DISSERTATION

THE RESPONSE OF A ROCKY MOUNTAIN FOREST SYSTEM TO A SHIFTING

DISTURBANCE REGIME

Submitted by

Amanda R. Carlson

Graduate Degree Program in Ecology

In partial fulfillment of the requirements

For the Degree of Doctor of Philosophy

Colorado State University

Fort Collins, Colorado

Fall 2019

Doctoral Committee:

    Advisor: Jason S. Sibold

    Timothy J. Assal
    N. Thompson Hobbs
    Monique E. Rocca

ABSTRACT

THE RESPONSE OF A ROCKY MOUNTAIN FOREST SYSTEM TO A SHIFTING

DISTURBANCE REGIME

Climate change is likely to drive widespread forest declines and transitions as

temperatures shift beyond historic ranges of variability. Warming temperatures and shifting

precipitation patterns may lead to increasing disturbances from wildfire, insect outbreaks,

drought, and extreme weather events, which may greatly accelerate rates of ecosystem change.

However, the role of disturbance in shaping forest response to climate change is not well

understood. Better understanding the impacts of changing disturbance patterns on forest decline

and recovery will allow us to better predict how forest ecosystems may adapt to a warming

world.

Severe wildfires and bark beetle outbreaks are currently affecting large areas of forest

throughout western North America, and increasing disturbance size and severity will have

uncertain impacts on forest persistence. The goal of my dissertation was to investigate the factors

shaping disturbance response in a region of the San Juan Mountains, Colorado, which has

undergone impacts from a high-severity spruce beetle outbreak and wildfire in the last 15 years. I

conducted three separate studies in the burn area of the West Fork Complex wildfire, which

burned in 2013, and in surrounding beetle-affected spruce-fir forests. The goals of each study

were to 1) assess whether the severity of spruce beetle outbreaks occurring before wildfire

resulted in compounded disturbance interactions affecting vegetation recovery, 2) determine how

the severity of each disturbance type influenced fine-scale below-canopy temperature patterns

across the landscape, and 3) assess how conifer seedling regeneration densities were influenced by effects of disturbance severity on seed dispersal, temperature, and vegetation structure.

I found that disturbances influenced seedling regeneration and ecosystem resilience through several mechanisms. First, pre-fire beetle outbreak severity was negatively correlated with post-fire vegetation cover, indicating that the combined disturbances were inhibiting regeneration beyond what may have been expected with fire alone. Second, disturbances had significant effects on below-canopy temperatures, with burned areas ~0.5 °C warmer than unburned forest areas and differences in overnight minimum temperatures resulting from loss of live canopy in unburned, beetle-killed forests. Third, the large fire size and high severity resulted in very little spruce seed dispersal or conifer regeneration in most of the burned area, while spruce regeneration in unburned forest was negatively correlated with increasing overstory mortality from the spruce beetle.

My results indicate that disturbance is playing an important role in determining the future trajectory of the forest in my study area. The West Fork Complex fire has caused a severe ecosystem transformation, has increased landscape exposure to warming temperatures, and is preventing forest re-establishment as a result of a lack of seed sources. The spruce beetle outbreak has not resulted in such a severe transformation, but is possibly leading to reduced forest resilience by reducing spruce seedling re-establishment and by altering fuel structures to make forests more prone to high soil burn severity if fire follows within ~10 years. Warming of below-canopy microclimates is not exacerbated by spruce beetle outbreak, and is rather partially offset by cooling of overnight temperatures. These findings provide insights into how forest responses to climate change may be shaped by disturbance processes, which are occurring with increasing severity and frequency worldwide.

ACKNOWLEDGEMENTS

to thank my past and current labmates, Doug Ouren, Ari Porter, and Carlyn Perovich for their help with fieldwork preparations, logistics, and execution. Thanks as well to all of the undergraduate lab assistants who helped with field data collection and data entry, who dealt heroically with rain, hail, and some non-ideal field site placements.

Pursuing a PhD was only possible with the support of the teachers and friends that have helped me along the way. I thank the GDPE community for providing me with a fantastic graduate school experience, with plenty of opportunities for stimulating conversation and friendly support. Thank you to all of my friends and family who made this an enjoyable experience and who provided constant encouragement and beers. Thank you especially to Mike for all of the love and support. Last but not least, I thank my dog Scout for providing good company throughout long hours of data analysis and writing.

TABLE OF CONTENTS

LIST OF TABLES

LIST OF FIGURES

CHAPTER 1: Introduction

Climate Change, Disturbance, and the Future of Forests

Climate change is expected to have a dramatic impact on forest ecosystems worldwide. Global average surface temperatures have increased by 0.85 °C since 1880, and are projected to increase by an additional 1-2 °C by the mid-21st century (IPCC, 2014). Relative to the pace of observed climate change, forests are dominated by slow-growing organisms that may have difficulty adapting to novel conditions. Forest species which are unable to adapt in place may therefore undergo declines in regions where climate is becoming unsuitable, and will only persist by colonizing newly suitable areas (Aitken et al., 2008). This response is likely to lead to widespread shifts in forest distributions and productivity across the globe, with implications for global terrestrial carbon pools, nutrient and water cycling, and wildlife habitat (Kirschbaum, 2000; Lenoir et al., 2008).

Some of the most severe climate impacts to forests may arise from amplifying effects of disturbances (Overpeck et al., 1990; Dale et al., 2001; Allen et al., 2010; Bentz et al., 2010; Seidl et al., 2017). A warming atmosphere increases evaporative demand and will thereby increase drought stress on vegetation (Williams et al., 2010; Berg et al., 2016), especially in regions such as the subtropical latitudes and Mediterranean where mean annual precipitation is projected to decrease (IPCC, 2014). Severe drought stress on forests increases the likelihood of widespread tree die-offs and increases tree susceptibility to insect infestation (Allen et al., 2010). Warming also prolongs fire seasons and leads to low fuel moisture, increasing wildfire occurrence in flammable forest types where there are sources of ignitions (Jolly et al., 2015). In regions where precipitation is expected to increase, such as the equatorial and high latitudes, increasing wetness

and heavy rainstorms may facilitate pathogen spread (IPCC, 2014; Pautasso et al., 2015). Climate change is also expected to increase the frequency and severity of extreme weather events, increasing forest impacts from tropical storms, cyclones, winter storms, tornadoes, windthrow, floods, and avalanches (Dale et al., 2001; Seidl et al., 2017).

Disturbance Regimes

Forest disturbances are relatively discrete biotic or abiotic events that significantly alter the structure of an ecosystem, usually by causing high mortality in dominant species (White & Pickett, 1985). Interactions among climate, geomorphology, and species assemblages may determine a recurring pattern of particular disturbance types, known as the disturbance regime (Sousa, 1984; White & Pickett, 1985; Turner et al., 1998). These regimes may be an integral part of ecosystem functioning, contributing to movement of nutrients and organisms, regeneration, succession, and landscape diversity (Turner, 2010). Disturbance regimes are also an important evolutionary filter for organisms on the landscape and play a role in shaping species assemblages and adaptations (Johnstone et al., 2016). Changing disturbance regimes therefore have the potential to alter forest ecosystem structure and function, amplifying changes driven by shifting climates.

Climate change is modifying disturbance regimes by changing the size, severity, and frequency of multiple disturbance types (Turner, 2010). Increasing disturbance frequencies and footprints also increase the probability of disturbances interacting in space and time, potentially producing disturbance interactions or compounded effects on vegetation recovery (Paine et al., 1998; Buma, 2015). Interacting disturbances may produce negative feedbacks in many cases, such as when past disturbances reduce forest density and create forest gaps, which limit the severity of future disturbance by insect outbreaks or fire (Bigler et al., 2005; Kulakowski &

2

Veblen, 2007). On the other hand, positive feedbacks may result from other types of disturbance interactions, such as windthrow events leading to localized insect outbreaks (Seidl & Rammer, 2017). Additionally, compounded effects from multiple disturbances may arise when the combination of two events produces unexpected effects on ecosystem recovery that would not result from one event alone (Paine et al., 1998). This may occur when two disturbances closely overlap in time. For example, shortening fire return intervals may cause forests regenerating from pre-fire seed banks to re-burn before trees have matured, leaving no seed bank for a second regeneration (Buma et al., 2013).

Ecosystem Resilience and Transitions

Ecosystem transformations may occur where the cumulative impacts from disturbances and reduced climate suitability prevent dominant species from adapting to or recovering from changing conditions (Johnstone et al., 2016). Conversely, ecosystem resilience allows systems to absorb change and maintain relationships between populations and state variables (Holling, 1973). Ecosystem stability, a related concept, refers to the capacity of the system to resist being altered by external perturbations (Lewontin, 1969; Holling, 1973). Most ecosystems that appear stable over time have evolved species assemblages and individual species adaptations that confer resilience to localized disturbances, allowing the ecosystem to return to a prior state each time a disturbance occurs (Johnstone et al., 2016). Recovery from disturbances at specific places and times results in stability over large spatial and temporal scales. However, species' adaptations to a particular disturbance regime may not result in resilience when disturbances begin to routinely increase in extent or severity or create novel disturbance interactions. Resilience may be further undermined by climatic shifts that make dominant species less well-adapted to the physical environment.

Declines in forest resilience to disturbance may result in state transitions to non-forest ecosystems, or to systems with altered species composition and structure. These novel states may represent alternative stable states which cannot be expected to return to the prior, forested state even if warming temperatures stabilize or decrease or if disturbance regimes return to historic norms. Alternative stable states exist where multiple ecosystem types may arise from alternate disturbance trajectories and shifts in environmental parameters, and which require large perturbations to destabilize once established (Lewontin, 1969; Beisner et al., 2003). Disturbances not only allow species to more rapidly re-assemble in alignment with novel climate conditions, but also remove biological material from the landscape that would allow for forest recovery (i.e. seeds banks, resprouting roots) and may help to drive transitions to alternative stable states (Holling & Gunderson, 2002; Johnstone et al., 2016). Warming conditions increase the likelihood of these transitions by reducing the stability of species assemblages formed by past climates.

Alternative state transitions may be highly beneficial for adaptation to climate change in long-lived species (Thom et al., 2017). Some disturbance types, such as fire and insect outbreaks, may be more likely to occur at the warmest ends of a species' distribution where trees are under the greatest climatic stress. Tree die-offs may then allow more warm-adapted species to colonize sites without competition from the overstory (Iverson et al., 2011; Serra-Diaz et al., 2015). Disturbances also create a transition from forest dominance by large, well-established trees to dominance by regenerating seedlings, which are typically more susceptible to mortality from high temperatures and drought (Grubb, 1977). Seedling mortality may drive more gradual ecosystem transitions if novel climate conditions are sustained during the period of tree re-establishment.

Understanding Forest Trajectories in a Changing Climate

Impacts of climate change on particular species can be estimated using future climate projections made by general circulation models (GCMs). These projections can be used to predict future areas of potential decline and colonization based on change in suitability of climate variables correlated with historical species distributions, an exercise known as bioclimate modeling (Box, 1981; Guisan & Zimmerman, 2000). Bioclimate models have been widely used to assess the impacts of various climate change scenarios on forest species (Pearson & Dawson, 2003; Hijmans & Graham, 2006). However, it is not well understood how predictions based on climate suitability alone will ultimately be influenced by complex processes arising from changing disturbance regimes, processes of species movement, and species interactions (Franklin, 2010; Iverson et al., 2011). Given the occurrence of widespread forest disturbances associated with current warming, understanding the effects of changing climates on future distributions depends on understanding how disturbance patterns and recovery processes may help guide ecosystems toward alternative stable states.

Assessing impacts of climate on forest communities is often limited by a lack of available climate data at spatial scales relevant to biological processes. Mismatches between scales of observation and scales of process can significantly affect the assessed relationships between ecosystem variables, and is a common problem in ecology (Levin, 1992). Observed climate data is typically interpolated from weather stations and projected onto spatial grids with cell sizes ~1 km^2 or greater, and future projections are typically made at scales of several km^2 (IPCC, 2014; Harris et al., 2014). However, biotic processes such as seedling establishment and survival occur at much finer scales. It has been demonstrated that the spatial scale of climate representations can

strongly affect assessments and projections of the influences of climate on vegetation (Austin & van Niel, 2011; Slavich et al., 2014).

'Topoclimate' refers to the influence of topographic variations on temperature and moisture patterns along gradients of elevation, aspect, and slope position at spatial scales typically < 1 km (Dobrowski, 2011). In forest ecosystems, temperature and moisture may also be strongly affected by canopy structure and variation in microclimate as well (de Frenne et al., 2016). These complex variations may be of importance for predicting broader-scale patterns of decline, as pockets of cooler temperatures and elevated moisture can provide microrefugia within landscapes where species may be at risk of extirpation (Ashcroft, 2010). Landscape patterns in which climatically unsuitable areas are interrupted by microrefugia may allow particular species and cover types to persist with patchy distributions rather than become extirpated completely. Microrefugia can also preserve seed sources, provide bases for expansion during favorable climate windows, and create 'stepping stones' for dispersal to more suitable climates (Hannah et al., 2014). Understanding how forest species trajectories may be influenced by microrefugia requires that climate influences be considered at the relatively fine topoclimate scale.

Climate and disturbances may also influence future forest distributions through effects on species dispersal mechanisms. Species cannot realize their potential distributions in locations with improving climate suitability if they cannot disperse to those locations, and seed availability may additionally influence the likelihood of species persistence and the available genetic diversity for *in situ* adaptation (Clark et al., 2001; Kremer et al., 2012; Corlett & Wescott, 2013). Canopy disturbances have the potential to cause ecosystem transitions by limiting seed availability. For example, forest recovery after a large wildfire may be mediated not only by climate, but by the severity of the wildfire and the availability of live seed sources within the

burned patch (Turner et al., 1999). Long distances between seed sources and suitable sites for germination can mediate species' relationships to climatic factors across landscapes, particularly for wind-dispersed species with small dispersal ranges (Urza & Sibold, 2017; Kemp et al., 2019). Partial canopy disturbance may also reduce the numbers of large, high seed crop-producing trees in forests that reproduce through seed masting. In some circumstances, warming temperatures can further limit overall seed production in surviving trees (Zlotin & Parmenter, 2008; Smaill et al., 2011).

Disturbance and Recovery in Forests of the Southern Rockies

The Southern Rocky Mountains extend from southern Wyoming to northern New Mexico. Most of the region is dominated by conifer forest, with high-elevation subalpine zones (~2,700-3,600 m) dominated by Engelmann spruce (*Picea engelmannii*), subalpine fir (*Abies lasiocarpa*), lodgepole pine (*Pinus contorta*) and aspen (*Populus tremuloides*). Mid-elevation zones are dominated by aspen stands and mixed-conifer forests composed of spruces, firs, ponderosa pine, and Douglas fir (*Pseudotsuga menziesii*). Montane zones (~1,800-2,700 m elevation) are mainly dominated by ponderosa pine (*Pinus ponderosae*) and transition to woodlands dominated by piñon pine (*Pinus edulis*) and Rocky Mountain juniper (*Juniperus scopulorum*) at lower elevations.

The region has warmed significantly in the past century (~ +0.2-0.8 °C) and has experienced several severe, multi-year droughts since 1999 (Gonzalez et al., 2018). In the last three decades, forests of the Southern Rockies have seen a severe increase in the number of large wildfires and in annual area burned (Dennison et al., 2014). These increases have been attributed to higher summer temperatures, earlier snowmelt, and more frequent severe droughts as a result of anthropogenic warming (Westerling et al., 2006; Abatzoglou & Williams, 2016). Factors

driving fire regime changes in montane ponderosa pine and mixed-conifer forests are complex, as historic fire patterns are influenced by indigenous land use, European settlement, and 20th-century fire suppression leading to densely stocked forests in some areas (Brown et al., 1999). In higher-elevation subalpine forests, historic fire occurrence has not been as greatly influenced by human activities and has been more strongly linked to warm and dry climate conditions (Schoennagel et al., 2004; Sibold & Veblen, 2006). Warming and increasing aridity therefore may increase fire frequency and alter fire regimes in high-elevation forest zones.

Fires in subalpine forests have historically occurred infrequently (~50-300 year return intervals) and tend to be stand-replacing, as dominant spruces, firs, and lodgepole pine have not evolved fire-resistant traits such as thick bark (Agee, 1998). Rather, subalpine forest species have mainly evolved fire-resilient traits such as serotinous cones and wind-dispersed seeds (Enright et al., 2014). These resilience mechanisms may be highly sensitive to shifting fire regimes if increasing fire size, severity, and frequency result in large burned areas with few surviving trees or seed sources. Evidence from throughout the U.S. Rockies shows that many fires in the last decade have been followed by limited conifer re-establishment (Stevens-Rumann & Morgan, 2019). While regeneration failures have been primarily documented in lower-elevation dry forests, limited seedling numbers have also been observed in subalpine forests due to a combination of limited seed dispersal and post-fire drought conditions (Harvey et al., 2016; Urza & Sibold, 2017). These limits to seedling re-establishment may indicate that fires are catalyzing ecosystem transitions, and that these patterns are likely to become more widely observed with continued warming and severe fire seasons.

In addition to the increase in fire activity, western North America has also experienced unprecedented bark beetle outbreaks in the last two decades. Bark beetles are wood-boring

insects that lay larvae in the phloem of host trees, causing tree mortality as the growing larvae cut off nutrient flow to the canopy. While large outbreaks have occurred in the past, typically associated with blowdown events, recent outbreaks have been exacerbated by widespread and prolonged droughts that weaken tree defenses (Bentz et al., 2010; Hart et al., 2014). Warming winters also allow for larger beetle populations, as beetles are killed by extreme cold temperatures (Bentz et al., 2009). The extent and synchronicity of bark beetle outbreaks in multiple host forest types had not been previously documented, and is thought to be a symptom of a climatic shift which will leave a long-lasting legacy on western conifer forests (Raffa et al., 2008).

Bark beetle activity in the Southern Rockies has declined in the last several years as infestations have spread through mature host trees (CSFS, 2018). Beetles prefer large-diameter trees that may be several hundred years old, meaning that forests affected by severe outbreaks will not be susceptible again in the foreseeable future. In high-elevation forests affected by mountain pine beetle (*Dendroctonus ponderosae*; lodgepole pine hosts) or spruce beetle (*Dendroctonus rufipennis*; Engelmann spruce hosts), post-beetle recovery is typically dominated by advanced regeneration of seedlings established prior to the outbreak (DeRose & Long, 2007; Collins et al., 2011; Kayes & Tinker, 2012). Unlike wildfire, bark beetle outbreaks have not led to documented regeneration failures or abrupt ecosystem transformations.

Since extensive beetle outbreaks begin in the late 1990s, the potential for disturbance interactions with wildfire has been a major management concern. Beetle-killed stands may experience understory regeneration that may increase fine surface fuel loads, while large fuel loads may increase as dead trees fall (Jenkins et al., 2008). These changes to fuel structure can theoretically increase wildfire severity and lead to more active crown fire (Schoennagel et al.,

2012). However, a number of studies have shown that this is not necessarily the case, and that the links between fuel structure and fire activity may be irrelevant in relation to the influences of fire weather and topography (Simard et al., 2011; Harvey et al., 2014; Andrus et al., 2016).

Research Objectives

My dissertation research focused on the effects of recent, severe wildfire and spruce beetle outbreak in the eastern San Juan Mountains of southwest Colorado. Fieldwork for each chapter took place near Wolf Creek Pass in the Rio Grande National Forest, straddling the Continental Divide. The area is dominated by Engelmann spruce and mixed-fir forests with interspersed aspen stands. Spruce beetles in the San Juans were first detected in the Weminuche Wilderness Area in 2004 and had become widespread throughout the study area by ~2008. My study area also included area burned by the West Fork Complex wildfire in 2013. The West Fork Complex was composed of three individual lightning-caused fires and was the second-largest fire ever recorded in Colorado, burning over 44,000 ha of recently beetle-killed spruce-fir forest.

Severe disturbances in this region of the San Juan Mountains provided an opportunity to conduct a detailed examination of ecosystem response. Forest recovery in this area is influenced by multiple factors, including compounded disturbance interactions, novel disturbance severities and extents, and complex warming patterns over a landscape with varying topography. Chapters 2-4 of this dissertation explore various components of the potential effects of changing disturbance regimes on future forest trajectories and the potential implications for climate change response. In Chapter 2, I examined the effects of high-severity wildfire interacting with prior high-severity spruce beetle outbreak to produce compounded effects on vegetation recovery. I present a remote sensing methodology for assessing pre-fire spruce beetle disturbance severity, and use a spatially structured model to determine the relationship between spruce beetle severity

and post-fire vegetation cover. In Chapter 3, I used *in situ* temperature sensor data to assess the influences of fine-scale topography and disturbance impacts to forest overstory on below-canopy temperatures. The results of this study have implications for understanding how ecosystem recovery may vary as a result of heterogeneity in exposure to broader warming at the below-canopy scale. In Chapter 4, I utilized below-canopy temperature records, topography, canopy structure, and understory cover data to determine the relative influence of these factors on spruce and fir seedling establishment. These results provide an indication of ecosystem resilience to each disturbance. Results from Chapters 2-4 are synthesized in Chapter 5.

LITERATURE CITED

Abatzoglou, J. T., & Williams, A. P. (2016). Impact of anthropogenic climate change on wildfire across western US forests. *PNAS*, *113*(42), 11770–11775.

Agee, J. K. (1998). The landscape ecology of western forest fire regimes. *Northwest Science*, *72*(17), 24–34.

Aitken, S. N., Yeaman, S., Holliday, J. A., Wang, T., & Curtis-McLane, S. (2008). Adaptation, migration or extirpation: Climate change outcomes for tree populations. *Evolutionary Applications*, *1*(1), 95–111.

Allen, C. D., Macalady, A. K., Chenchouni, H., Bachelet, D., McDowell, N., Vennetier, M., … others. (2010). A global overview of drought and heat-induced tree mortality reveals emerging climate change risks for forests. *Forest Ecology and Management*, *259*(4), 660–684.

Andrus, R. A., Veblen, T. T., Harvey, B. J., & Hart, S. J. (2016). Fire severity unaffected by spruce beetle outbreak in spruce-fir forests in southwestern Colorado. *Ecological Applications*, *26*(3), 700–711.

Ashcroft, M. B. (2010). Identifying refugia from climate change. *Journal of Biogeography*, *37*(8), 1407–1413.

Beisner, B., Haydon, D., & Cuddington, K. (2003). Alternative stable states in ecology. *Frontiers in Ecology and the Environment*, *1*(7), 376–382.

Bentz, B. J., Logan, J., MacMahon, J., Allen, C. D., Ayres, M., Berg, E., … Joyce, L. (2009). *Bark beetle outbreaks in western North America: Causes and consequences*. 42. Salt Lake City, UT: University of Utah Press.

Bentz, B. J., Régnière, J., Fettig, C. J., Hansen, E. M., Hayes, J. L., Hicke, J. A., … Seybold, S. J. (2010). Climate Change and Bark Beetles of the Western United States and Canada: Direct and Indirect Effects. *BioScience*, *60*(8), 602–613.

Berg, A., Findell, K., Lintner, B., Giannini, A., Seneviratne, S. I., van den Hurk, B., … Milly, P. C. D. (2016). Land–atmosphere feedbacks amplify aridity increase over land under global warming. *Nature Climate Change*, *6*, 869.

Bigler, C., Kulakowski, D., & Veblen, T. T. (2005). Multiple disturbance interactions and drought influence fire severity in Rocky Mountain subalpine forests. *Ecology*, *86*(11), 3018–3029.

Box, E. O. (1981). Predicting physiognomic vegetation types with climate variables. *Vegetatio*, *45*(2), 127–139.

Brown, P. M., Kaufmann, M. R., & Shepperd, W. D. (1999). Long-term, landscape patterns of past fire events in a montane ponderosa pine forest of central Colorado. *Landscape Ecology*, *14*(6), 513–532.

Buma, B. (2015). Disturbance interactions: Characterization, prediction, and the potential for cascading effects. *ECOSPHERE*, *6*(4).

Buma, Brian, Brown, C. D., Donato, D. C., Fontaine, J. B., & Johnstone, J. F. (2013). The Impacts of Changing Disturbance Regimes on Serotinous Plant Populations and Communities. *BioScience*, *63*(11), 866–876.

Clark, J., Silman, M., Kern, R., Macklin, E., & HilleRisLambers, J. (1999). Seed dispersal near and far: Patterns across temperate and tropical forests. *Ecology*, *80*(5), 1475–1494.

Collins, B. J., Rhoades, C. C., Hubbard, R. M., & Battaglia, M. A. (2011). Tree regeneration and future stand development after bark beetle infestation and harvesting in Colorado lodgepole pine stands. *Forest Ecology and Management*, *261*(11), 2168–2175.

Corlett, R. T., & Westcott, D. A. (2013). Will plant movements keep up with climate change? *Trends in Ecology & Evolution*, *28*(8), 482–488.

CSFS. (2018). *2018 Report on the Health of Colorado's Forests*. Fort Collins, CO: Colorado State Forest Service.

Dale, V. H., Joyce, L. A., McNulty, S., Neilson, R. P., Ayres, M. P., Flannigan, M. D., … Wotton, M. (2001). Climate Change and Forest Disturbances: Climate change can affect forests by altering the frequency, intensity, duration, and timing of fire, drought, introduced species, insect and pathogen outbreaks, hurricanes, windstorms, ice storms, or landslides. *BioScience*, *51*(9), 723–734.

De Frenne, P., Rodríguez-Sánchez, F., Coomes, D. A., Baeten, L., Verstraeten, G., Vellend, M., … Verheyen, K. (2013). Microclimate moderates plant responses to macroclimate warming. *PNAS*, *110*(46), 18561–18565.

Dennison, P. E., Brewer, S. C., Arnold, J. D., & Moritz, M. A. (2014). Large wildfire trends in the western United States, 1984–2011. *Geophysical Research Letters*, *41*(8), 2928–2933.

DeRose, R. J., & Long, J. N. (2007). Disturbance, structure, and composition: Spruce beetle and Engelmann spruce forests on the Markagunt Plateau, Utah. *Forest Ecology and Management*, *244*(1), 16–23.

Dobrowski, S. Z. (2011). A climatic basis for microrefugia: The influence of terrain on climate. *Global Change Biology*, *17*(2), 1022–1035.

Enright, N. J., Fontaine, J. B., Lamont, B. B., Miller, B. P., & Westcott, V. C. (2014). Resistance and resilience to changing climate and fire regime depend on plant functional traits. *Journal of Ecology*, *102*(6), 1572–1581.

Franklin, J. (2010). Moving beyond static species distribution models in support of conservation biogeography. *Diversity and Distributions*, *16*(3), 321–330.

González, P., Garfin, G. M., Breshears, D. D., Brooks, K. M., Brown, H. E., Elias, E. H., … Udall, B. H. (2018). *Ch. 25: Southwest* (pp. 1101–1184). Washington, D.C.: U.S. Global Change Research Program.

Grubb, P. J. (1977). The maintenance of species-richness in plant communities: The importance of the regeneration niche. *Biological Reviews*, *52*(1), 107–145.

Guisan, A., & Zimmermann, N. E. (2000). Predictive habitat distribution models in ecology. *Ecological Modelling*, *135*(2), 147–186.

Hannah, L., Flint, L., Syphard, A. D., Moritz, M. A., Buckley, L. B., & McCullough, I. M. (2014). Fine-grain modeling of species' response to climate change: Holdouts, stepping-stones, and microrefugia. *Trends in Ecology & Evolution*, *29*(7), 390–397.

Harris, R. M. B., Grose, M. R., Lee, G., Bindoff, N. L., Porfirio, L. L., & Fox-Hughes, P. (2014). Climate projections for ecologists. *Wiley Interdisciplinary Reviews: Climate Change*, *5*(5), 621–637.

Hart, S. J., Veblen, T. T., Eisenhart, K. S., Jarvis, D., & Kulakowski, D. (2014). Drought induces spruce beetle (Dendroctonus rufipennis) outbreaks across northwestern Colorado. *Ecology*, *95*(4), 930–939.

Harvey, B. J., Donato, D. C., Romme, W. H., & Turner, M. G. (2014). Fire severity and tree regeneration following bark beetle outbreaks: The role of outbreak stage and burning conditions. *Ecological Applications*, *24*(7), 1608–1625.

Harvey, B. J., Donato, D. C., & Turner, M. G. (2016). High and dry: Post-fire tree seedling establishment in subalpine forests decreases with post-fire drought and large stand-replacing burn patches. *Global Ecology and Biogeography*, *25*(6), 655–669.

Hijmans, R. J., & Graham, C. H. (2006). The ability of climate envelope models to predict the effect of climate change on species distributions. *Global Change Biology*, *12*(12), 2272–2281.

Holling, C. S. (1973). Resilience and stability of ecological systems. *Annual Review of Ecology and Systematics*, *4*(1), 1–23.

Holling, C. S., & Gunderson, L. H. (2002). Resilience and adaptive cycles. In *Panarchy: Understanding Transformations in Human and Natural Systems* (pp. 25–62). Washington, D.C.: Island Press.

IPCC. (2014). *Climate Change 2014: Synthesis Report. Contribution of Working Groups I, II and III to the Fifth Assessment Report of the Intergovernmental Panel on Climate Change*. IPCC. Geneva, Switzerland: IPCC.

Iverson, L. R., Prasad, A. M., Matthews, S. N., & Peters, M. P. (2011). Lessons Learned While Integrating Habitat, Dispersal, Disturbance, and Life-History Traits into Species Habitat Models Under Climate Change. *Ecosystems*, *14*(6), 1005–1020.

Jenkins, M. J., Hebertson, E., Page, W., & Jorgensen, C. A. (2008). Bark beetles, fuels, fires and implications for forest management in the Intermountain West. *Forest Ecology and Management*, *254*(1), 16–34.

Johnstone, J. F., Allen, C. D., Franklin, J. F., Frelich, L. E., Harvey, B. J., Higuera, P. E., … Turner, M. G. (2016). Changing disturbance regimes, ecological memory, and forest resilience. *Frontiers in Ecology and the Environment*, *14*(7), 369–378.

Jolly, W. M., Cochrane, M. A., Freeborn, P. H., Holden, Z. A., Brown, T. J., Williamson, G. J., & Bowman, D. M. J. S. (2015). Climate-induced variations in global wildfire danger from 1979 to 2013. *Nature Communications*, *6*, 7537.

Kayes, L. J., & Tinker, D. B. (2012). Forest structure and regeneration following a mountain pine beetle epidemic in southeastern Wyoming. *Forest Ecology and Management*, *263*, 57–66.

Kemp, K. B., Higuera, P. E., Morgan, P., & Abatzoglou, J. T. (2019). Climate will increasingly determine post-fire tree regeneration success in low-elevation forests, Northern Rockies, USA. *Ecosphere*, *10*(1), e02568.

Kirschbaum, M. U. F. (2000). Forest growth and species distribution in a changing climate. *Tree Physiology*, *20*(5–6), 309–322.

Kremer, A., Ronce, O., Robledo-Arnuncio, J. J., Guillaume, F., Bohrer, G., Nathan, R., … Schueler, S. (2012). Long-distance gene flow and adaptation of forest trees to rapid climate change. *Ecology Letters*, *15*(4), 378–392.

Kulakowski, D., & Veblen, T. T. (2007). Effect of prior disturbances on the extent and severity of wildfire in Colorado subalpine forests. *Ecology*, *88*(3), 759–769.

Lenoir, J., Gégout, J. C., Marquet, P. A., de Ruffray, P., & Brisse, H. (2008). A significant upward shift in plant species optimum elevation during the 20th century. *Science*, *320*(5884), 1768–1771.

Levin, S. A. (1992). The Problem of Pattern and Scale in Ecology: The Robert H. MacArthur Award Lecture. *Ecology*, *73*(6), 1943–1967.

Lewontin, R. C. (1969). The meaning of stability. *Brookhaven Symposia in Biology*, *22*, 13–24.

Overpeck, J. T., Rind, D., & Goldberg, R. (1990). Climate-induced changes in forest disturbance and vegetation. *Nature*, *343*(6253), 51–53.

Paine, R., Tegner, M., & Johnson, E. (1998). Compounded perturbations yield ecological surprises. *ECOSYSTEMS*, *1*(6), 535–545.

Pautasso, M., Schlegel, M., & Holdenrieder, O. (2015). Forest Health in a Changing World. *Microbial Ecology*, *69*(4), 826–842.

Pearson, R. G., & Dawson, T. P. (2003). Predicting the impacts of climate change on the distribution of species: Are bioclimate envelope models useful? *Global Ecology and Biogeography*, *12*(5), 361–371.

Raffa, K. F., Aukema, B. H., Bentz, B. J., Carroll, A. L., Hicke, J. A., Turner, M. G., & Romme, W. H. (2008). Cross-scale drivers of natural disturbances prone to anthropogenic amplification: The dynamics of bark beetle eruptions. *Bioscience*, *58*(6), 501–517.

Schoennagel, T., Veblen, T. T., & Romme, W. H. (2004). The Interaction of Fire, Fuels, and Climate across Rocky Mountain Forests. *BioScience*, *54*(7), 661–676.

Seidl, R., & Rammer, W. (2017). Climate change amplifies the interactions between wind and bark beetle disturbances in forest landscapes. *Landscape Ecology*, *32*(7), 1485–1498.

Seidl, R., Thom, D., Kautz, M., Martin-Benito, D., Peltoniemi, M., Vacchiano, G., … Reyer, C. P. O. (2017). Forest disturbances under climate change. *Nature Climate Change*, *7*(6), 395–402.

Serra-Diaz, J. M., Scheller, R. M., Syphard, A. D., & Franklin, J. (2015). Disturbance and climate microrefugia mediate tree range shifts during climate change. *Landscape Ecology*, *30*(6), 1039–1053.

Sibold, J. S., & Veblen, T. T. (2006). Relationships of subalpine forest fires in the Colorado Front Range with interannual and multidecadal-scale climatic variation. *Journal of Biogeography*, *33*(5), 833–842.

Simard, M., Romme, W. H., Griffin, J. M., & Turner, M. G. (2011). Do mountain pine beetle outbreaks change the probability of active crown fire in lodgepole pine forests? *ECOLOGICAL MONOGRAPHS*, *81*(1), 3–24.

Slavich, E., Warton, D. I., Ashcroft, M. B., Gollan, J. R., & Ramp, D. (2014). Topoclimate versus macroclimate: How does climate mapping methodology affect species distribution models and climate change projections? *Diversity and Distributions*, *20*(8), 952–963.

Smaill, S. J., Clinton, P. W., Allen, R. B., & Davis, M. R. (2011). Climate cues and resources interact to determine seed production by a masting species. *Journal of Ecology*, *99*(3), 870–877.

Sousa, W. P. (1984). The Role of Disturbance in Natural Communities. *Annual Review of Ecology and Systematics*, *15*(1), 353–391.

Stevens-Rumann, C. S., & Morgan, P. (2019). Tree regeneration following wildfires in the western US: a review. *Fire Ecology*, *15*(1), 15.

Thom, D., Rammer, W., & Seidl, R. (2017). Disturbances catalyze the adaptation of forest ecosystems to changing climate conditions. *Global Change Biology*, *23*(1), 269–282.

Turner, M. G. (2010). Disturbance and landscape dynamics in a changing world. *Ecology*, *91*(10), 2833–2849.

Turner, M. G., Baker, W. L., Peterson, C. J., & Peet, R. K. (1998). Factors Influencing Succession: Lessons from Large, Infrequent Natural Disturbances. *Ecosystems*, *1*(6), 511–523.

Turner, M. G., Romme, W. H., & Gardner, R. H. (2000). Prefire heterogeneity, fire severity, and early postfire plant reestablishment in subalpine forests of Yellowstone National Park, Wyoming. *International Journal of Wildland Fire*, *9*(1), 21–36.

Urza, A. K., & Sibold, J. S. (2017). Climate and seed availability initiate alternate post-fire trajectories in a lower subalpine forest. *Journal of Vegetation Science*, *28*(1), 43–56.

Westerling, A. L., Hidalgo, H. G., Cayan, D. R., & Swetnam, T. W. (2006). Warming and earlier spring increase western U.S. forest wildfire activity. *Science*, *313*(5789), 940–943.

White, P. S., & Pickett, S. T. A. (1985). Natural disturbance and patch dynamics. In *The ecology of natural disturbance and patch dynamics: An introduction* (pp. 3–13). New York, NY: Academic Press.

Williams, A. P., Allen, C. D., Millar, C. I., Swetnam, T. W., Michaelsen, J., Still, C. J., & Leavitt, S. W. (2010). Forest responses to increasing aridity and warmth in the southwestern United States. *Proceedings of the National Academy of Sciences*, *107*(50), 21289–21294.

Zlotin, R. I., & Parmenter, R. R. (2008). Patterns of mast production in pinyon and juniper woodlands along a precipitation gradient in central New Mexico (Sevilleta National Wildlife Refuge). *Journal of Arid Environments*, *72*(9), 1562–1572.

CHAPTER 2: Evidence of Compounded Disturbance Effects on Vegetation Recovery
Following High-Severity Wildfire and Spruce Beetle Outbreak

Summary

Spruce beetle (*Dendroctonus rufipennis*) outbreaks are rapidly spreading throughout

subalpine forests of the Rocky Mountains, raising concerns that altered fuel structures may

increase the ecological severity of wildfires. Although many recent studies have found no

conclusive link between beetle outbreaks and increased fire size or canopy mortality, few studies

have addressed whether these combined disturbances produce compounded effects on short-term

vegetation recovery. We tested for an effect of spruce beetle outbreak severity on vegetation

recovery in the West Fork Complex fire in southwestern Colorado, USA, where much of the

burn area had been affected by severe spruce beetle outbreaks in the decade prior to the fire.

Vegetation recovery was assessed using the Landsat-derived Normalized Difference Vegetation

Index (NDVI) two years after the fire, which occurred in 2013. Beetle outbreak severity, defined

as the basal area of beetle-killed trees within Landsat pixels, was estimated using vegetation

index differences (dVIs) derived from pre-outbreak and post-outbreak Landsat images. Of the

seven dVIs tested, the change in Normalized Difference Moisture Index (dNDMI) was most

strongly correlated with field measurements of beetle-killed basal area ($R^2 = 0.66$). dNDMI was

included as an explanatory variable in sequential autoregressive (SAR) models of $NDVI_{2015.}$

Models also included pre-disturbance NDVI, topography, and weather conditions at the time of

burning as covariates. SAR results showed a significant correlation between $NDVI_{2015}$ and

dNDMI, with more severe spruce beetle outbreaks corresponding to reduced post-fire vegetation

cover. The correlation was stronger for models which were limited to locations in the red stage

of outbreak (outbreak ≤ 5 years old at the time of fire) than for models of gray-stage locations

(outbreak > 5 years old at the time of fire). These results indicate that vegetation recovery processes may be negatively impacted by severe spruce beetle outbreaks occurring within a decade of stand-replacing wildfire.

Introduction

Climate-related disturbances in North American forests have been increasing in frequency and extent in recent decades (Cohen et al., 2016). In the Rocky Mountain region, the increasing pressures of novel climate conditions, prolonged droughts, insect outbreaks, and larger and more severe wildfires have sparked concerns that multiple disturbances may drive fundamental shifts in species compositions and ecosystem processes (Buma, 2015; Kulakowski, Matthews, Jarvis, & Veblen, 2013; Stephens et al., 2013). Events which alter recovery processes and drive ecosystems toward new stable states are known as 'compound disturbances' (Paine, Tegner, & Johnson, 1998), and may play an important role in shaping the structure and composition of future forests (Dale et al., 2001; Turner, 2010). However, evidence supporting clear compounded effects of multiple disturbances in western forest systems is not well documented. An improved understanding of interactions between disturbances is important for building an understanding of multiple disturbance processes, and for informing management decisions in systems undergoing changes in disturbance regimes.

One of the most pressing research questions related to multiple disturbances in western forest systems is whether severe bark beetle outbreaks can increase the ecological severity of subsequent wildfires (Hicke, Johnson, Hayes, & Preisler, 2012; Jenkins, Hebertson, Page, & Jorgenen, 2008; Negrón et al., 2008). Millions of hectares of western conifer forests have been recently affected by several species of bark beetle, including the mountain pine beetle (*Dendroctonus ponderosae*), spruce beetle (*Dendroctonus rufipennis*), western balsam bark

beetle (*Dryocoetes confusus*), Douglas-fir beetle (*Dendroctonus pseudotsugae*), and pinyon Ips beetle (*Ips confusus*) (Meddens, Hicke, & Ferguson, 2012). These insects have caused forest mortality at an unprecedented scale over the last two decades, due in large part to warming temperatures and aging forest stands (Negrón & Fettig, 2014; Raffa et al., 2008). The spruce beetle in particular is spreading rapidly through high-elevation subalpine forests as a possible result of increasing summer temperatures, which may shorten beetle development cycles, and increasing winter temperatures, which may allow larger populations to survive (DeRose & Long, 2012; Hansen & Bentz, 2003). Spruce beetles are likely to continue spreading to higher elevations and more northerly latitudes throughout the Rocky Mountain region (Bentz et al., 2010).

In the southern Rockies (southern Wyoming to northern New Mexico), the primary spruce beetle host species is Engelmann spruce (*Picea engelmannii*). *P. engelmannii* typically co-occurs with subalpine fir (*Abies lasiocarpa*) at elevations ranging from about 2,850-3,500 m a.s.l. (Peet, 1978). Spruce-fir forests are characterized by infrequent, high-severity wildfire and fire occurrence is climate-limited rather than fuel-limited (Agee, 1998; Arno, 1980; Bessie & Johnson, 1995; Romme & Knight; 1981; Sibold, Veblen, & González, 2006). As a result of the typically long intervals between fires in these systems, fuels tend to be densely stocked (Bessie & Johnson, 1995; Sibold et al., 2006). However, surface fuels are often limited (Schoennagel, Veblen, & Romme, 2004), and beetle outbreaks may affect the fuel structure of recently killed stands by transferring fine fuels from the canopy to the forest floor.

Severe spruce beetle outbreaks can cause up to 100% mortality in mature spruce stands and result in complete loss of overstory canopy (Bentz et al., 2009). During an outbreak, host trees are killed within 1-2 years of attack as beetles bore into the bark and feed on phloem

tissues. Loss of canopy needles continues for 2-5 years after the initial attack, after the tree has been killed (known as the "red stage") (Bentz et al., 2009). The red stage is followed by a "gray stage" in which all needles have been shed and fine fuels begin to decompose on the forest floor (Hicke et al., 2012). During this time, coarse surface fuel loads may increase as standing dead trees begin to fall from root rotting and blowdowns (Meigs, Kennedy, & Cohen, 2011). Accumulation of fuels on the forest floor can potentially increase the severity of surface fire (Agee & Skinner, 2005), leading managers to speculate that fuel removal may be necessary to mitigate wildfire impacts (Collins, Rhoades, Hubbard, & Battaglia, 2011).

Assessing the impact of bark beetle outbreaks on fire severity is challenging, due to the difficulty in accurately quantifying outbreak severity (referring to the number or density of killed trees within a stand) after fires have damaged physical evidence of beetle activity (Assal, Sibold, & Reich, 2014). Although aerial imagery and aerial detection survey (ADS) data can be used to classify where outbreaks have occurred at broad scales, it is difficult to determine how severity may vary at fine spatial scales. ADS is carried out annually by multiple resource agencies in the US and provides classifications of severity within hand-drawn outbreak extent polygons, but these classifications provide only a single severity estimate within areas which may vary widely in size (e.g. >1,000 ha). Remotely sensed vegetation indices (VIs) derived from satellite imagery offer the potential to estimate outbreak severity with greater spatial accuracy than ADS (30-m resolution from Landsat imagery), and can be used to characterize canopy change from outbreaks over a greater spatial extent than is feasible using field methods. Remote sensing techniques have been widely applied to detect canopy change from bark beetle outbreaks and other types of disturbance (Assal et al., 2014; Assal, Anderson, & Sibold, 2016; Goodwin et al., 2008; Hais, Jonášová, Langhammer, & Kučera, 2009; Hart & Veblen, 2015; Havašová, Bucha, Ferenčik, &

Jakuš, 2015; Meddens, Hicke, Vierling, & Hudak, 2013; Walter & Platt, 2013; Wilson & Sader, 2002). Multi-date image differencing of VIs provides a quantitative indicator of spectral change from forest canopy mortality (Healey, Yang, Cohen, & Pierce, 2006; Jin & Sader, 2005), which may serve as an effective metric for canopy loss from beetle outbreak.

An additional challenge in assessing the relationship between outbreak severity and fire impacts is that a number of contingent factors may affect the nature of the disturbance interaction. These factors may complicate the effect of beetle outbreaks on fuel structures, alter the effect of fuel structure on fire behavior and burning intensity, or may affect vegetation recovery independently from fuel structure. First, the fuel structure of beetle-killed stands changes with time following the initial outbreak. Older beetle-killed stands contain greater amounts of downed woody material and ladder fuels from sapling regeneration, which allow faster surface spread and increase the probability of fire spreading to the crown (Harvey, Donato, Romme, & Turner, 2014). However, more recently killed stands may retain more fallen needles on the forest floor which increase fine surface fuel loads (Simard, Romme, Griffin, & Turner, 2011). The effect of fuel structure on fire severity can also vary with weather conditions at the time of burning, such that extreme temperatures, humidity levels, and wind speed are more likely to result in faster fire spread and complete combustion of fuels (Bebi, Kulakowski, & Veblen, 2003; Harvey et al., 2014; Kulakowski, Veblen, & Bebi, 2003). Additionally, topographic factors influence fire behavior (e.g., fire intensity may be greater on steeper slopes or at high slope positions) (Bigler et al., 2003) and spatial patterns in vegetation recovery (e.g., faster recovery on north-facing slopes due to greater moisture availability, or at lower elevations due to warmer temperatures and longer growing season) (Ireland & Petropoulos, 2015; Petropoulos, Griffiths, & Kalivas, 2014).

Several recent studies have assessed impacts of beetle outbreaks on fire severity, and many have found no evidence of a conclusive link between disturbances (Agne, Woolley, & Fitzgerald, 2016; Andrus, Veblen, Harvey, & Hart, 2016; Bebi et al., 2003; Bigler et al., 2005; Harvey et al., 2014; Harvey, Donato, Romme, & Turner, 2013; Hicke et al., 2012; Kulakowski et al., 2003; Kulakowski & Veblen, 2007; Meigs, Zald, Campbell, Keeton, & Kennedy, 2016; Meng, Dennison, Huang, Moritz, & D'Antonio, 2015; Simard et al., 2011). However, previous methods of assessing fire severity may not thoroughly address all potential effects on ecosystem recovery. "Fire severity" is a somewhat ambiguous term in the literature (Keeley, 2009), and most beetle-wildfire interaction studies have primarily focused on impacts to canopy vegetation and aboveground cover immediately after the fire. These methods do not directly account for impacts to belowground soil properties which may have a longer-term effect on vegetation recovery, such as destruction of the seed bank, alteration of soil structure, loss of organic matter, or increases in hydrophobicity (Certini, 2005; DeBano, Neary, & Ffolliott, 1998). Because the primary effect of spruce beetle outbreaks on forest stands is to shift fuels from the canopy to the forest floor, it is possible that outbreaks may impact these properties without creating any significant effect on canopy mortality. Moreover, in forests characterized as having stand-replacing fire regimes where nearly all canopy trees are killed (Sibold et al., 2006), it is not clear how bark beetles could exacerbate mortality associated with wildfire.

To determine whether spruce beetle outbreak severity shows an effect on short-term vegetation recovery from fire, we used the Landsat-derived Normalized Difference Vegetation Index (NDVI) to assess understory vegetation recovery two years after a large, high-severity wildfire. NDVI provides an indicator of grass and herbaceous cover in early recovery stages (Hope, Tague, & Clark, 2007; Ireland & Petropoulos, 2015; Petropoulos et al., 2014). We chose

the West Fork Complex fire in southwestern Colorado, USA, as a case study because this event exemplifies an extreme wildfire event co-occurring with severe spruce beetle disturbance. The goals of the study were to 1) determine a Landsat-derived index which would allow us to estimate pre-fire spruce beetle severity using a multi-date image difference, and 2) determine the relationship of NDVI two years after the burn to pre-fire beetle outbreak severity, accounting for the influences of topography, weather at time of burning, and pre-disturbance NDVI.

Methods

Study Area

The West Fork Complex fire burned from June 5 – July 6, 2013. The complex consisted of three lightning-caused wildfires: Papoose (20,084 ha), West Fork (23,705 ha), and Windy Pass (573 ha). A total of over 44,000 hectares of subalpine spruce/fir forest in the Rio Grande National Forest, San Juan National Forest, and private lands northeast of Pagosa Springs, Colorado, were burned (Figure 2-1). Fire spread was driven by strong winds and high temperatures, causing up to 7,500 ha of spread in a single day. Firefighting management was minimal due to steep terrain and hazardous conditions presented by fire behavior in beetle-killed forest, and because the fire primarily burned areas designated as wilderness. The US Forest Service's Burned Area Emergency Response (BAER) program classified the majority of the burn as 'high-severity', indicating complete canopy mortality and loss of understory vegetation (US Forest Service Remote Sensing Applications Center, 2015).
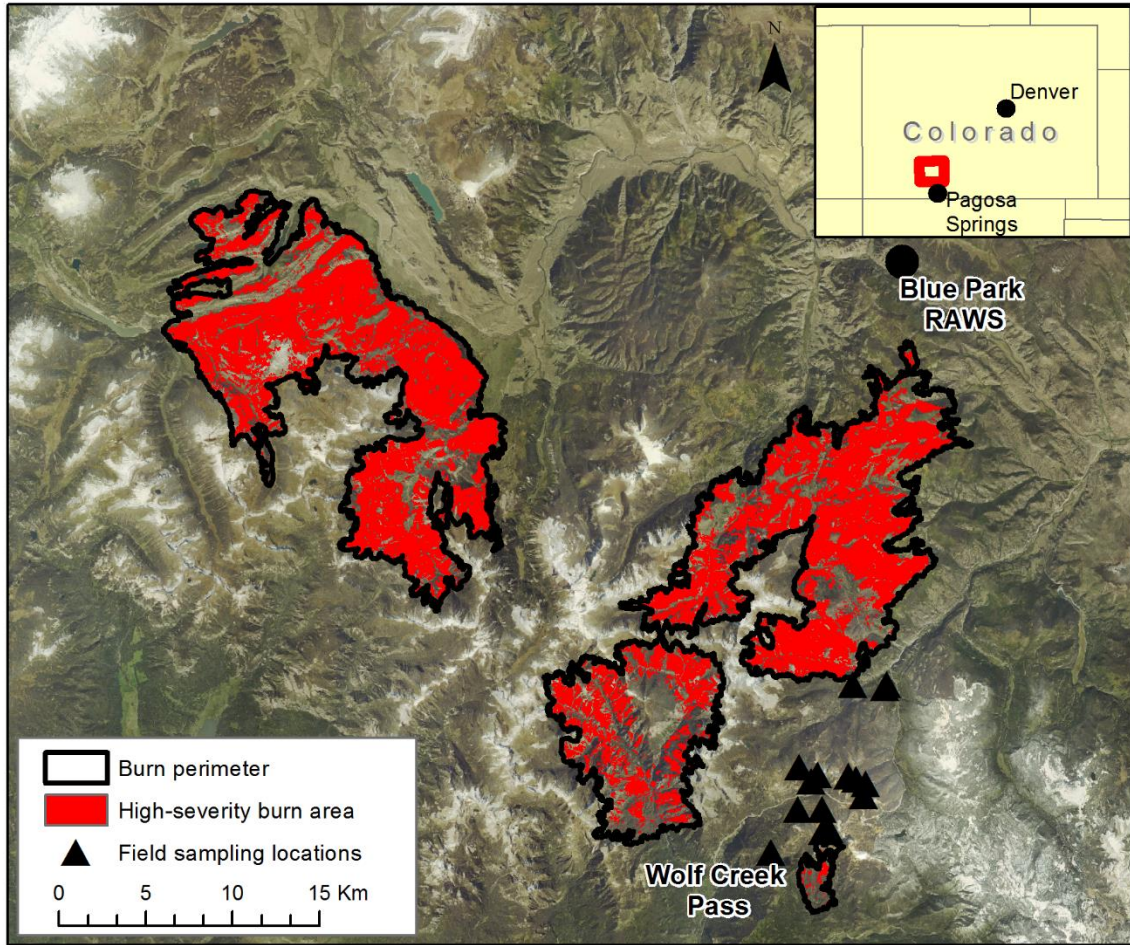
Figure 2-1. Overview map of the West Fork Complex burn area. Locations of the nearest weather station (Blue Park RAWS) and field sampling locations around Wolf Creek Pass are indicated. Area in red indicates burn area classified as 'high severity' by the US Forest Service Burned Area Emergency Response (BAER). Red square in inset shows the location of the study area within Colorado. Base imagery is from the USGS National Map server.

The burn area was dominated by *P. engelmannii* and *A. lasiocarpa*, with some lodgepole pine (*Pinus contorta*), quaking aspen (*Populus tremuloides*), and Douglas fir (*Pseudotsuga menziesii*). Elevation ranges from ~2700 – 4000 m a.s.l. with steep slopes and rugged topography. Mean temperatures range from -7.80° C in January to 11.50° C in July, and annual precipitation is 95 cm (PRISM climate data; http://www.prism.oregonstate.edu/). Significant spruce beetle activity within the burn perimeter was first detected by ADS in 2004 (data

available from US Forest Service; https://www.fs.usda.gov/detail/r2/forest-grasslandhealth/?cid=fsbdev3_041629). The outbreak was very severe, affecting more than 80% of spruce/fir forest within the study area by the time of the 2013 fire.

Landsat Image Processing

Processing steps for Landsat images and other explanatory variables are outlined in Figure 2-2. We acquired Landsat 7 ETM+ and Landsat 8 OLI (path 34, row 34) surface reflectance images collected in 2002, 2006, 2012, 2013, and 2015 (see Table 2-1 for image dates and sensor types). Images were pre-processed to surface reflectance using the Landsat Ecosystem Disturbance Adaptive Processing System (LEDAPS) (Masek et al., 2006). The 2002 image predated the earliest detection of spruce beetle mortality by ADS, and was assumed to represent undisturbed canopy conditions. Subsequent images represent distinct points in the disturbance history of the site: mid-beetle outbreak (2006), mid-beetle outbreak and immediately pre-fire (2012), immediately post-fire (2013), and following two years of post-fire recovery (2015). We selected cloud-free images representing growing-season conditions at each time point (August, or the latest available growing-season date for which a cloud-free image was available). The 2006 and 2012 images contained missing data areas due to Landsat 7's Scan Line Corrector Error, which accounted for ~5% of the study area. We excluded these missing data areas in the 2012 image from the final analysis.
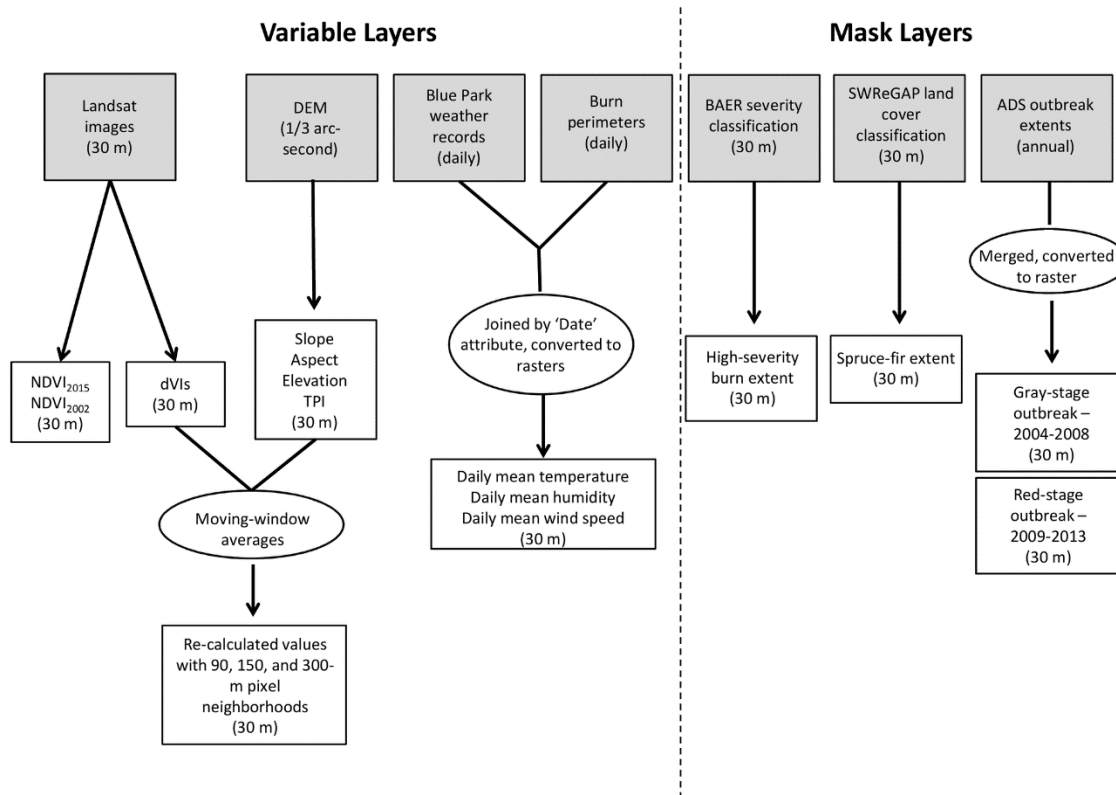
Figure 2-2. Processing steps used to derive model variable layers from data sources.

Table 2-1. Date and sensor type for Landsat scenes used in analysis.

Image	Sensor	Date
Pre-disturbance	L7 ETM+	August 10, 2002
Mid-beetle outbreak	L7 ETM+	June 18, 2006
Post-beetle outbreak, pre-fire	L7 ETM+	June 18, 2012
Immediately post-fire	L8 OLI	August 16, 2013
2 years post-fire	L8 OLI	August 06, 2015

Although the images were pre-processed to eliminate atmospheric biases between image dates, slight band differences between Landsat 7 ETM+ and Landsat 8 OLI may result in systematic biases between images collected with the different sensor types. In order to eliminate this bias when comparing images, we applied a normalization technique to the 2015 image using pseudo-invariant features (PIFs). We manually selected 40 PIFs as single pixels representing non-vegetative features where reflectance should be constant between image dates (such as bare soil above tree line, water bodies, and major roads). A linear regression calculation between each image band was used to adjust the 2015 image according to the method described by Schott et al. (Schott, Salvaggio, Volchok, 1988). In all cases the fit of the regression line used in band adjustment calculations was $R^2 \geq 0.86$.

Beetle Severity Indices

i.   Field Validation

We assessed the ability of Landsat-derived VIs to approximate spruce beetle severity using field measurements of beetle-caused spruce mortality. In August of 2015, we collected measurements in 58 unburned, beetle-affected spruce/fir plots within ~5 km of the West Fork Complex burn perimeter (see Figure 2-1). Fifteen sampling locations were chosen in ArcMap 10.0 (ESRI, 2010) to achieve a diverse representation of topographic characteristics, outbreak severities, and outbreak ages (determined by ADS). Including plots in different outbreak stages accounted for potential differences in spectral response caused by regeneration in older beetle-killed stands. Each sampling location consisted of a 180 m-long east-west transect with four 20 x 20 m evenly spaced sampling plots. In one transect we only established two plots, because spruce stands were surrounded by flat, wet subalpine fir-dominated site conditions which are uncharacteristic

28

of the total study area. Outbreak severities ranged from 0 - 100% beetle-caused mortality in overstory trees.

We used a handheld GPS to place plots within ~3 m of the center of a 2 x 2 Landsat pixel grid (60 x 60 m). We measured diameter at breast height (DBH) of all dead *P. engelmannii* trees with evidence of recent beetle activity within each 20 x 20 m plot area, and converted these measurements to total basal area. Basal area of beetle-killed trees within plot areas (400 m^2) was our selected metric of beetle outbreak severity, and was assumed to estimate total change in canopy cover from pre-outbreak to post-outbreak. Our metric of beetle severity is therefore an absolute value of beetle-killed *P. engelmannii* basal area per 400 m^2 (20 x 20 m plot area) rather than a percentage of total canopy. Standing dead trees with no evidence of beetle activity were small in diameter, and we assumed that these trees did not significantly affect the spectral changes resulting from beetle outbreak.

ii.   Vegetation Indices

We tested seven VIs which have been shown to respond to canopy disturbance: the Normalized Difference Moisture Index (NDMI; Gao, 1996; Wilson & Sader, 2002), Normalized Burn Ratio (NBR; Key & Benson, 1999; Meigs et al., 2011), Vegetation Condition Index (VCI; Havašová et al., 2015; Vogelmann, 1990), Moisture Stress Index (MSI; Havašová et al., 2015; Jakubauskas & Price, 2000), and two Disturbance Indices (DI and DI') based on the Tasseled Cap transformation (Crist & Cicone, 1984; Hais et al., 2009; Healey, Cohen, Zhiqiang, & Krankina, 2005; Liu, Liu, Huang, Liu, & Zhao, 2014). VIs were calculated using combinations of two or more Landsat bands (see Table 2-2 for index calculations).

Table 2-2. Equations used to calculate Landsat vegetation indices (VIs) used to approximate beetle severity.

Index	Equation
NDVI	(Near-infrared – Red)/(Near-infrared + Red)
NDMI	(Near-infrared – Mid-infrared)/(Near-infrared + Mid-infrared)
NBR	(Near-infrared – Thermal-infrared)/(Near-infrared + Thermal-infrared)
VCI	Thermal-infrared/Near-infrared
MSI	Mid-infrared/Near-infrared
DI	TCBright – (TCGreen + TCWet)*
DI'	TCWet - TCBright*

*Refers to Tasseled Cap Brightness, Greenness, and Wetness transformations of Landsat bands, rescaled according to the method described by Healey et al. [67].

For each VI, we calculated a multi-date image difference by subtracting 2002 pre-disturbance values from the 2015 value ($dVI = VI_{2015} – VI_{2002}$). We compared these image differences to field measurements of beetle-caused overstory mortality by calculating the means of dVI values extracted from the 2 x 2 (60 x 60 m) pixel grid area surrounding field plot centers. We used mean values to account for potential spatial inaccuracies in the GPS location of the plot and overlay with the Landsat grid. Relationships between dVIs and plot-level values of basal area of beetle-killed trees were assessed using ordinary least squares (OLS) regression. The dVI which yielded the highest OLS R^2 value was assumed to be the best indicator of beetle outbreak severity, and the difference in the selected index from 2002 to 2012 ($VI_{2012} – VI_{2002}$) was included as an explanatory variable in post-fire NDVI models.

Other Explanatory Variables

 i. Topography

    Topographic variables included slope, elevation, aspect, and topographic position index (TPI). TPI is a numeric indicator of slope position, with higher values representing locations closer to ridgetops and lower values representing valley bottoms (Wilson & Gallant, 2000). Aspect was transformed to relative 'northness' using the formula abs(aspect – 180), so that values range from 0-180 as aspect increases from south-facing to north-facing. All topographic predictor variables were derived from a 1/3 arc-second digital elevation model (DEM), resampled to a resolution of 30 m.

 ii. Weather

    NDVI models included variables accounting for daily weather conditions over the two-week burn period. This was done using daily burn perimeter maps, which we obtained from the USGS Geospatial Multi-agency Coordination (GeoMAC) Wildland Fire Support service (US Geological Survey, 2015a). Each of these daily burn areas was classified with the corresponding mean daily values for air temperature, humidity, and wind speed. Daily weather station data was obtained from the Blue Park Remote Automated Weather Station (RAWS; National Interagency Fire Center, 2015).

 iii. Outbreak Stage

    We determined outbreak stage using the earliest year of spruce beetle detection from ADS data. Using annual ADS extents for all years since 1994, we determined that 2004 was the earliest year when significant spruce beetle activity was mapped within the study area. Polygon areas with detection years 2004-2008 were classified as gray-stage,

while polygons with detection years 2009-2013 were classified as red-stage (Figure 2-3). These areal extent layers were used to clip explanatory variable areas to red and gray-stage locations. We examined red and gray-stage locations in separate models to determine how relationships between outbreak severity and vegetation recovery varied between outbreak stages.
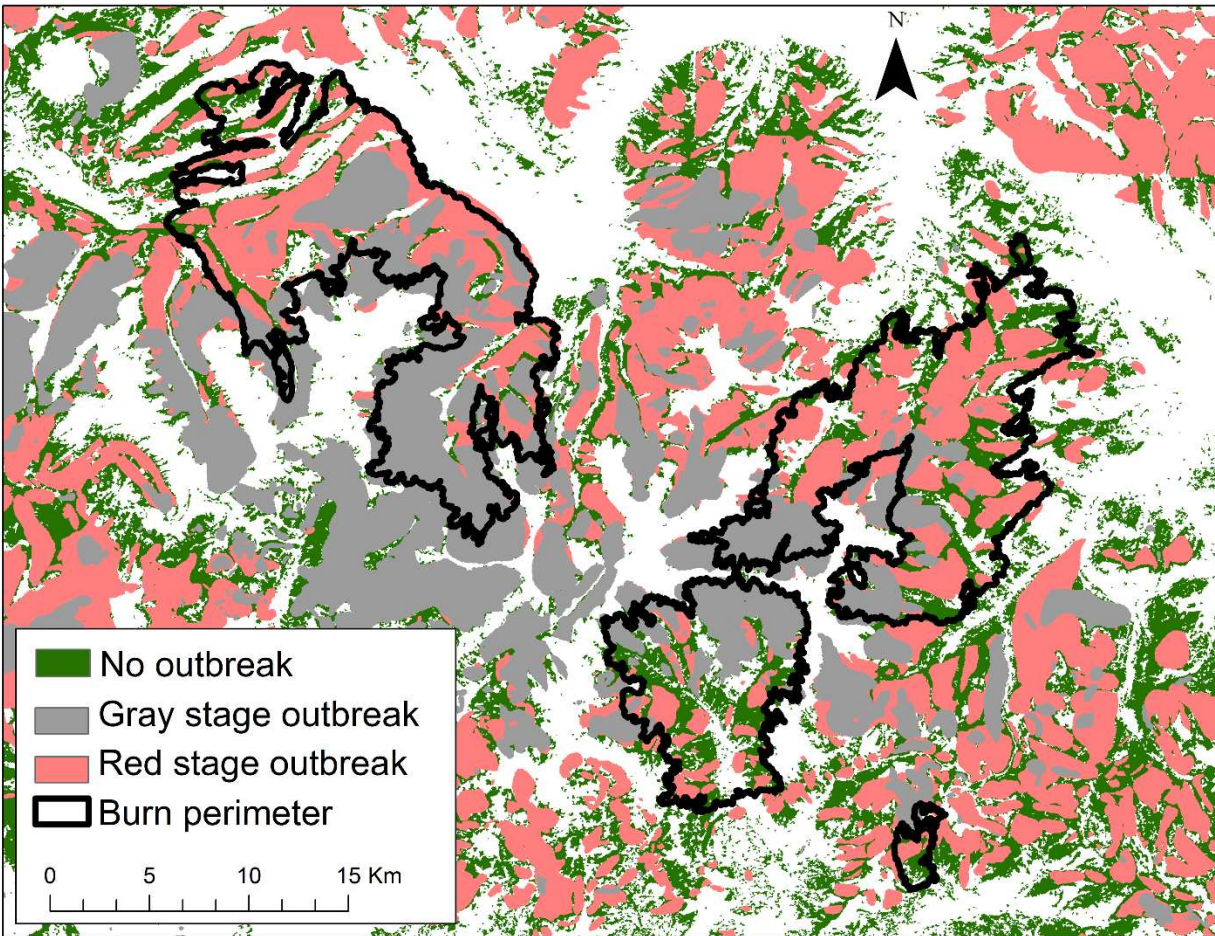
Figure 2-3. Extent of study area classified as red or gray-stage beetle outbreak in 2012. Green area depicts spruce/fir forest with no outbreak detected.

NDVI Models

Explanatory variable layers were clipped to areas of spruce/fir forest cover type which burned at high severity. The spruce/fir forest cover mask layer was derived from the Southwest

Regional Gap Assessment (SWReGAP) land cover classification (US Geological Survey, 2015b), using category labels which corresponded to subalpine spruce/fir forest type (Figure 2-3). The high severity mask layer was derived from a 4-level BAER classification product based on the Landsat-derived relativized change in Normalized Difference Burn Ratio (RdNBR; Figure 2-1). We generated a predictor variable matrix by sampling pixel values from clipped layers along a 60x60 m point lattice (sampling at every other pixel).

    i.   Sequential Autoregression

        The effects of spatial autocorrelation must be taken into account when assessing patterns in a contagious disturbance such as wildfire, because spatial dependence in either the response or the explanatory variables can violate assumptions of observation independence and inflate parameter values (Lennon, 2000; Wimberly, Cochrane, Baer, & Pabst, 2009). Variogram analysis revealed spatial autocorrelation in the NDVI layers for up to ~500 m of lag distance. We therefore modeled post-fire vegetation cover using spatial error sequential autoregressive models (SAR) to account for the effects of positive spatial autocorrelation in the data. The formula for the error SAR model is given by the equation

$$y = x\beta + \lambda W(y - x\beta) + \varepsilon$$

where y is the dependent variable (modeled with a gamma likelihood), x is a vector of predictor variables, β is a vector of coefficients, λ is the autoregressive coefficient, W is a spatial weights matrix, and ε is a random error term. All variables in x are assumed to be measured without error. We determined the spatial weights matrix W using the inverse distance of neighbors within 125 m of sample locations. All statistical analyses were

carried out in R 3.3.1 (R Core Development Team, 2013) using the 'spdep' package (Bivand, 2014).

ii.   Variable Scale

To further account for the spatially connected nature of wildfire, we considered how variable scale may affect relationships between vegetation recovery patterns and explanatory variables. Wildfire is a rapid-spreading, contagious process, and fire behavior is likely to be influenced by topographic and fuel characteristics over a broader area than that covered by a 30-m Landsat pixel. Because fire behavior influences the degree of fuel consumption and burning intensity across the landscape, and can ultimately influence patterns of vegetation recovery (Odion & Davis, 2000), we expect that spatial neighborhood effects influence the relationship of topographic and fuel variables to post-recovery NDVI assessed at 30-m resolution. We accounted for neighborhood effects of explanatory variables using square moving-window average functions on our topographic variables and beetle severity index, which implicitly accounts for fuel structure. This process generated new 30-m raster layers by calculating new values for each pixel using the averages of surrounding pixels within our selected window sizes of 90, 150, and 300 m (corresponding to 3x3, 5x5, and 10x10 pixel grids, respectively). We determined the most appropriate scale of analysis for each variable using univariate SAR models for each variable at each scale to predict $NDVI_{2015}$. The best-fitting model based on Akaike's Information Criterion (AIC) value was used to select the scale for each variable to be included in the final multivariate model. This scale selection process ensures that the explanatory power of each variable is maximized in the

final multivariate model (Falk, Miller, McKenzie, & Black, 2007; Parks, Parisien, & Miller, 2011).

    iii.   Multivariate Models

After determining the best-fitting scales for explanatory variables, we used a stepwise selection procedure to select a model from a full set of explanatory variables:

$$NDVI_{2015} \sim dVI + slope + northness + elevation + TPI \\ + mean\ air\ temp. + mean\ humidity + mean\ wind\ speed \\ + NDVI_{2002}$$

We selected the combination of variables that minimized AIC value for both the red and gray stage. Relative importance of each variable to the final model was determined by removing variables from the final selected model and calculating the change in AIC (ΔAIC).

Results

Beetle Severity Indices

R^2 values indicated that dNDMI was the index most strongly correlated to field-measured basal area of beetle-killed spruce (Table 2-3). The R^2 value of the OLS regression was 0.66, indicating a relatively strong correlation (Figure 2-4). Furthermore, visual inspection of spatial patterns in dNDMI at multiple time points showed that values were responsive to outbreaks detected by ADS (Figure 2-5). Although the magnitude of dNDMI values varies as a result of scale differences in the post-outbreak image, there were clear spatial patterns within images indicating that lower values of dNDMI (darker-colored areas in the right-hand column of Figure 2-5) correspond to known beetle outbreaks (areas detected by ADS; shaded orange in the left-hand column of Figure 2-5) at multiple time points. The close relationship between dNDMI and

field-measured spruce mortality, in addition to temporal trends of ADS detection, indicates that

dNDMI is a good proxy for beetle outbreak severity. dNDMI was therefore selected as a proxy

for beetle outbreak severity in NDVI models.

Table 2-3. R^2 values from OLS regression tests comparing changes in each vegetation index from 2002-2015 (dVIs) to the beetle-killed basal area of spruce in field plots measured in 2015.

Index	R^2
dNDMI	0.66
dDI	0.65
dVCI	0.62
dNBR	0.61
dNDVI	0.60
dMSI	0.60
dDI'	0.56
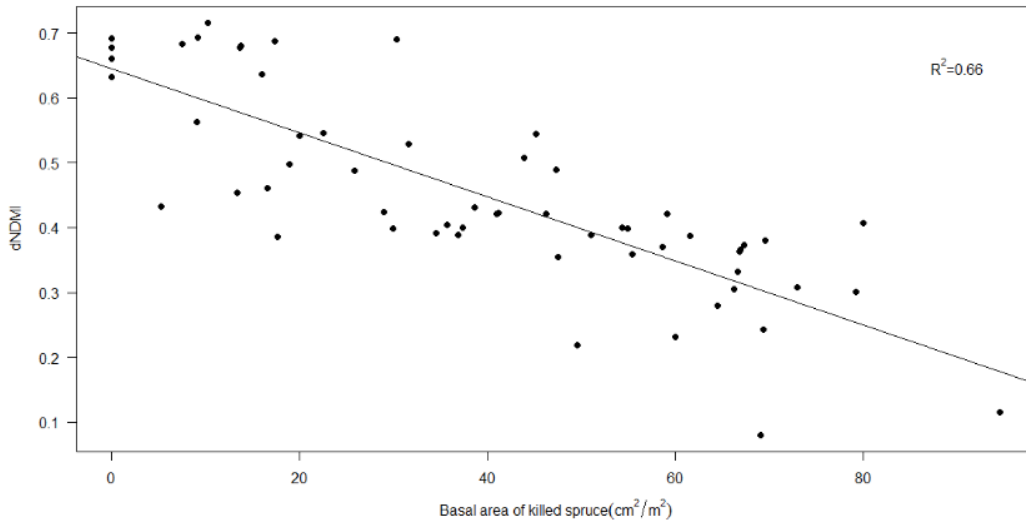
Figure 2-4. Relationship of observed basal area of killed *P. engelmannii* in 20 m × 20 m field plots to the mean change in Normalized Difference Moisture Index (NDMI) from 2002 to 2015 (dNDMI) for a 4x4 neighborhood of 30-m grid cells surrounding plot centers.
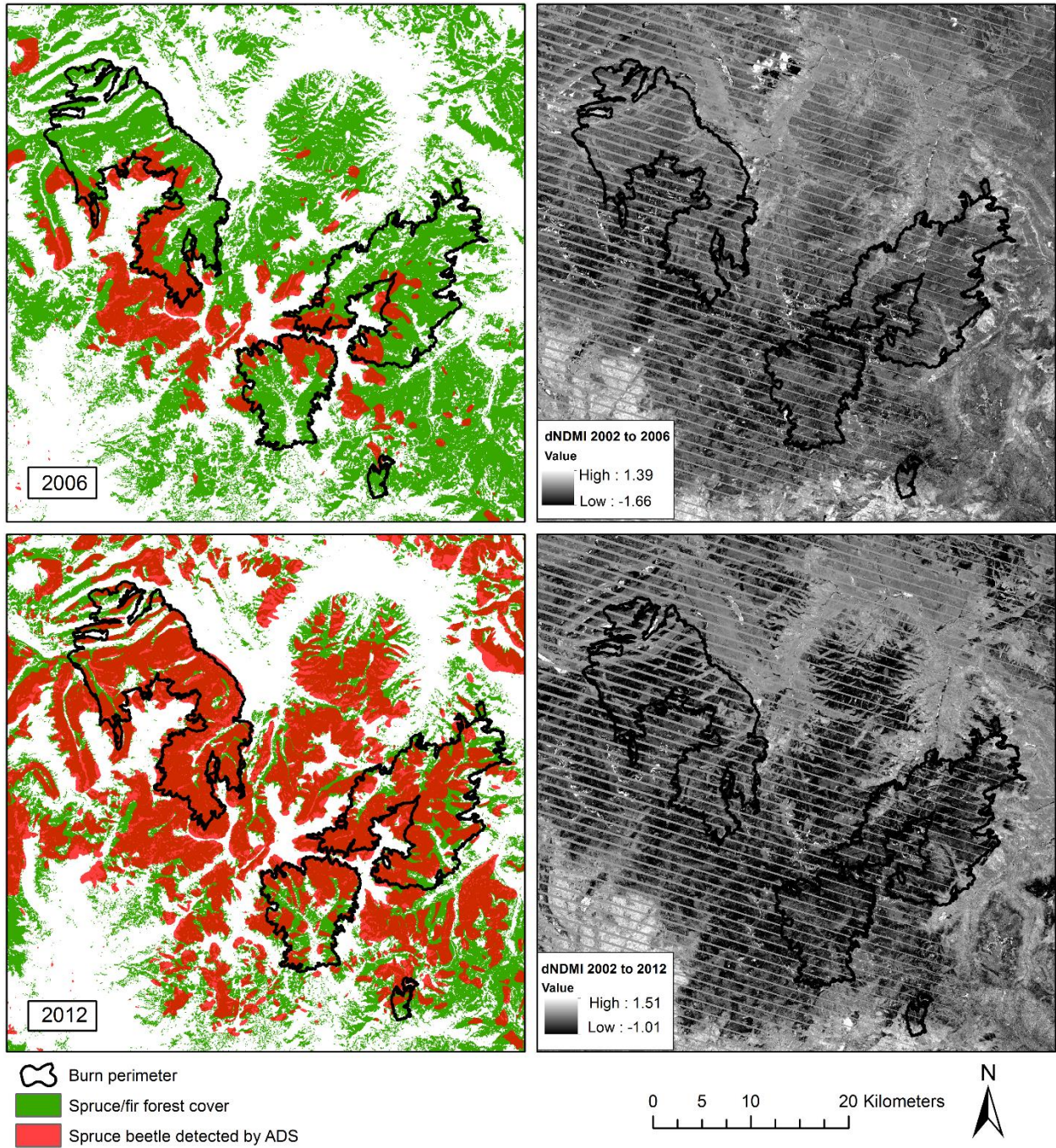
Figure 2-5. Comparison between spruce beetle outbreak extent detected by ADS from 2002 to the indicated year (left; ADS polygons shown in orange) and dNDMI (right). Top dNDMI = $NDMI_{2006} - NDMI_{2002}$; bottom dNDMI = $NDMI_{2012} - NDMI_{2002}$. Color scale for dNDMI is based on standard deviations within images.

NDVI Recovery

Comparison of NDVI$_{2013}$ and NDVI$_{2015}$ to NDVI$_{2002}$ reveals that NDVI has increased toward pre-disturbance values in the two years following wildfire, compared to relatively homogenous values in 2013 (Figure 2-6). However, NDVI$_{2015}$ values are generally lower than their corresponding 2002 values. The pattern of recovery is heterogeneous, with some areas in the southern portions of the West Fork and Papoose burn areas showing slower recovery compared to the rest of the burn area (Figure 2-7).
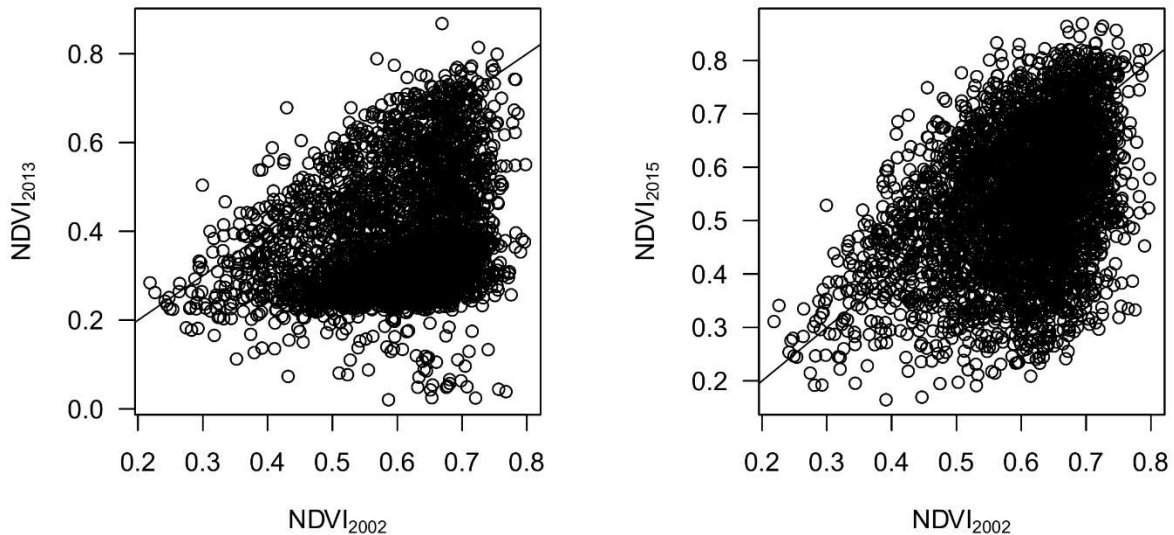
Figure 2-6. Pattern in Landsat-derived NDVI for locations in the West Fork Complex burn area that burned at high severity, compared to undisturbed 2002 conditions. NDVI$_{2013}$ is the growing-season NDVI immediately after the fire (August, 2013) and NDVI$_{2015}$ is the NDVI two years after the fire (August, 2015). Solid line represents a 1:1 relationship.
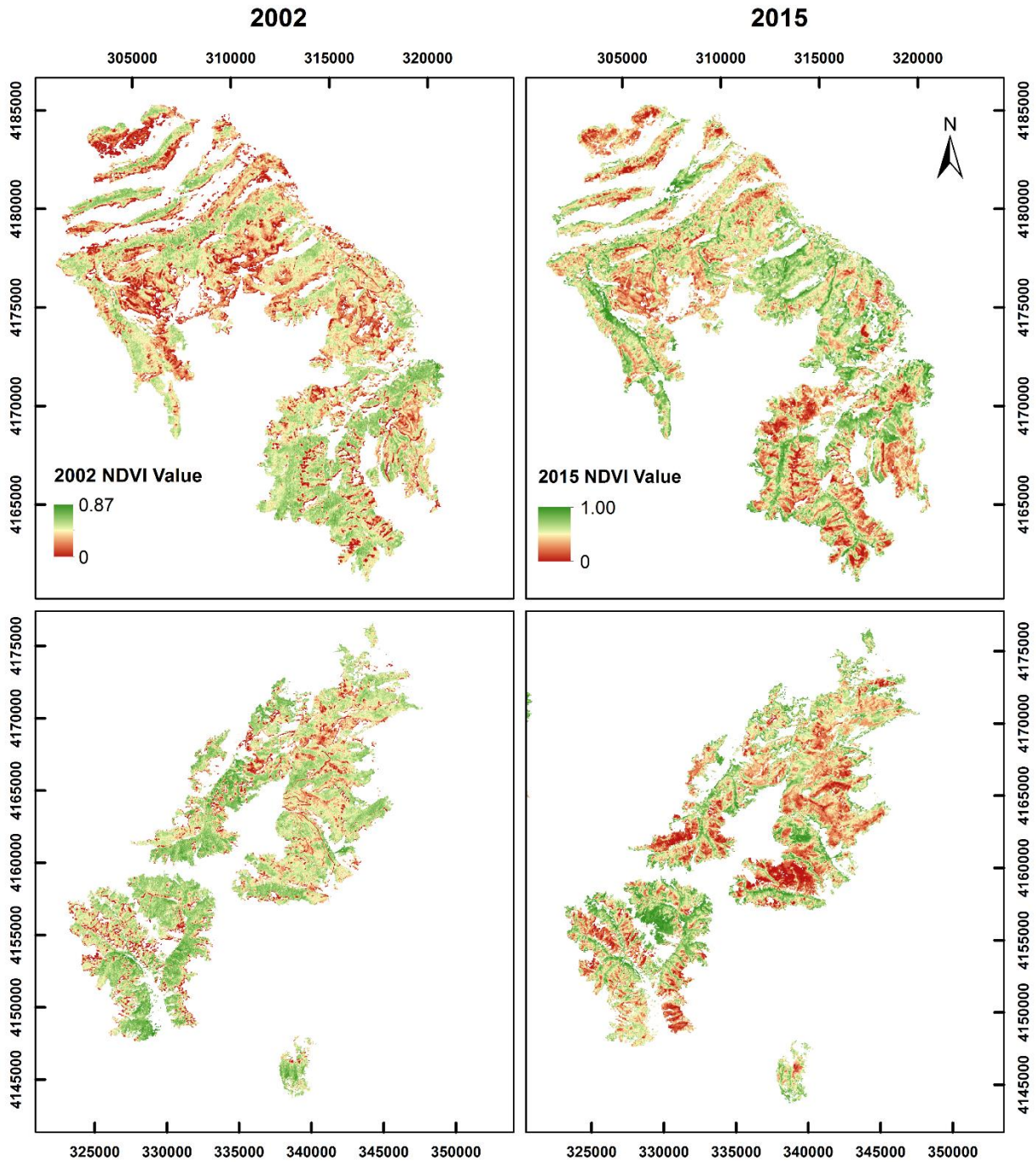
Figure 2-7. Growing-season NDVI for the Papoose burn area (top row), and West Fork and Windy Pass burn areas (bottom row). NDVI images are clipped to spruce/fir forest cover type. Left images are from August, 2002 (pre-disturbance) and right images are from August, 2015 (2 years post-fire recovery).

SAR Model Results

    i.   Univariate

Univariate relationships between explanatory variables and $NDVI_{2015}$ determined by SAR are summarized in Table 2-4. These results present the best-fitting scales for all variables where a moving-window average calculation was applied. The relationship of vegetation cover to dNDMI is highly significant ($p < 0.0001$) in both the red-stage and gray-stage sample subset, but the slopes of the relationships are opposite. dNDMI is positively correlated to $NDVI_{2015}$ in red-stage models, indicating that lower values of dNDMI (indicating greater mortality from spruce beetle outbreak) are correlated with lower vegetation cover in 2015. This relationship is negative in gray-stage models.

$NDVI_{2002}$ is the strongest single-variable predictor in both red and gray-stage models, based on AIC value. All topographic variables are significant in both subsets, while weather variables are not consistently significant. Topographic variables were selected at greater spatial scales, either at 150 m or 300 m. In the gray-stage subset, all topographic variables predicted $NDVI_{2015}$ more accurately than dNDMI. In the red-stage subset, dNDMI was a more accurate predictor than either slope or TPI, or any weather variable.

Table 2-4. Results of univariate SAR models predicting 2015 NDVI for point locations in gray-stage and red-stage pre-fire spruce beetle outbreak, with the best-performing scale of moving-window averages selected for dNDMI, slope, northness, and TPI. Variables in bold are significant within a 95% confidence interval. Models are ranked by AIC value.

Gray-stage:

Variable	β	Std. error	AIC	p
$NDVI_{2002}$	**0.48**	**8.9×10^{-3}**	**-51473**	**<0.0001**
northness150	**6.9×10^{-4}**	**3.7×10^{-5}**	**-49056**	**<0.0001**
elevation	**-3.0×10^{-4}**	**1.6×10^{-5}**	**-49047**	**<0.0001**
slope300	**-3.7×10^{-3}**	**3.3×10^{-4}**	**-48844**	**<0.0001**
TPI300	**-0.16**	**0.033**	**-48738**	**<0.0001**
dNDMI90	**-0.068**	**0.015**	**-48736**	**<0.0001**
air temperature	**2.6×10^{-3}**	**1.0×10^{-3}**	**-48723**	**<0.05**
humidity	-2.5×10^{-4}	1.8×10^{-4}	-48718	0.16
wind speed	5.8×10^{-4}	2.5×10^{-3}	-48716	0.82

Red-stage:

Variable	β	Std. error	AIC	p
2002 NDVI	**0.49**	**7.8×10^{-3}**	**-59878**	**<0.0001**
elevation	**-2.3×10^{-4}**	**1.1×10^{-5}**	**-56696**	**<0.0001**
northness150	**3.5×10^{-4}**	**3.3×10^{-5}**	**-56410**	**<0.0001**
TPI300	**-0.27**	**0.028**	**-56397**	**<0.0001**
dNDMI300	**0.24**	**0.028**	**-56373**	**<0.0001**
slope150	**-7.7×10^{-4}**	**1.6×10^{-4}**	**-56323**	**<0.0001**
humidity	**5.0×10^{-4}**	**1.9×10^{-4}**	**-56306**	**<0.01**
air temperature	8.6×10^{-4}	7.5×10^{-4}	-56301	0.25
wind speed	-1.2×10^{-3}	2.1×10^{-3}	-56300	0.56

ii.　　　Multivariate

In both gray-stage and red-stage models, including dNDMI as a predictor

improved model fit according to AIC. The best-fitting models selected from a full set of

variables are given in Table 2-5. The best-fitting model for gray-stage locations explained

71% of variance in $NDVI_{2015}$, and included all explanatory variables except air

temperature and wind speed. The top-performing model for red-stage locations explained

68% of variance in $NDVI_{2015}$ and included all explanatory variables except humidity and

wind speed. Variable importance calculations showed that $NDVI_{2002}$ is by far the most

important variable in both red and gray-stage models (Figure 2-8). dNDMI had a higher

importance value in both models than any other explanatory variables.

Table 2-5. Top-performing multivariate SAR models predicting 2015 NDVI for point
locations in red-stage and gray-stage of spruce beetle outbreak prior to fire. R^2 values
give the overall fit between predictions and observations.

Stage	Best-fitting model	R^2
Gray-stage	$NDVI_{2015}$ ~ $NDVI_{2002}$ + dNDMI90 + slope300 + northness150 + TPI300 + elevation + humidity	0.71
Red-stage	$NDVI_{2002}$ + dNDMI300 + slope150 + northness150 + TPI300 + elevation + air temp.	0.68
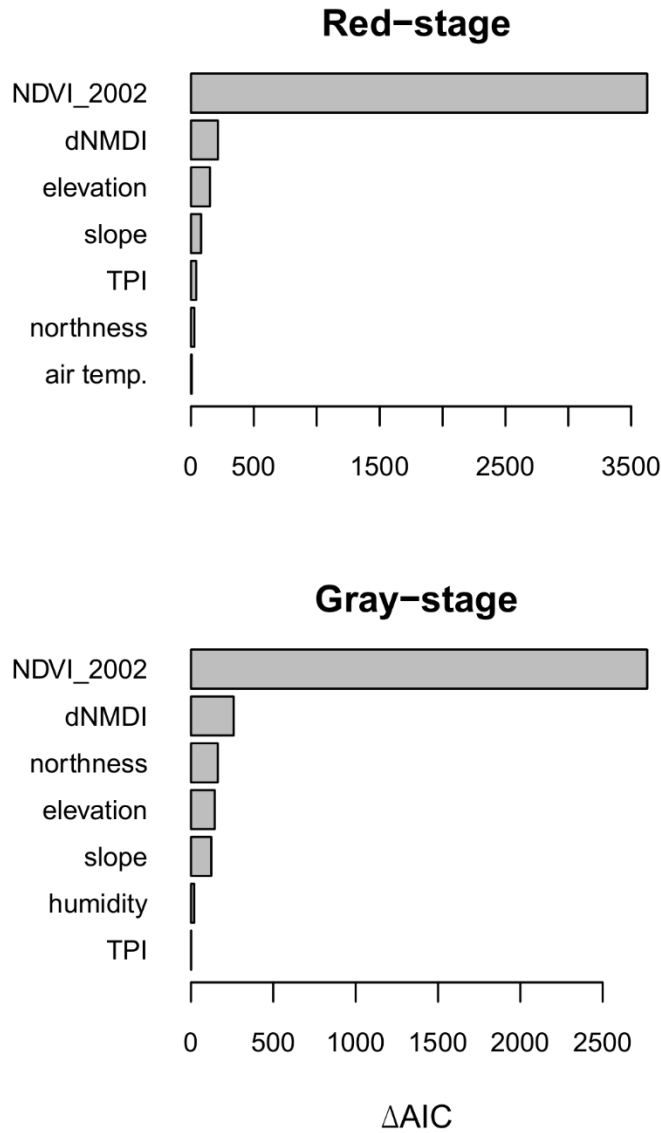
Figure 2-8. Variable importance plots for the best-fitting multivariate models for red and gray-stage outbreak locations. Variable importance is determined by the ΔAIC between the full model and model with the indicated variable removed.

Parameter estimates for the top-performing multivariate SAR models revealed variable relationships similar to those determined by univariate models (Table 2-6). dNDMI is highly significant (p <0.0001) and exhibits a positive relationship to $NDVI_{2015}$ in both gray-stage and red-stage models, but $NDVI_{2002}$ is the strongest predictor in both model subsets. Topographic variables are also significant predictors in all models, with

43

slope, elevation, and TPI exhibiting negative correlations with $NDVI_{2015}$ while northness exhibits a positive correlation. Humidity is negatively correlated with $NDVI_{2015}$ in the gray-stage model while air temperature is negatively correlated with $NDVI_{2015}$ in the red-stage model. All signs of variable relationships are consistent between gray-stage and red-stage models. The parameter estimate for dNDMI is greater in magnitude in the top-performing red-stage model ($\beta = 0.40 \pm 0.027$) than in the top-performing gray-stage model ($\beta = 0.25 \pm 0.015$), indicating that dNDMI has a greater influence on $NDVI_{2015}$ in the red-stage model.

Table 2-6. Parameter estimates, standard errors, and significance values for top-performing multivariate SAR models predicting 2015 NDVI. Variables in bold are significant within a 95% confidence interval.

Gray-stage:

Variable	β	Std. Error	p-value
dNDMI90	**0.25**	**0.015**	**<0.0001**
$NDVI_{2002}$	**0.52**	**9.5×10^{-3}**	**<0.0001**
slope300	**-3.4×10^{-3}**	**3.0×10^{-4}**	**<0.0001**
northness150	**4.5×10^{-4}**	**3.5×10^{-5}**	**<0.0001**
elevation	**-1.9×10^{-4}**	**1.6×10^{-5}**	**<0.0001**
TPI300	**-0.065**	**0.031**	**<0.05**
humidity	**-7.4×10^{-4}**	**1.6×10^{-4}**	**<0.0001**

Red-stage:

Variable	β	Std.Error	p-value
dNDMI300	**0.40**	**0.027**	**<0.0001**
$NDVI_{2002}$	**0.49**	**7.9×10^{-3}**	**<0.0001**
slope150	**-1.3×10^{-3}**	**1.4×10^{-4}**	**<0.0001**
northness150	**1.8×10^{-4}**	**3.3×10^{-5}**	**<0.0001**

elevation	**-1.4×10^{-4}**	**1.2×10^{-5}**	**<0.0001**
TPI300	**-0.17**	**0.026**	**<0.0001**
air temperature	**-1.9×10^{-3}**	**6.6×10^{-4}**	**<0.01**

Discussion

Because dNDMI is negatively correlated with spruce beetle outbreak severity, the results of multivariate SAR models indicate that recovery of NDVI in the West Fork Complex fire was negatively correlated with the severity of spruce beetle outbreaks which occurred in the decade or so prior to the fire. The direction of the univariate relationship between dNDMI and $NDVI_{2015}$ matched that of the multivariate relationship in red-stage models but was reversed in gray-stage models, possibly indicating that the compounded disturbance effect becomes less significant with increasing time between disturbances. However, when all relevant variables were accounted for there was a consistently negative relationship between beetle outbreak severity and $NDVI_{2015}$ in both stages. Although dNDMI did not explain $NDVI_{2015}$ as strongly as $NDVI_{2002}$ (according to ΔAIC), the significant correlation between the indicator of beetle severity and $NDVI_{2015}$ suggests the presence of a compounded disturbance effect on the rate and trajectory of vegetation recovery.

Our results add a new dimension of understanding to those of recent studies which have found no correlation between outbreak severity and subsequent fire severity when accounting for differences in outbreak stage, burning conditions, or topography (Hicke et al., 2012). Most of these studies have assessed fire severity by measuring immediate post-fire impacts to aboveground vegetation, using remotely sensed indices such as dNBR or RdNBR (Andrus et al., 2016; Bigler et al., 2005; Harvey et al., 2013; Meigs et al., 2016; Meng et al., 2015) or field-based metrics such as scorch height, percent surface char, or percent overstory mortality (Andrus

45

et al., 2016; Harvey et al, 2013; Harvey et al., 2014). We focused on the effects of high-severity fire only, which made up a majority of the West Fork Complex burn area. Previous studies have addressed whether there is a linked interaction between beetle outbreaks and the impact of fire on existing vegetation, but may not fully address all mechanisms of compounded interactions on vegetation recovery (see Buma [2015] for a review of linked and compound disturbance). We propose that a significant negative relationship between beetle outbreak severity and vegetation recovery was observed in the West Fork Complex because the pre-fire beetle outbreak may have played a significant role in fire behavior at the soil surface; an effect which has not been thoroughly explored by previous beetle-wildfire interaction studies.

This difference in linked vs. compounded disturbance effects can be seen when comparing the results of our study to the findings of Andrus et al. (2016), who also examined beetle-wildfire interactions in the West Fork Complex. That study found no effect of spruce beetle outbreak on canopy tree mortality, percent surface char, or RdNBR immediately after the fire. Although those results provide important insights into the effect of spruce beetle outbreaks on fire behavior and canopy mortality, these metrics of fire severity may not account for ecologically important impacts to chemical properties of soils, vegetative seed banks, or resprouting roots. Moreover, remotely sensed metrics based on differences between pre-fire and post-fire imagery may underestimate fire severity if greenness in the pre-fire imagery is reduced by a severe beetle outbreak (Falk et al., 2007). This may be a reason why previous studies have found a consistently negative correlation between bark beetle outbreaks and RdNBR in subsequent fires (Meigs et al., 2016; Meng et al., 2015).

Effects of spruce beetle outbreak on regeneration processes may be a more significant ecological impact than effects to canopy loss, due to the typical high severity of fires in

subalpine forests. High canopy mortality is expected in subalpine systems because climatic conditions typically make fires infrequent, and the long interval between fire results in dense fuel stocking (Sibold et al., 2006). *P. engelmannii* and *A. lasiocarpa* are shade-tolerant species, meaning that mature stands become stocked with ladder fuels which incur a high probability of active crown fire (Schoennagel et al., 2004). They are also thin-barked species, and mortality can be high from low-intensity surface fire alone (Bessie & Johnson, 1995; McCarley et al., 2017). Because we expect subalpine fires to be stand-replacing regardless of beetle-caused changes to canopy structure (Ryan & Reinhardt, 1988), it is important to consider other mechanisms by which multiple disturbances may interact to produce compounded effects. If beetle outbreaks are significantly increasing surface fuel loads, this may explain impacts on vegetation recovery resulting from increased heat released by burning at the soil surface (DeRose & Long, 2009).

dNDMI as an Indicator of Beetle Severity

Past studies have assessed pre-fire beetle mortality in the field after fire has occurred, which requires close examination of all trees within a field plot for larval galleries beneath the bark. This is a time-consuming process, and may also be prone to underestimation of mortality when the bark and wood surface have been damaged by fire (Assal et al., 2014). Differencing and single-date classification of NDMI time series have proven to be effective methods for detecting and quantifying outbreaks of North American and European spruce beetle (Hais et al., 2009; Havašová et al., 2015; Meddens et al., 2013), mountain pine beetle (Goodwin et al., 2008; Walter & Platt, 2013), and canopy gaps due to disturbance in coniferous forests (Assal et al., 2016). In our study, dNDMI was a reliable estimator of spruce mortality from bark beetles, and other dVIs also correlated well with field measurements. Remote sensing estimates likely

provide a more objective measurement of pre-fire beetle disturbance compared to field measurements taken after fires have occurred.

We observed that spruce cover was high in most of our study area and that high abundance of subalpine fir was restricted to flat valley bottoms, which made up a low proportion of the total area. Our severity quantification method was therefore focused on spruce-dominated stands (where spruce made up >50% of total basal area). Consideration should be taken in applying the dNDMI severity quantification method to areas with more mixed forest communities, as it is possible that growth in secondary species between image dates could cause dNDMI to underestimate spruce mortality (Hart & Veblen, 2015). In our study area these areas included stands classified as aspen woodlands, which represented ~8% of the total burn area and were not included in models.

NDVI and Vegetation Recovery

NDVI tends to increase rapidly in the two years following fire occurrence (Ireland & Petropoulos, 2015; Petropoulos et al., 2014). NDVI in the West Fork Complex also increased rapidly, and overall NDVI values are correlated with pre-disturbance values. Post-fire vegetation is characterized by grass and forb understory rather than by the pre-fire forest canopy, but because NDVI is sensitive to understory vegetation (Buma, 2012), the importance of $NDVI_{2002}$ in models of $NDVI_{2015}$ indicates that some factors relating to site greenness are unaltered by fire. Differences between pre-disturbance and post-disturbance NDVI may be the result of alteration of soils and microclimate which affect the ability of understory species to re-establish.

It is important to note that understory recovery is not necessarily an indicator of overstory regeneration (Buma, 2012). However, rates of understory succession have been shown to affect

forest seedling regrowth, community resilience, and recovery of soil properties. For example, reduced cover following high-severity wildfire in subalpine forests has been found to correlate with reduced soil nitrogen, which could have long-term impacts on seedling establishment (Turner, Romme, Smithwick, Tinker, & Zhu, 2011). Reduced recruitment of early successional species can also be an indicator of severely altered soil properties following fire (Dzwonko, Loster, & Gawrónski, 2015). Given the high severity of the West Fork Complex, it is likely that altering of soil properties will influence variation in overall vegetation recovery across the burn area. However, future differences in vegetation composition will be also determined by climate, seed dispersal, topography, and future disturbance (Healey et al., 2006).

Mediating Factors in the Relationship Between Beetle Severity and Vegetation Recovery

Comparing univariate to multivariate relationships between beetle outbreak severity and NDVI$_{2015}$ in red and gray stages reveals that in the gray stage, the effect of beetle severity is mediated to a greater extent by other explanatory variables. This difference may indicate that the effect of beetle-caused canopy mortality on fire impacts diminishes over time. This may be due to the fact that fine surface fuels decompose or are lost from the site after the initial outbreak [10]. Canopy loss from spruce beetle outbreak also allows for the recruitment of grass, forbs, and shrubs in the understory, which may be able to germinate or resprout rapidly after the fire (Aplet, Laven, & Smith, 1988; Hicke et al., 2012).

Multivariate models indicated that outbreak severity has a significant influence on post-fire recovery, but did not have a greater effect than topography or pre-disturbance NDVI. Topography is important in influencing fire behavior and micro-climate conditions which can promote or impede vegetation recovery (Meng et al., 2018; Prichard & Kennedy, 2014). The influence of topographic variables in multivariate models was expected, given results of previous

NDVI recovery studies (Ireland & Petropoulos, 2015; Petropoulos et al., 2014). The selection of topographic variables at coarser spatial scales was also expected, given that fire spread is rapid and is unlikely to respond to topographic variation over fine scales, and that vegetation recovery is likely to be somewhat homogenous within small areas with similar species compositions.

Weather within daily burn perimeters did not play a significant role in predicting NDVI recovery in our models. This result is not unexpected due to the coarse resolution of the data, where the entirety of a daily burn area was attributed with a single value of mean air temperature, humidity, and wind speed. Weather factors at the time of burning certainly play a role in the spread of fire and consumption of vegetation and litter, but in this study weather did not appear to have a strongly significant influence on soil alteration and post-fire recovery. This may be due to the coarse scale of weather data applied to daily burn extents, or because the majority of the study area burned under extreme conditions beyond a threshold where weather may have become more significant.

Management Implications

Warming climates are resulting in a shift toward large, high-impact wildfires occurring at greater frequency throughout western North America (Westerling, Hidalgo, Cayan, & Swetnam, 2006), and the question of whether bark beetles and wildfires produce compounded effects has important implications for managing to promote ecosystem resilience (Jenkins, Page, Hebertson, & Alexander, 2012). Salvage logging has been proposed to mitigate the effects of beetle disturbance and fuel loading on high-severity wildfire. Our results suggest that increased severity of beetle outbreak can inhibit short-term post-fire vegetation recovery, which may be caused by accumulation of surface fuels. This mechanism may suggest that treatments to reduce surface fuels can promote ecosystem resilience from fire. However, these activities pose a risk toward

altering recovery dynamics and facilitating future species composition shifts (Jonášová & Prach, 2008), and may reduce long-term carbon storage in forests (Donato, Simard, Romme, Harvey, & Turner, 2013). Two additional issues suggest that salvage logging would not mitigate the compounded impacts of beetles and wildfire. First, because salvage logging is focused on the removal of dead trees in contrast to fuels on the forest floor, it would not be expected to alter beetle-fire implications for fire characteristics at the soil level. Second, the short period of time in which surface fuels increase the ecological consequences of fire and the highly random nature of wildfires in time and space, implies that salvage logging with the goal of averting the impacts of beetle-wildfire interactions is not a logical management action. Nonetheless, salvage prescriptions have the potential to contribute to other land management objectives in addition to timber production. For example, salvage prescriptions located close to communities in the wildland-urban interface may act as fire breaks and contribute to community and fire fighter safety, and give fire managers confidence in allowing some natural fires to burn.

Impacts of severe beetle outbreak on vegetation recovery also create additional need for enhanced post-fire restoration efforts in areas where outbreak was known to have occurred prior to burning. Our model results indicate that these efforts should prioritize high-elevation, steep, south-facing slopes, as these topographic factors also show a significant effect on vegetation recovery. Restoration of ground vegetation mitigates flooding hazards, prevents soil erosion, and mitigates rising soil temperatures and evapotranspiration potential (Cawson, Sheridan, Smith, & Lane, 2013). Facilitating understory vegetation recovery may therefore prove beneficial for preventing drastic ecological change in severely burned landscapes affected by severe spruce beetle outbreaks.

Conclusions

Although many studies have tried to determine whether bark beetles lead to larger, more frequent, or more severe wildfires, there have been a number of limitations to determining the true ecological impacts of these overlapping disturbances. Our study quantified pre-fire beetle impacts using the Landsat-derived dNDMI, which likely provides a more accurate measure of beetle severity compared to studies focused on post-fire field measurements. We also used Landsat-based measurements of NDVI recovery to address how beetle-fire interactions may result in compounded effects on surface fuels and soil recovery, and found more conclusive evidence supporting a compounded disturbance interaction compared to studies which have assessed fire severity as a metric of canopy mortality. Future research should focus on long-term examinations of recovery dynamics following wildfires in beetle-killed forests, which will be important for improving understanding of how compounded disturbance interactions from bark beetles and wildfire will affect future forest communities. Additionally, future high-severity fires in beetle-killed spruce forests will need to be studied to determine whether the compounded effects observed in the West Fork Complex are consistent across geographic areas. Although many recent studies have concluded that there is no evidence of a link between beetle outbreaks and increased fire severity, our results indicate that the combined disturbances may result in compounded effects on vegetation recovery.

LITERATURE CITED

Agee, J.K. (1998). The landscape ecology of western forest fire regimes. *Northwest Science, 72*, 24.

Agee, J.K., & Skinner, C.N. (2005). Basic principles of forest fuel reduction treatments. *Forest Ecology and Management, 211*(1), 83-96.

Agne, M.C., Woolley, T., & Fitzgerald, S. (2016). Fire severity and cumulative disturbance effects in the post-mountain pine beetle lodgepole pine forests of the Pole Creek Fire. *Forest Ecology and Management, 366*, 73-86.

Andrus, R.A., Veblen, T.T., Harvey, B.J., & Hart, S.J. (2016). Fire severity unaffected by spruce beetle outbreak in spruce-fir forests in southwestern Colorado. *Ecological Applications, 26*(3), 700-711.

Aplet, G.H., Laven, R.D., & Smith, F.W. (1988). Patterns of community dynamics in Colorado Engelmann spruce-subalpine fir forests. *Ecology, 69*(2), 312-319.

Arno, S.F. (1980). Forest fire history in the northern Rockies. *Journal of Forestry, 78*(8), 460-465.

Assal, T.J., Anderson, P.J., & Sibold, J. (2016). Spatial and temporal trends of drought effects in a heterogeneous semi-arid forest ecosystem. *Forest Ecology and Management, 365*, 137-151.

Assal, T.J., Sibold, J., & Reich, R. (2014). Modeling a historical mountain pine beetle outbreak using Landsat MSS and multiple lines of evidence. *Remote Sensing of Environment, 155*, 275-288.

Bebi, P., Kulakowski, D., & Veblen, T.T. (2003). Interactions between fire and spruce beetles in a subalpine Rocky Mountain forest landscape. *Ecology, 84*(2), 362-371.

Bentz, B.J., Logan, J., MacMahon, J., Allen, C.D., Ayres, M., Berg, E., et al. (2009). Bark beetle ecology and biology. In: Bentz B (ed.) *Bark beetle outbreaks in western North America: Causes and consequences: Bark Beetle Symposium, 15-18 November 2005, Snowbird, Utah*. Salt Lake City: University of Utah Press, 6-15.

Bentz, B.J., Régnière, J., Fettig, C.J., Hansen, E.M., Hayes, J.L., Hicke, J.A., et al. (2010). Climate change and bark beetles of the western United States and Canada: direct and indirect effects. *BioScience, 60*(8), 602-613.

Bessie, W.C., & Johnson, E.A. (1995). The relative importance of fuels and weather on fire behavior in subalpine forests. *Ecology, 76*(3), 747-762.

Bigler, C., Kulakowski, D., & Veblen, T.T. (2005). Multiple disturbance interactions and drought influence fire severity in Rocky Mountain subalpine forests. *Ecology, 86*(11), 3018-3029.

Bivand, R. (2014). spdep: Spatial dependence: weighting schemes, statistics and models [software]. R package version 0.5-71.

Buma, B. (2012). Evaluating the utility and seasonality of NDVI values for assessing post-disturbance recovery in a subalpine forest. *Environmental Monitoring and Assessment, 184*(6), 3849-3860.

Buma, B. (2015). Disturbance interactions: characterization, prediction, and the potential for cascading effects. *Ecosphere, 6*(4), 1-5.

Cawson, J.G., Sheridan, G.J., Smith, H.G., & Lane, P.N. (2013). Effects of fire severity and burn patchiness on hillslope-scale surface runoff, erosion and hydrologic connectivity in a prescribed burn. *Forest Ecology and Management, 310*, 219-233.

Certini, G. (2005). Effects of fire on properties of forest soils: a review. *Oecologia, 143*(1), 1-10.

Cohen, W.B., Yang, Z., Stehman, S.V., Schroeder, T.A., Bell, D.M., Masek, J.G., et al. (2016). Forest disturbance across the conterminous United States from 1985–2012: The emerging dominance of forest decline. *Forest Ecology and Management, 360*, 242-252.

Collins, B.J., Rhoades, C.C., Hubbard, R.M., & Battaglia, M.A. (2011). Tree regeneration and future stand development after bark beetle infestation and harvesting in Colorado lodgepole pine stands. *Forest Ecology and Management, 261*(11), 2168-2175.

Crist, E.P., & Cicone, R.C. (1984). A physically-based transformation of Thematic Mapper data – The TM Tasseled Cap. *IEEE Transactions on Geoscience and Remote Sensing, 3*, 256-263.

Dale, V.H., Joyce, L.A., McNulty, S., Neilson, R.P., Ayres, M.P., Flannigan, M.D., et al. (2001). Climate change and forest disturbances: climate change can affect forests by altering the frequency, intensity, duration, and timing of fire, drought, introduced species, insect and pathogen outbreaks, hurricanes, windstorms, ice storms, or landslides. *BioScience, 51*(9), 723-734.

DeBano, L.F., Neary, D.G., & Ffolliott, P.F. (1998). *Fire effects on ecosystems*. John Wiley & Sons.

DeRose, R.J., & Long, J.N. (2009). Wildfire and spruce beetle outbreak: Simulation of interacting disturbances in the central Rocky Mountains. *Ecoscience, 16*(1), 28-38.

DeRose, R.J., & Long, J.N. (2012). Factors influencing the spatial and temporal dynamics of Engelmann spruce mortality during a spruce beetle outbreak on the Markagunt Plateau, Utah. *Forest Science, 58*(1), 1-4.

Donato, D.C., Simard, M., Romme, W.H., Harvey, B.J., & Turner, M.G. (2013). Evaluating post-outbreak management effects on future fuel profiles and stand structure in bark beetle-impacted forests of Greater Yellowstone. *Forest Ecology and Management, 303*, 160-174.

Dzwonko, Z., Loster, S., & Gawroński, S. (2015). Impact of fire severity on soil properties and the development of tree and shrub species in a Scots pine moist forest site in southern Poland. *Forest Ecology and Management, 342*, 56-63.

ESRI. (2010). ArcGIS for Desktop (Release 10.0) [software]. Redlands, CA: Environmental Systems Research Institute.

Falk, D.A., Miller, C., McKenzie, D., & Black, A.E. (2007). Cross-scale analysis of fire regimes. *Ecosystems, 10*(5), 809-823.

Gao, B.C. (1996). NDWI—A normalized difference water index for remote sensing of vegetation liquid water from space. *Remote Sensing of Environment, 58*(3), 257-266.

Goodwin, N.R., Coops, N.C., Wulder, M.A., Gillanders, S., Schroeder, T.A., & Nelson, T. (2008). Estimation of insect infestation dynamics using a temporal sequence of Landsat data. *Remote Sensing of Environment, 112*(9), 3680-3689.

Hais, M., Jonášová, M., Langhammer, J., & Kučera, T. (2009). Comparison of two types of forest disturbance using multitemporal Landsat TM/ETM+ imagery and field vegetation data. *Remote Sensing of Environment, 113*(4), 835-845.

Hansen, E.M., & Bentz, B.J. (2003). Comparison of reproductive capacity among univoltine, semivoltine, and re-emerged parent spruce beetles (Coleoptera: Scolytidae). *The Canadian Entomologist, 135*, 687-712.

Hart, S.J., & Veblen, T.T. (2015). Detection of spruce beetle-induced tree mortality using high- and medium-resolution remotely sensed imagery. *Remote Sensing of Environment, 168*, 134-145.

Harvey, B.J., Donato, D.C., Romme, W.H., & Turner, M.G. (2013). Influence of recent bark beetle outbreak on fire severity and postfire tree regeneration in montane Douglas-fir forests. *Ecology, 94*(11), 2475-2486.

Harvey, B.J., Donato, D.C., Romme, W.H., & Turner, M.G. (2014). Fire severity and tree regeneration following bark beetle outbreaks: the role of outbreak stage and burning conditions. *Ecological Applications, 24*(7), 1608-1625.

Havašová, M., Bucha, T., Ferenčík, J., & Jakuš, R. (2015). Applicability of a vegetation indices-based method to map bark beetle outbreaks in the High Tatra Mountains. *Annals of Forest Research, 58*(2), 295-310.

Healey, S.P., Cohen, W.B., Zhiqiang, Y., & Krankina, O.N. (2005). Comparison of Tasseled Cap-based Landsat data structures for use in forest disturbance detection. *Remote Sensing of Environment, 97*(3), 301-310.

Healey, S.P., Yang, Z., Cohen, W.B., & Pierce, D.J. (2006). Application of two regression-based methods to estimate the effects of partial harvest on forest structure using Landsat data. *Remote Sensing of Environment, 101*(1), 115-126.

Hicke, J.A., Johnson, M.C., Hayes, J.L., & Preisler, H.K. (2012). Effects of bark beetle-caused tree mortality on wildfire. *Forest Ecology and Management, 271*, 81-90.

Hope, A., Tague, C., & Clark, R. (2007). Characterizing post-fire vegetation recovery of California chaparral using TM/ETM+ time-series data. *International Journal of Remote Sensing, 28*(6), 1339-1354.

Ireland, G., & Petropoulos, G.P. (2015). Exploring the relationships between post-fire vegetation regeneration dynamics, topography and burn severity: A case study from the Montane Cordillera ecozones of western Canada. *Applied Geography, 56*, 232-248.

Jakubauskas, M.E., & Price, K. (2000). Regression-based estimation of lodgepole pine forest age from Landsat Thematic Mapper data. *Geocarto International, 15*(1), 21-26.

Jenkins, M.J., Hebertson, E., Page, W., & Jorgensen, C.A. (2008). Bark beetles, fuels, fires and implications for forest management in the Intermountain West. *Forest Ecology and Management, 254*(1), 16-34.

Jenkins, M.J., Page, W.G., Hebertson, E.G., & Alexander, M.E. (2012). Fuels and fire behavior dynamics in bark beetle-attacked forests in Western North America and implications for fire management. *Forest Ecology and Management, 275*, 23-34.

Jin, S., & Sader, S.A. (2005). Comparison of time series tasseled cap wetness and the normalized difference moisture index in detecting forest disturbances. *Remote Sensing of Environment, 94*(3), 364-372.

Jonášová, M., & Prach, K. (2008). The influence of bark beetles outbreak vs. salvage logging on ground layer vegetation in Central European mountain spruce forests. *Biological Conservation, 141*(6), 1525-1535.

Keeley, J.E. (2009). Fire intensity, fire severity and burn severity: a brief review and suggested usage. *International Journal of Wildland Fire, 18*(1), 116-126.

Key, C.H., & Benson, N.C. (1999). *The Normalized Burn Ratio, a Landsat TM radiometric index of burn severity incorporating multi-temporal differencing*. US Geological Survey.

Kulakowski, D., & Veblen, T.T. (2007). Effect of prior disturbances on the extent and severity of wildfire in Colorado subalpine forests. *Ecology, 88*(3), 759-769.

Kulakowski, D., Matthews, C., Jarvis, D., & Veblen, T.T. (2013). Compounded disturbances in sub-alpine forests in western Colorado favour future dominance by quaking aspen (*Populus tremuloides*). *Journal of Vegetation Science, 24*(1), 168-176.

Kulakowski, D., Veblen, T.T., & Bebi, P. (2003). Effects of fire and spruce beetle outbreak legacies on the disturbance regime of a subalpine forest in Colorado. *Journal of Biogeography, 30*(9), 1445-1456.

Lennon, J.J. (2000). Red-shifts and red herrings in geographical ecology. *Ecography 23*(1), 101-113.

Liu, Q., Liu, G., Huang, C., Liu, S., & Zhao, J. (2014). A tasseled cap transformation for Landsat 8 OLI TOA reflectance images. In: *Geoscience and Remote Sensing Symposium (IGARSS), 2014 IEEE International,* 541-544.

Masek, J.G., Vermote, E.F., Saleous, N.E., Wolfe, R., Hall, F.G., Huemmrich, K.F., et al. (2006). A Landsat surface reflectance dataset for North America, 1990-2000. *IEEE Geoscience and Remote Sensing Letters, 3*(1), 68-72.

McCarley, T.R., Kolden, C.A., Vaillant, N.M., Hudak, A.T., Smith, A.M., Wing, B.M., Kellogg, B.S., & Kreitler, J. (2017). Multi-temporal LiDAR and Landsat quantification of fire-induced changes to forest structure. *Remote Sensing of Environment, 191*, 419-432.

Meddens, A.J., Hicke, J.A., & Ferguson, C.A. (2012). Spatiotemporal patterns of observed bark beetle-caused tree mortality in British Columbia and the western United States. *Ecological Applications, 22*(7), 1876-1891.

Meddens, A.J., Hicke, J.A., Vierling, L.A., & Hudak, A.T. (2013). Evaluating methods to detect bark beetle-caused tree mortality using single-date and multi-date Landsat imagery. *Remote Sensing of Environment, 132*, 49-58.

Meigs, G.W., Kennedy, R.E,. & Cohen, W.B. (2011). A Landsat time series approach to characterize bark beetle and defoliator impacts on tree mortality and surface fuels in conifer forests. *Remote Sensing of Environment, 115*(12), 3707-3718.

Meigs, G.W., Zald, H.S., Campbell, J.L., Keeton, W.S., & Kennedy, R.E. (2016). Do insect outbreaks reduce the severity of subsequent forest fires? *Environmental Research Letters, 11*(4), 045008.

Meng, R., Dennison, P.E., Huang, C., Moritz, M.A., & D'Antonio, C. (2015). Effects of fire severity and post-fire climate on short-term vegetation recovery of mixed-conifer and red fir forests in the Sierra Nevada Mountains of California. *Remote Sensing of Environment, 171*, 311-325.

National Interagency Fire Center. *RAWS USA Climate Archive*. Retrieved from: http://www.raws.dri.edu/ [Accessed 14th April 2015].

Negrón, J.F., Bentz, B.J., Fettig, C.J., Gillette, N., Hansen, E.M., Hayes, J.L., et al. (2008). US Forest Service bark beetle research in the western United States: Looking toward the future. *Journal of Forestry, 106*(6), 325-331.

Negrón, J.F., Fettig, C.J. (2014). Mountain pine beetle, a major disturbance agent in US western coniferous forests: A synthesis of the state of knowledge. *Forest Science, 60*(3), 409.

Odion, D.C., & Davis, F.W. (2000). Fire, soil heating, and the formation of vegetation patterns in chaparral. *Ecological Monographs, 70*(1), 149-169.

Paine, R.T., Tegner, M.J., & Johnson, E.A. (1998). Compounded perturbations yield ecological surprises. *Ecosystems, 1*(6), 535-545.

Parks, S.A., Parisien, M.A., & Miller, C. (2011). Multi-scale evaluation of the environmental controls on burn probability in a southern Sierra Nevada landscape. *International Journal of Wildland Fire, 20*(7), 815-828.

Peet, R.K. (1978). Forest vegetation of the Colorado Front Range: patterns of species diversity. *Vegetatio, 37*(2), 65-78.

Petropoulos, G.P., Griffiths, H.M., & Kalivas, D.P. (2014). Quantifying spatial and temporal vegetation recovery dynamics following a wildfire event in a Mediterranean landscape using EO data and GIS. *Applied Geography, 50*, 120-131.

Prichard, S.J., & Kennedy, M.C. (2014). Fuel treatments and landform modify landscape patterns of burn severity in an extreme fire event. *Ecological Applications, 24*(3), 571-590.

R Core Development Team. (2013). R: A language and environment for statistical computing [software]. Vienna, Austria: R Foundation for Statistical Computing.

Raffa, K.F., Aukema, B.H., Bentz, B.J., Carroll, A.L., Hicke, J.A., Turner, M.G., et al. (2008). Cross-scale drivers of natural disturbances prone to anthropogenic amplification: the dynamics of bark beetle eruptions. *Bioscience, 58*(6), 501-17.

Romme, W.H., & Knight, D.H. (1981). Fire frequency and subalpine forest succession along a topographic gradient in Wyoming. *Ecology, 62*(2), 319-326.

Ryan, K.C., & Reinhardt, E.D. (1988). Predicting postfire mortality of seven western conifers. *Canadian Journal of Forest Research, 18*(10), 1291-1297.

Schoennagel, T., Veblen, T.T., & Romme, W.H. (2004). The interaction of fire, fuels, and climate across Rocky Mountain forests. *BioScience, 54*(7), 661-676.

Schott, J.R., Salvaggio, C., & Volchok, W.J. (1988). Radiometric scene normalization using pseudoinvariant features. *Remote Sensing of Environment, 26*(1), 1-16.

Sibold, J.S., Veblen, T.T., & González, M.E. (2006). Spatial and temporal variation in historic fire regimes in subalpine forests across the Colorado Front Range in Rocky Mountain National Park, Colorado, USA. *Journal of Biogeography, 33*(4), 631-647.

Simard, M., Romme, W.H., Griffin, J.M., & Turner, M.G. (2011). Do mountain pine beetle outbreaks change the probability of active crown fire in lodgepole pine forests? *Ecological Monographs, 81*(1), 3-24.

Stephens, S.L., Agee, J.K., Fulé, P.Z., North, M.P., Romme, W.H., Swetnam, T.W., et al. (2013). Managing forests and fire in changing climates. *Science, 342*(6154), 41-42.

Turner, M.G. (2010). Disturbance and landscape dynamics in a changing world. *Ecology, 91*(10), 2833-2849.

Turner, M.G., Romme, W.H., Smithwick, E.A., Tinker, D.B., & Zhu, J. (2011). Variation in aboveground cover influences soil nitrogen availability at fine spatial scales following severe fire in subalpine conifer forests. *Ecosystems, 14*(7), 1081-1095.

US Forest Service Remote Sensing Applications Center. (2015). Burned Area Emergency Response (BAER) Imagery Support. Retrieved from: https://www.fs.fed.us/eng/rsac/baer/ [Accessed 12th February 2015].

US Geological Survey, Gap Analysis Program. *Land Cover Dataset*. A from: http://swregap.nmsu.edu/ [Accessed 20th February 2015].

US Geological Survey. *GeoMAC Wildland Fire Support Application*. Retrieved from: http://rmgsc.cr.usgs.gov/outgoing/GeoMAC/ [Accessed 22nd April 2015].

Vogelmann, J.E. (1990). Comparison between two vegetation indices for measuring different types of forest damage in the north-eastern United States. *Remote Sensing, 11*(12), 2281-2297.

Walter, J.A., & Platt, R.V. (2013). Multi-temporal analysis reveals that predictors of mountain pine beetle infestation change during outbreak cycles. *Forest Ecology and Management, 302*, 308-318.

Westerling, A.L., Hidalgo, H.G., Cayan, D.R., & Swetnam, T.W. (2006). Warming and earlier spring increase western US forest wildfire activity. *Science, 313*(5789), 940-943.

Wilson, E.H., & Sader, S.A. (2002). Detection of forest harvest type using multiple dates of Landsat TM imagery. *Remote Sensing of Environment, 80*(3), 385-396.

Wilson, J.P., & Gallant, J.C. (2000). Secondary topographic attributes. *Terrain Analysis: Principles and Applications*, 87-131.

Wimberly, M.C., Cochrane, M.A., Baer, A.D., & Pabst, K. (2009). Assessing fuel treatment effectiveness using satellite imagery and spatial statistics. *Ecological Applications, 19*(6), 1377-1384.

CHAPTER 3: Effects of Wildfire and Spruce Beetle Disturbance on Topoclimate in a
Rocky Mountain Forest

Summary

Forests of the Rocky Mountains have recently experienced extensive and severe canopy

loss from wildfires and bark beetle outbreaks. Recovery of these ecosystems will take several

decades, and it is difficult to project how current and future warming temperatures will affect

forest persistence and extirpation in the future. Recent work has highlighted the potential

importance of fine-scale topography and canopy cover in determining the below-canopy

environment in mountain forests, which may have an important mediating effect on regional-

scale climate changes. The aim of this study was to determine how fire and spruce beetle

outbreak within the last 10-15 years have impacted below-canopy temperatures in a region of the

San Juan Mountains, southwest Colorado, USA, where these disturbances have been particularly

severe. We used a network of sensors to record temperatures for a full year in burned and beetle-

impacted areas. Using a Bayesian multiple regression model that accounted for spatial structure,

we assessed the relative influence of topographic variables (elevation, aspect, slope, topographic

position, and solar radiation), live tree basal area, and burned/unburned status on daily maximum

and minimum temperatures. Model parameters indicated that burned area was warmer than

unburned forest by ~0.5 °C. Conversely, increasing spruce mortality in unburned, beetle-killed

forests did not meaningfully affect daily maximum temperatures but resulted in cooling of daily

minimum temperatures by up to ~1.0 °C. These results indicate that severe wildfire may

exacerbate effects of climate change and increase the probability of ecosystem transitions.

However, the effects of bark beetle outbreaks are more complex. Cooling of overnight minimum

temperatures may counteract warming trends, but an increase in diurnal temperature ranges may have uncertain ecological consequences.

Introduction

Spatial variability in warming trends can strongly influence biotic community responses to climate change (Ackerly et al., 2010). This is particularly true in mountain regions, where broad-scale warming patterns may be substantially buffered by variations in elevation, aspect, exposure, and cold air drainage across small geographic areas (Dobrowski, 2011; Lenoir et al., 2013). Canopy structure in mountain forests plays an additional role in mediating surface-level microclimates (Ashcroft & Gollan, 2012; Chen et al., 1999; Geiger, 1950). Understanding the effects of climate change on fine-scale biotic processes, such as seedling establishment and survival, therefore depends on accurate representation of fine-scale temperature patterns determined by physiography and overstory condition. Disturbances may create abrupt changes in overstory that may result in shifts in below-canopy temperatures even when physiographic conditions remain constant over time. However, effects of canopy disturbance on microclimates are not well understood.

Disturbances such as fires, insect outbreaks, blowdowns, and drought-related die-offs alter the below-canopy environment by removing overstory vegetation. Overstory loss increases the amount of daytime shortwave radiation reaching the ground surface, which can elevate daytime maximum temperatures and evapotranspiration potential. Such changes may exacerbate broader warming trends and limit seedling recruitment in locations where dominant species are at risk of warming-related decline (Dobrowski et al., 2015). However, canopy loss can also lead to greater overnight cooling, as forest canopies intercept outgoing ground-surface longwave radiation (Geiger, 1950). Although some studies have demonstrated that canopy cover plays a

significant role in buffering extreme daytime maximum temperatures and overnight minimum temperatures (Frey et al., 2016; Holden et al., 2016; Ma, Concilio, Oakley, North, & Chen, 2010), it is not clear how overall below-canopy microclimates are altered by varying disturbance types or severities. Furthermore, the importance of disturbance on microclimate is not typically considered at the landscape scale in relation to other drivers of spatial variability.

Investigating the effects of disturbance and topographic variation on below-canopy temperatures is limited by a scarcity of long-term temperature data in forest stands. However, a number of recent studies have investigated the use of inexpensive temperature logger networks to create high-resolution topoclimate models in topographically complex areas (e.g. Ashcroft & Gollan, 2012; Bruening, Tran, Bunn, Weiss, & Salzer, 2017; Greiser et al., 2018; Holden et al., 2016; Isaak, Wenger, & Young, 2017; Meineri & Hylander, 2017). These studies used detailed physiographic data and remotely-sensed canopy variables to model climate variability at resolutions of < 1 km. Detailed climate models in mountain regions are valuable for understanding species-climate relationships at fine scales, as well as for identifying potential microrefugia where species may be protected from climate stress in the near future (Ashcroft, 2010; Dobrowski, 2011). Additionally, understanding how disturbances influence these fine-scale patterns is increasingly important as anthropogenic climate change causes forests to experience increasing disturbance frequency and severity (Seidl et al., 2017).

Mountain forests in the western United States are currently facing risks of decline and species transitions as a result of warming and associated disturbance. Over the past century the region has seen a temperature increase of ~1.5 °C (González et al., 2018), with resulting increases in wildfire area (Abatzoglou & Williams, 2016) and tree mortality from bark beetles and drought (Allen et al., 2010; Meddens, Hicke, & Ferguson, 2012) in the last few decades.

Many of these changes are taking place in topographically complex landscapes with high spatial variability in warming patterns. Whether these disturbances drive permanent transitions to new forest cover types, or from forest to non-forest, will depend on the extent to which disturbance severity and climate shifts over the next few decades will overcome resilience mechanisms favoring ecosystem stability (Johnstone et al., 2016; Turner, 2010). It is largely thought that disturbances reduce forest resilience to climate change, and will ultimately accelerate forest adaptations by allowing species to migrate to more suitable climates (Overpeck, Rind, & Goldberg, 1990; Thom, Rammer, & Seidl, 2017).

There is evidence that recent climate shifts are limiting forest regeneration and allowing for expansion of warm-adapted species in severely disturbed areas in the southern Rockies (Bell, Bradford, & Lauenroth, 2014a; Landhaeusser, Deshaies, & Lieffers, 2010; Rother & Veblen, 2016). However, a thorough understanding of the effect of climate on post-disturbance ecosystem change is limited when coarse-scale climate data is used to explain fine-scale biotic processes (Austin & Van Niel, 2011). Microrefugia may play a more important role in buffering climate change than what has previously been assumed, while topographic exposure to high temperatures on low-elevation, southwest-facing slopes may accelerate change (Wilkin, Ackerly, & Stephens, 2016). Extensive, severe forest disturbances have the potential to modify these patterns of climate change exposure for biota affected by temperatures below the canopy.

In this study, we used a network of temperature loggers to collect a 1-year record of below-canopy temperatures in a topographically complex mountain forest recently affected by severe disturbances. Our study region in the San Juan Mountains, southwest Colorado, USA, was impacted by the West Fork Complex wildfire in 2013 and by severe overstory mortality from a spruce beetle outbreak beginning ca. 2004. The outbreak was in the early gray stage at the time

63

of sampling, in which dead trees remained standing but had lost needles and fine twigs from the canopy. The area is dominated by subalpine spruce-fir forests which are expected to decline by the end of the 21st century as a result of shifting climate suitability (Bell, Bradford, & Lauenroth, 2014b). The goal of the study was to quantify differences in temperature in burned vs. unburned forest and across a gradient of beetle kill severity in unburned forest. We used spatially structured Bayesian multiple regression models in order to determine the relative influence of topographic gradients and disturbance type and severity, while accounting for the inherent spatial structure of landscape temperature patterns.

Methods

Study Area

The study focused on an approximately 25 x 25 km area in the Rio Grande National Forest in the San Juan Mountains, Colorado. Study sites were located within ~20 km of the Wolf Creek Pass summit on US Highway 160, straddling the Continental Divide. Elevations of study sites ranged from ~2,700 m to 3,300 m a.s.l. The forest in this area is dominated by subalpine species including Engelmann spruce (*Picea engelmannii*) and subalpine fir (*Abies lasiocarpa*) with lower abundances of white fir (*Abies concolor*), Douglas fir *(Pseudotsuga menziesii)*, blue spruce (*Picea pungens*) and lodgepole pine (*Pinus contorta*). Quaking aspen (*Populus tremuloides*) is present at lower elevations north of the Continental Divide. The high-elevation climate is characterized by cool summers (12 °C average July mean), cold winters (-8 °C average January mean) and high precipitation (1,200 cm annual average). Most precipitation falls as winter snow or in monsoonal rainstorms in July and August.

The West Fork Complex fire burned over 44,500 ha of spruce and fir-dominated forest in June-July, 2013. Our study area included one of the three distinct burn areas making up the

complex, the West Fork burn (Figure 3-1). Most of the burn area was high-severity, consuming

nearly all overstory vegetation (MTBS, 2013). By the time of the fire much of the burn area had

already experienced significant mortality from a spruce beetle outbreak which had killed a

majority of overstory *P. engelmannii* trees (CSFS, 2018). The forest outside of the burn area has

similarly experienced a large degree of beetle-caused mortality. The greatest outbreak severity

occurred in the Weminuche Wilderness area, with severity decreasing east of Highway 160

(Carlson, Sibold, Assal, & Negron, 2017).
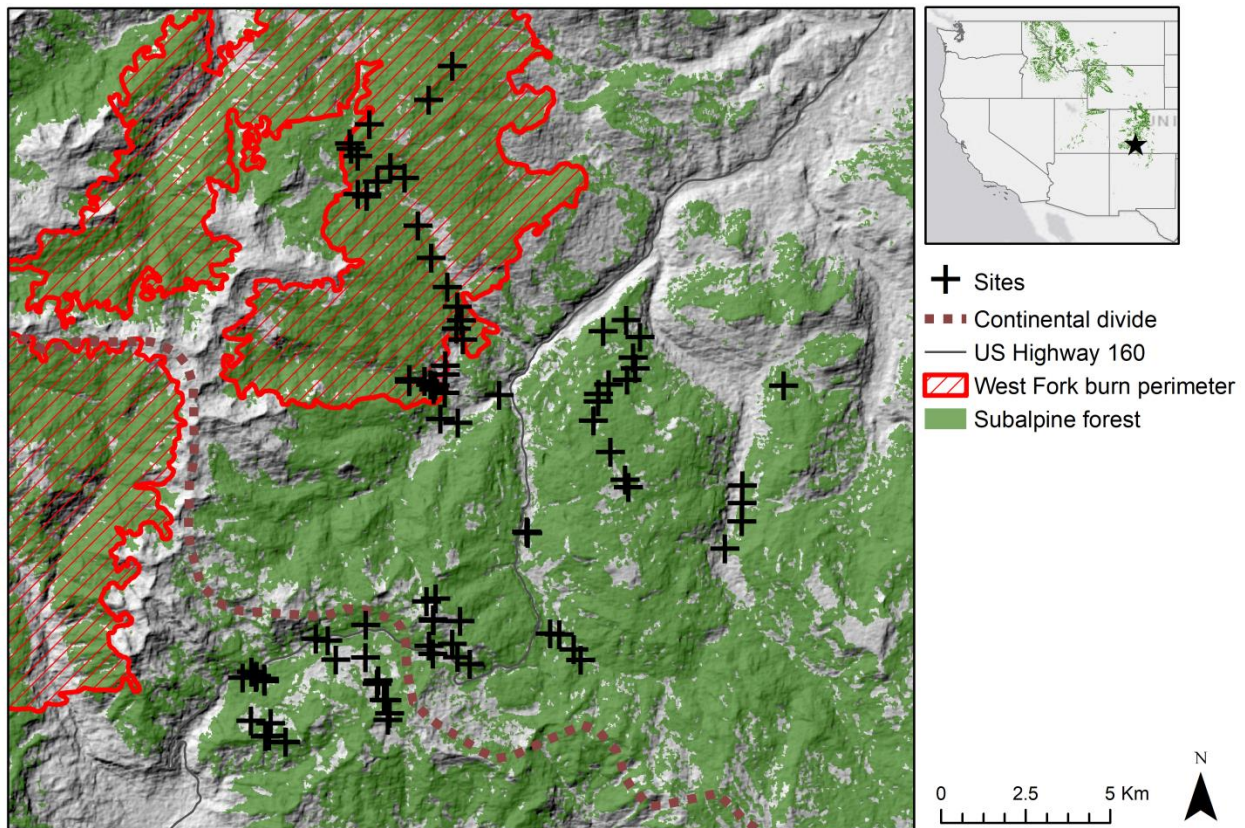
Figure 3-1. Study area map with study sites indicated. Star in inset map indicates the location of
the study area within the western United States.

Site Selection

We selected 90 sites in burned and unburned forest to evaluate temperatures in relation to topography and canopy cover. We selected sites in a Geographic Information System (GIS) to achieve an optimal representation of elevations, aspects, slope positions, and spruce beetle outbreak severities. In order to evaluate temperatures along a gradient of canopy cover in beetle-killed forest, we placed a greater number of sites in unburned than in burned areas (30 burned, 60 unburned). We recorded the precise location of sites in the field using a handheld Global Positioning System (GPS) device.

Temperature Data

We used Logtag TRIX-8® temperature sensors to record below-canopy temperatures at each study site. Sensors were programmed to record every 3 hours beginning at midnight. We housed sensors within plastic shields covered in reflective tape so that they would not be encased in snow and so that readings would not be influenced by direct solar radiation (Holden, Klene, Keefe, & Moisen, 2013). Sensor shields were attached to the north-facing sides of tree trunks ~2 m above the ground. We initially placed sensors in September of 2016 and downloaded all temperature data in the summer of 2018. Temperature records were summarized as a daily time series of maximum and minimum temperatures (Tmax, Tmin).

i. Data Cleaning

Of the 90 sensors placed in the field, 85 were successfully recovered with a complete data record (27 burned, 58 unburned). We were unable to use data from the winter of 2016-2017 due to a clear influence of snow insulation at many sites. However, data from the winter of 2017-2018 did not show this effect, presumably due to drought and high winter temperatures in that year. Furthermore, some sites showed anomalously

high daytime temperatures (>30 °C) which were perhaps influenced by direct solar radiation penetrating the radiation shield. We checked for temperature anomalies at each site by plotting a time series of daily maxima and minima against data recorded at the Wolf Creek Summit Snow Telemetry (SNOTEL) weather station (NRCS, 2018). There was a strong linear correlation between Logtag® data and SNOTEL data, and we were able to visually identify outliers (Figure 3-2). Outlying values were removed from the dataset.
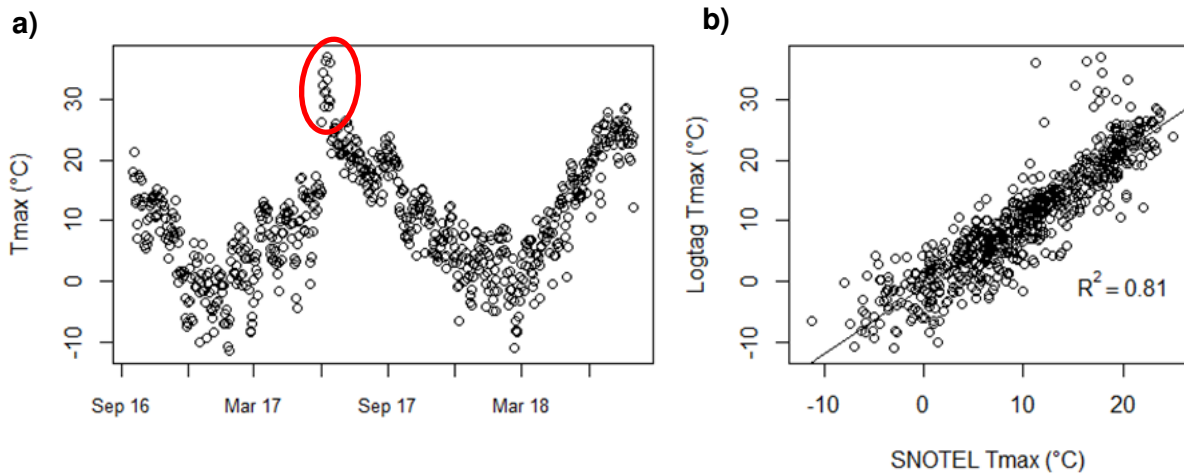
Figure 3-2. a) Example time series used to identify erroneous temperature records. Daily maximum temperature is subtracted from SNOTEL weather station values to identify outliers. Outliers (circled in red) were removed from the dataset and filled using a linear regression based on SNOTEL data (b).

Because missing values at certain sites influence seasonal temperature averages derived from 3-hourly records, we filled in the manually removed records using ordinary least squares regression. For each site, we fit a regression function between the Logtag® daily maximum/minimum temperatures and corresponding SNOTEL temperatures. Fit was high for all sites ($R^2 > 0.8$). The regression function was then used to predict the removed daily values from corresponding SNOTEL values. We used this procedure to fill data gaps

no longer than 12 consecutive days and no more than 12 days out of the complete record for any site.

Field Data

Basal area of live trees was used as a proxy for canopy cover at each temperature sensor site. We measured basal area within a 20x20 m plot area centered on the sensor and oriented along north-south and east-west axes. We measured diameter at breast height (DBH) of all trees rooted within the plot area and recorded species and live/dead status. DBH measurements were then converted to total live and dead basal area for each species. We additionally recorded slope and aspect at plot centers. Aspect was transformed along a northeast to southwest-facing scale according to the following formula: Taspect = sin(aspect + 45) + 1 (Beers, Dress, & Wensel, 1966).

Topographic Variables in GIS

We used a 1/3-arcsecond digital elevation model (DEM) to calculate elevation, relative elevation, and equinox solar radiation for DEM cells overlapping plot GPS coordinates. All variables were calculated in ArcMap 10.4 (ESRI, 2016). Relative elevation was calculated by subtracting elevation of the DEM cell overlaying the plot center from the mean of a 5x5 cell neighborhood. This method gives an estimate of slope position along a numeric scale, with more negative values indicating valley bottoms and higher values indicating peaks. Slope position serves as an indicator of cold-air drainage, as valley bottoms collect cool, dense air and thereby may experience lower nighttime and winter temperatures compared to surrounding upslope locations (Bergen, 1968). Similarly, sites with greater topographic exposure to solar radiation may experience higher daytime maximum temperatures (Bristow & Campbell, 1984). Solar radiation was calculated in ArcMap using the Solar Radiation tool.

Analysis

We used a Bayesian multiple linear regression approach to determine relative influences of each explanatory variable (Table 3-1) on temperature averages. We fit models using four different averages of temperatures – summer Tmax, summer Tmin, winter Tmax, and winter Tmin, where summer is defined as the (mostly) snow-free season of June-October and winter is defined as November-May. Tmax and Tmin are the seasonal averages of daily maximum and minimum temperatures. For each temperature summary, we fit models using two different formulations. The first included all burned and unburned sites and included a binary 'Burned' covariate (0 = unburned, 1 = burned). These models were designed to determine the overall temperature difference between the burned area and surrounding unburned forest, and did not include a live canopy covariate because the majority of burned sites contained no live canopy. The second set of models included a live canopy covariate and used unburned sites only.

Table 3-1. Variables used in Bayesian multiple regression models.

Variable	Description
Topography	
Elevation	DEM values
Relative elevation	Elevation of sites relative to the mean elevation of neighboring DEM grid cells within a 5x5 cell neighborhood
Slope	Measured in the field at plot centers
Solar radiation at equinox	Calculated from a DEM using ArcGIS tools
Taspect	Transformation of aspect measured in the field at plot centers (Beers et al., 1966)
Disturbance	
log(Canopy)	Total basal area of all live trees >1 m in height within 20 x 20 m plot areas, log-transformed (measured in unburned plots only)
Burned/Unburned	Binary variable (0 – unburned, 1 – burned)

The linear regression equation for each model takes the form

$$y_i \sim \text{normal}(\mu_i, \sigma^2)$$
$$\mu_i = \beta_0 + \boldsymbol{\beta}\boldsymbol{X}_i{}'$$

where y_i is the is the observed average temperature for a given site, i in $\{1, \dots n\}$, derived from the Logtag record, μ_i and σ^2 are the mean and variance of the normal distribution from which y_i is drawn, β_0 is a random intercept, $\boldsymbol{X}$ is a matrix of observed explanatory variables, and $\boldsymbol{\beta}$ is a vector of unknown coefficients. We assumed temperatures and explanatory variables were measured without error.

i.   Spatial Modeling with INLA/SPDE

While we expected that topography and canopy variables would explain observed temperature patterns well, temperatures are also influenced by large-scale atmospheric processes which are not explicitly modeled here. We therefore expected that model residuals would show spatial autocorrelation, and that a modeling approach accounting for spatial covariance in the data was needed. We addressed this by adding a spatial random effects term to the model using the stochastic partial differential equation (SPDE) approach described by Lindgren, Rue, & Lindstrom (2011). The SPDE method represents space as a continuous Gaussian field and uses Matérn covariance functions to derive a discrete Gaussian Markov random field (GMRF) from observed point locations, using measured GPS coordinates as spatial indices. The GMRF is defined by creating a mesh over the spatial domain using Delaunay triangulation, allowing for a finite combination of piecewise functions based on Matérn covariance parameters which are used to populate a sparse precision

matrix (Lindgren & Rue, 2015; Figure 3-3). The sparse precision matrix allows for computationally efficient model fitting based on approximations of spatial covariance parameters.

a)

b)
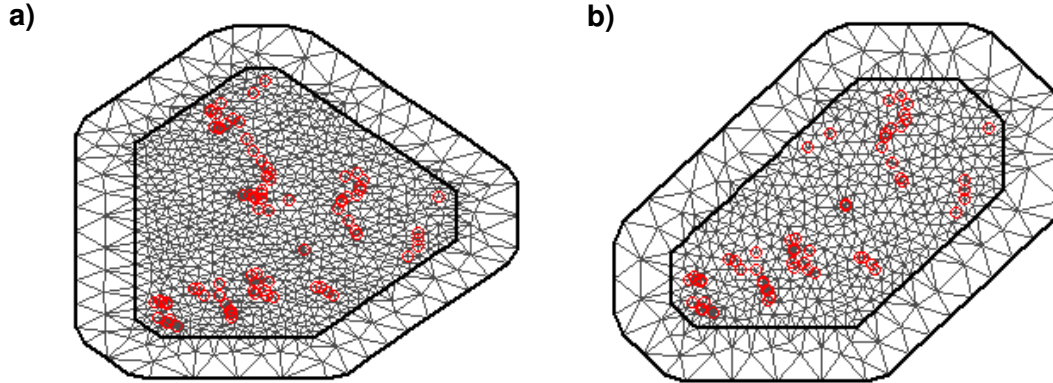
Figure 3-3. Delaunay triangulations of point data, used to build Gaussian Markov Random Field precision matrices for a) all burned and unburned sites and b) unburned sites only.

The Bayesian linear predictor model including the GMRF spatial effects term, u_i, is written as

$$\mu_i = \beta_0 + \boldsymbol{\beta X}_i + u_i$$

where u_i is approximated from a 0-mean GMRF with precision matrix, $\boldsymbol{Q}$, with the equation

$$\boldsymbol{u} \sim \text{multivariate normal}(\boldsymbol{0}, \boldsymbol{Q}^{-1}(\kappa, \tau))$$

where κ and τ are parameters for the Matérn covariance function used to populate $\boldsymbol{Q}$. The spatial process for all points in the spatial domain ($\boldsymbol{s}$) is modeled as a continuous field $u(\boldsymbol{s})$ where the Gaussian white noise process is modeled with a stationary solution to the Mátern covariance function. The solution is given by the equation

71

$$(\kappa^2 - \Delta)^{\frac{\alpha}{2}}(\tau u(\boldsymbol{s})), \qquad \boldsymbol{s} \in \Omega$$

where κ is the spatial scale parameter, Δ is the Laplacian differential operator, α is a smoothness parameter (set to 2), τ is a variance parameter, and Ω is the spatial domain. For a set of discrete locations $i = \{1, \dots n\}$ in a 2-dimensional spatial field, $u(\boldsymbol{s})$ can be estimated by the equation

$$u(\boldsymbol{s}) = \sum_{i=1}^{n} \psi_i(\boldsymbol{s})u_i$$

where $\psi_i(\cdot)$ are piecewise linear basis functions and $\boldsymbol{u} = \{u_1, \dots u_n\}$ are fitted on covariances between observed data points (see Lindgren et al., 2011).

The full model expression for the posterior and joint distribution is as follows:

$$[\boldsymbol{\beta}, \sigma^2, \kappa, \tau | \boldsymbol{y}] \propto \prod_{i=1}^{n} [y_i | \boldsymbol{\beta}, \boldsymbol{X}_i', u_i, \sigma^2][\boldsymbol{u}|\boldsymbol{0}, \boldsymbol{Q}^{-1}(\kappa, \tau)][\boldsymbol{\beta}][\sigma^2][\kappa][\tau]$$

where $\boldsymbol{y}$ are observed temperature averages for each site and n is the number of observed sites (n=87 for all sites, n=58 for unburned sites). The model was fit using Integrated Nested Laplace Approximation (INLA) with the R package 'INLA' (Rue, Martino, & Chopin, 2009; R Core Team, 2019). The observed data, $\boldsymbol{y}$, was modeled with a Gaussian likelihood, with the mean predicted by the linear function and variance (σ^2) as an unknown parameter. Prior distributions for parameters $\boldsymbol{\beta}$, σ^2, κ, and τ were set using a Penalized Complexity (PC) method developed for SPDE spatial models by Fuglstad, Simpson, Lindgren, & Rue (2018; also see Simpson, Rue, Riebler, Martins, & Sorbye, 2017). PC priors are designed to shrink unknown parameters to an effect of 0, resulting in

weakly informative priors for the fixed effects, the variance, and the spatial field. In R-INLA, the SPDE parameters κ and τ are reformulated as r and σ, which can be more intuitively defined as the empirical range and marginal standard deviation of the GMRF (see Lindgren & Rue, 2015).

Hyperparameters r_o, r_P, σ_o, and σ_P are defined such that $\Pr(r < r_o) = r_P$ and $\Pr(\sigma < \sigma_o) = \sigma_P$. We specified values r_o=sd($\boldsymbol{y}$)/10, r_P=0.5, σ_o=12, and r_P=0.5, according to the method suggested by Bakka et al. (2018) in which the standard deviation is about 20% of the diameter of the study region and range is about 10% of the standard deviation of the data. We set weakly informative PC priors for the fixed effects parameters and random error, $\boldsymbol{\beta}$ and σ^2.

ii.   Model Evaluation

We used 3-fold cross-validation to evaluate the predictive performance of our models. For each model, we withheld observed values at 1/3 of sites (n=29 for burned/unburned models, n=19 for beetle-killed models). Models were fit using the remaining observations, and predictions were compared to the withheld observed data using log-predictive densities (LPD, Gelman, Hwang, & Vehtari., 2014) of M=10,000 posterior samples. LPD gives the total probability density of the observed out-of-sample data, $\boldsymbol{y}_{oos}$, conditioned on predictions made by a model fit with withheld data, and is defined by the equation

$$\log[\boldsymbol{y}_{oos}|\boldsymbol{y}] \approx \log\left(\frac{\sum_{m=1}^{M}[\boldsymbol{y}_{oos}|\boldsymbol{y}, \boldsymbol{\theta}^{(m)}]}{M}\right)$$

where y is the observed data used to fit the model, and $\theta^{(m)}$ is the full set of parameters for the kth sample. We withheld a different random subset of sites in each cross-validation run and averaged log-predictive densities across all three runs. We additionally performed diagnostics for models fit to the complete dataset using the probability integral transform (PIT; Angus, 1994), computed using a leave-one-out cross-validation procedure included in the R-INLA package. PIT gives the likelihood of an observation being less than or greater than the predicted value, such that a uniform distribution indicates a lack of model bias.

iii.   Estimating Change in Temperature Due to Beetle-Kill

In order to estimate the temperature effect of partial canopy loss from spruce beetles, we used models to estimate the difference in temperatures before and after beetle kill. After fitting initial models using field measurements of live canopy basal area, we re-fit models using the sum of live tree basal area and standing dead spruce basal area. n=1000 samples were drawn from the posterior distribution of estimated y values and subtracted by observed y values to obtain a posterior for the temperature difference for each site.

Results

The mean of all summer and winter temperatures for all sites was 5.0 °C (std. dev. = 8.3 °C). The mean temperature for sites in the burned area was 5.4 °C and mean temperature for sites in unburned forests was 4.8 °C. Temperature ranges for all sites were as follows – mean summer Tmax: 12.2 – 20.6 °C; mean summer Tmin: 1.8 – 8.2 °C; mean winter Tmax: -0.5 – 9.8 °C; mean winter Tmin:-10.8 – -3.8 °C. Our Logtag®-recorded mean temperature is similar to the mean of monthly PRISM temperatures for June 2017-May 2018 (5.3 °C), and is 1.7 °C warmer

than the 1981-2010 normal annual mean temperature for Wolf Creek Pass (PRISM online data; prism.nacse.org).

Model Performance

Validations using withheld sites indicated a good overall correlation between predicted values (95% credible intervals) and observed values (Figure 3-4). Fit was highest for summer mean Tmax for both burned/unburned and beetle-killed models (mean LPDs of 1,398 and 947, respectively) and lowest for winter Tmin (mean LPDs of 894 and 537, respectively). PIT plots revealed a uniform distribution for all models, indicating no significant model bias.
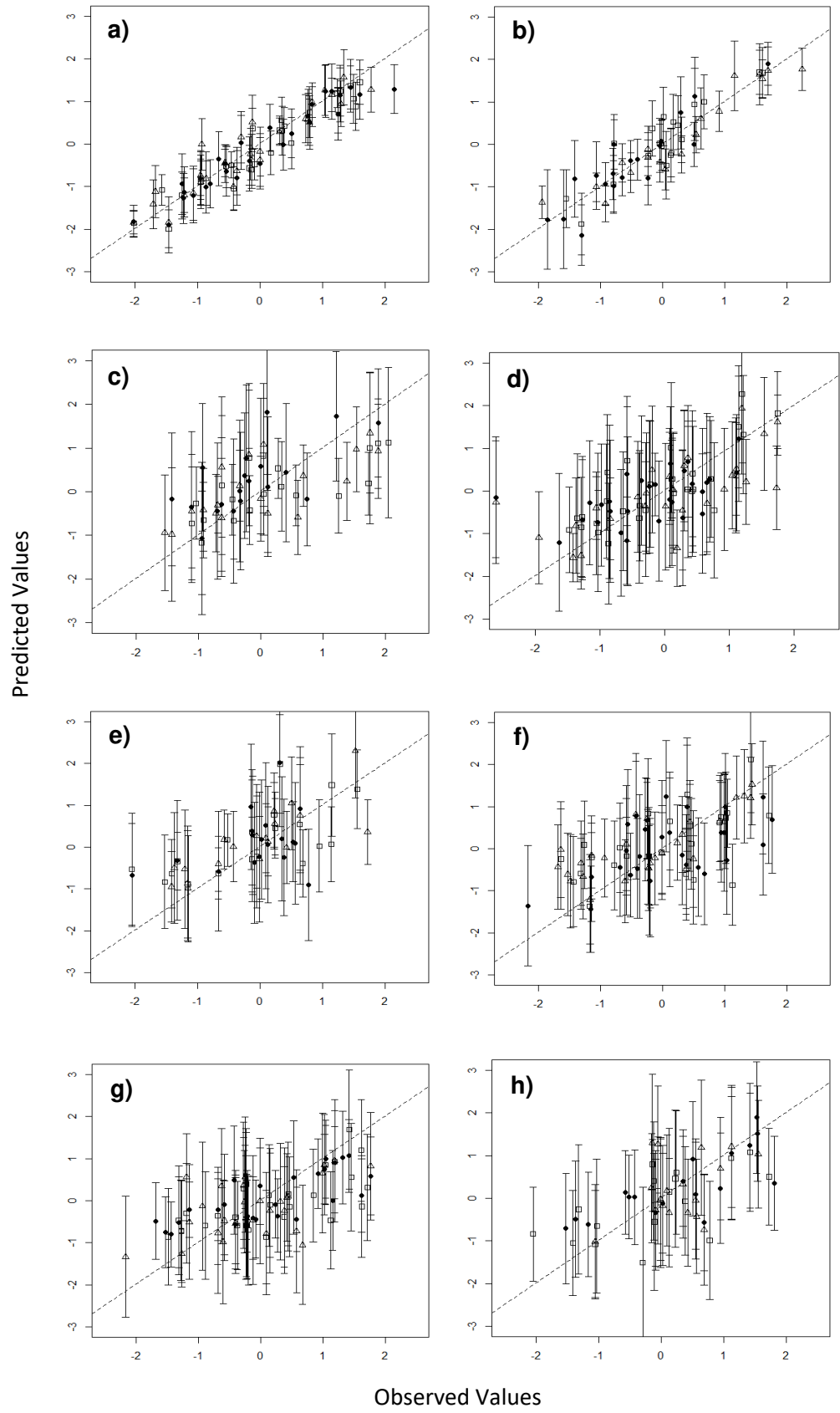
Figure 3-4. Comparisons of predicted vs. observed values for 4 temperature summaries, from 3-fold model cross-validation runs using randomly withheld sites. Left column: models fit using all sites and a binary Burned variable; right column: models fit using unburned sites only and a live canopy basal area variable. a-b): average summer Tmax, c-d): average summer Tmin, e-f): average winter Tmax, g-h): average winter Tmin. Dashed lines indicate 1:1 relationships. Error bars indicate equal-tailed 95% credible intervals for predicted value posterior distributions; points indicate posterior means. Point symbols correspond to individual validation runs.

Parameter Estimates

We determined the relative effects of each explanatory variables on temperatures by plotting the posterior means and equal-tailed 95% credible intervals (CIs) for β's from models fit using standardized covariates (Figure 3-5). Elevation had a strong negative effect on summer Tmax (>95% probability that $\beta < 0$) but not on other temperature variables. Relative elevation had a strong effect on winter Tmax/Tmin and winter Tmax (>95% probability that $\beta > 0$), such that temperatures increased with increasing topographic relief (conversely, temperatures were colder in valley bottoms). Temperatures were also higher in burned than in unburned areas (>95% probability that $\beta > 0$) for all temperature variables except summer Tmin. In unburned-only models, live canopy basal area had a positive effect on Tmin and winter Tmax (>90% probability that $\beta > 0$) but did not have a strong effect on summer Tmax. Temperatures additionally increased with increasing solar radiation and with decreasing Taspect, corresponding with more southwest-facing slopes. There was no strong effect of the field-measured slope on Tmax or Tmin in either season, although DEM-derived slope is a component of the solar radiation calculation. Posterior means and 95% CIs for β's based on unstandardized covariate values are listed in Table 3-2.
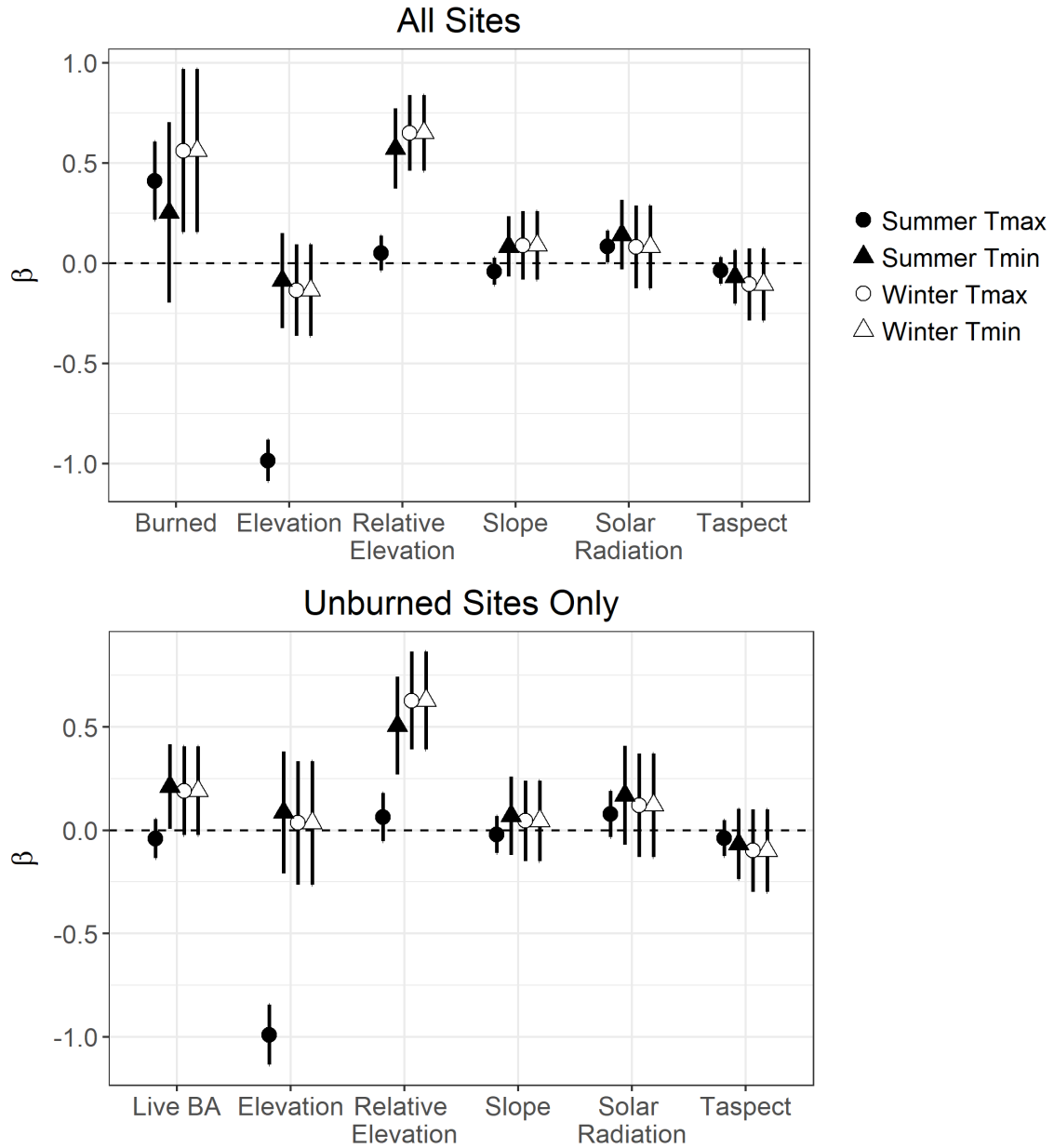
Figure 3-5. Posterior means (points) and equal-tailed 95% credible intervals (vertical lines) for predictor variable coefficients (β) in models predicting each of 4 temperature summaries (average summer Tmax, average summer Tmin, average winter Tmax, and average winter Tmin). Top row shows results for models fit using all sites and a binary Burned variable; bottom row gives results for models fit using unburned sites only and a live canopy basal area variable (Live BA). Coefficient values are based on standardized predictor variables.

Table 3-2. Posterior means (in parentheses) and equal-tailed 95% credible intervals for β's for all 8 models. β's are for unstandardized covariates.

Model #	Disturbance covariate	y	Intercept	Burned	Live Canopy Basal Area (cm²/m²)	Elevation (m)	Relative elevation (m)	Slope (°)	Solar rad. (WH m⁻²)	Taspect (no units)
1	Burned vs. unburned	Summer mean Tmax	12.04 – 14.68 (13.36)	0.215 – 0.604 (.410)	-	-0.0050 – -0.0040 (-0.0045)	-0.0006 – 0.0023 (0.0008)	-0.012 – 0.003 (-0.0043)	0.0000 – 0.0001 (0.0001)	-0.140 – 0.042 (-0.0492)
2		Summer mean Tmin	-3.86 – 2.25 (1.56)	-0.197 – 0.702 (0.253)	-	-0.0015 – -0.0006 (-0.0004)	0.006 – 0.013 (0.010)	-0.010 – 0.023 (0.007)	0.0000 – 0.0005 (0.0002)	-0.227 – 0.092 (-0.092)
3		Winter mean Tmax	10.72 – 14.04 (12.38)	0.487 – 0.986 (0.737)	-	-0.0048 – -0.0036 (-0.0042)	-0.0017 – 0.0018 (0.0000)	-0.0153 – 0.0020 (-0.0066)	0.0000 – 0.0003 (0.0002)	-0.316 – -0.102 (-0.209)
4		Winter mean Tmin	-2.65 – 3.02 (0.19)	0.156 – 0.966 (0.561)	-	-0.0017 – 0.0004 (-0.0007)	0.008 – 0.014 (0.011)	-0.012 – 0.025 (0.007)	-0.0002 – 0.0005 (0.0002)	-0.383 – 0.106 (-0.138)
5	Live canopy cover (unburned sites only)	Summer mean Tmax	39.99 – 47.73 (43.86)	-	-0.188 – 0.079 (-0.054)	-0.0104 – -0.0078 (-0.0091)	-0.002 – 0.005 (0.002)	-0.025 – 0.014 (-0.006)	-0.0001 – 0.0006 (0.0003)	-0.350 – 0.135 (-0.107)
6		Summer mean Tmin	-7.19 – 3.33 (-1.93)	-	0.004 – 0.382 (0.193)	-0.0013 – 0.0023 (0.0005)	0.005 – 0.014 (0.010)	-0.017 – 0.037 (0.010)	-0.0043 – 0.0009 (0.0004)	-0.436 – 0.181 (-0.127)
7		Winter mean Tmax	27.13 – 38.46 (32.80)	-	-0.245 – 0.073 (-0.086)	-0.0112 – -0.0074 (-0.0093)	-0.0050 – 0.0043 (-0.0004)	-0.028 – 0.017 (-0.005)	0.0000 – 0.0008 (0.0004)	-0.672 – -0.070 (-0.371)
8		Winter mean Tmin	-17.38 – -5.43 (-11.40)	-	-0.026 – 0.416 (0.195)	-0.0018 – 0.0022 (0.0002)	0.0085 – 0.0188 (0.0137)	-0.024 – 0.038 (0.007)	-0.0003 – 0.0009 (0.0003)	-0.617 – 0.205 (-0.206)

Disturbance Effects on Temperature

We observed a very slight decrease in predicted summer Tmax with increasing live tree basal area when all other standardized covariates were held at their zero means (Figure 3-6). Predicted summer Tmin and winter Tmax/Tmin increased with increasing live tree basal area such that sites with no live overstory were expected to have winter minimum temperatures approximately 1-2 °C cooler than sites with the highest amounts of live basal area (~45 cm^2/m^2). Figure 3-7 shows simulated temperature changes from pre- to post-beetle outbreak for sampled sites along an axis of overstory *P. engelmannii* percent mortality (dead spruce basal area as a percent of total live/dead basal area). Simulated values gave a maximum difference in winter Tmin of ~1.5 °C at sites with 100% beetle-caused mortality. Credible intervals (95%) for temperature differences in burned vs. unburned sites with similar topographic settings are ~0.2 – 1.0 °C for Tmax and ~-0.2 – 1.0 °C for Tmin.
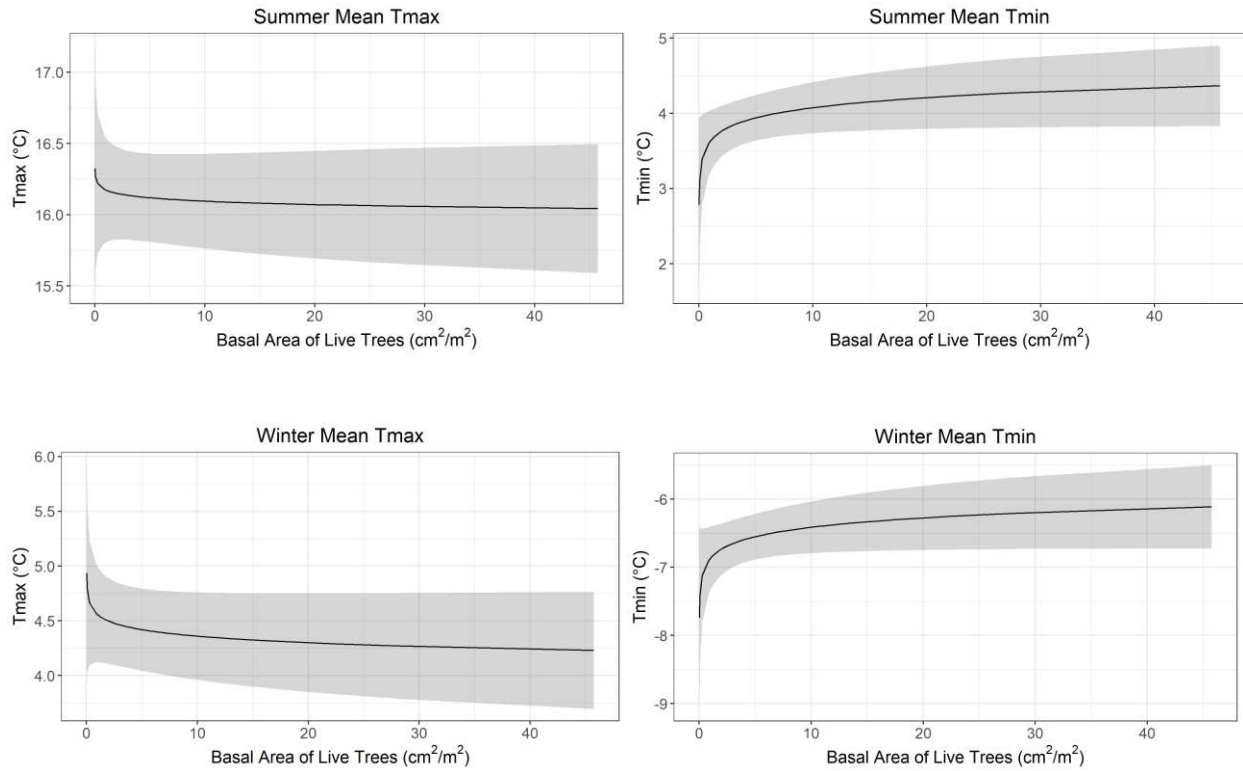
Figure 3-6. Marginal effects plots showing the effect of increasing live tree basal area on summer mean Tmax/Tmin and winter mean Tmax/Tmin at mean values of all topographic variables in unburned, beetle-killed models. Black line indicates mean of the posterior distribution for predicted temperature values, gray ribbon indicates 95% credible interval.
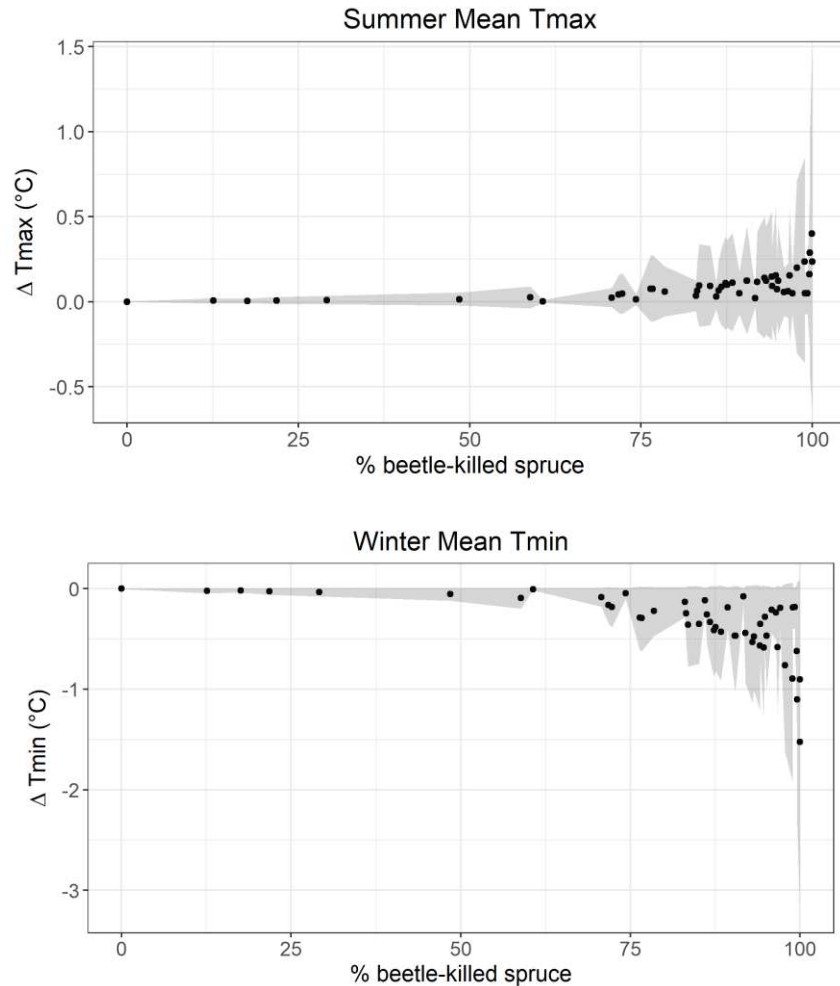
Figure 3-7. Simulated difference in summer Tmax and winter Tmin in beetle-killed sites, plotted along an axis of spruce overstory mortality %. Points indicate means of posterior distributions for predicted values, gray ribbon indicates 95% confidence intervals.

Discussion

SPDE model results indicate that canopy-removing disturbances influence below-canopy microclimates, although the nature and magnitude of the change varies with disturbance type and severity. Burned sites are, on average, ~0.25 – 0.50 °C warmer than unburned sites when topographic variables are included. Conversely, beetle-killed sites experience mean overnight cooling of ~1.0 °C compared to sites with abundant live canopy in comparable topographic settings, but do not experience significantly warmer daytime maximum temperatures. These

temperature effects are small but significant in relation to the overall range of temperatures resulting from topographic variation (~10 °C difference between highest and lowest-elevation sites).

Importance of Topography and Canopy Variables

Our modeled coefficients for topographic variables are mostly consistent with those of previous studies modeling topoclimate at fine spatial scales. Working in the Sierra Nevadas, Dobrowski, Abatzoglou, Greenberg, & Schladow (2009) similarly found that elevation was a strong driver of daytime maximum temperatures but that relative elevation was a more significant driver of overnight minimum temperatures. Topographic relief and cold air drainage is typically an important process in steep mountain environments when temperatures are cold (Barry, 2008), which likely explains why relative elevation had a strong effect on daily maximum temperatures in winter but not summer. Additionally, we found that increasing Taspect (i.e., more northeast-facing slopes) were associated with lower wintertime maximum temperatures but showed no effect on summertime temperatures. This may be because north-facing slopes retain more snowpack at high-elevation Rocky Mountain sites, which may contribute more substantially to cooling in the winter than in the summer when snow has melted on both north and south-facing slopes (Tennant et al., 2017). Our temperature records represent a year with exceptionally low snowpack and a warm winter, so it is not clear whether these effects would be seen in years with normal snowpack. However, winters like the one of 2017-2018 may be indicative of normal conditions in the next few decades.

In contrast to our results, other studies have previously shown that forest canopies have a significant cooling effect on daytime maximum temperatures (Ashcroft & Gollan, 2012; Greiser et al., 2018). A key difference between our study and previous studies is that we examined the

effect of canopy variation due to spruce beetle disturbance as opposed to harvesting or variations in forest vs. non-forest. Spruce beetle-killed sites contain many dead standing trees which may still play a functional role in shading the ground surface, while a lack of soil disturbance allows for greater understory vegetation cover which may reduce temperatures through evapotranspiration (Geiger, 1950; Jonášová & Prach, 2004). It is also important to note that our study sites were all located in stands which had been impacted by bark beetle in approximately the last decade, and that killed spruce trees still retain branches and larger twigs after losing their needles (Figure 3-8). The burned area also contained many standing dead trees, but the fire had consumed most canopy material but the boles (Figure 3-8). Furthermore, Ashcroft & Gollan (2012) noted that cooling effects were only significant when canopies were very dense (>90% canopy cover). While our study sites included undisturbed canopies, it is possible that coniferous forest at our maximum measured live basal area (~45 m^2/ha) was not sufficient to create an observable cooling effect.

Figure 3-8. Left: A typical beetle-killed spruce stand with fine material attached to standing dead trees. Right: Burned trees with only boles and large branches remaining.

Ecological Implications

We found that sites within the West Fork Complex burn area experience warmer maximum and minimum daily temperatures compared to sites in similar topographic settings in forested area outside the burned area. This warming can potentially exacerbate broader warming trends, leading to reduced snowpack, earlier snowmelt, and greater soil drying throughout the summer (González et al., 2018). This drying effect may limit germination of *P. engelmannii* and *A. lasiocarpa* seedlings in years where precipitation is too low to provide adequate moisture (Andrus, Harvey, Rodman, Hart, & Veblen, 2018). However, snowpack depletion and limitations in seedling establishment will vary along substantial topographic gradients. Lower-elevation, more southwest-facing sites are more likely to experience depleted snowpack and limited seedling re-establishment than higher-elevation, northeast-facing sites. Furthermore, our results suggest that sites with low relative elevation (i.e., valley bottoms) experience cooler minimum and wintertime maximum temperatures, though they will not necessarily mitigate extreme summer maximum temperatures. These cooler temperatures may favor snowpack retention and reduce overall soil moisture loss, creating more favorable conditions for spruce-fir regeneration and refugia for forest species during periods of drought.

Our results indicate that disturbance from spruce beetle outbreak, in contrast to disturbance from high-severity fire, does not exacerbate warming trends. Rather, partial canopy removal appears to reduce mean temperatures by increasing overnight cooling. This disturbance may therefore favor continued seedling germination for *P. engelmannii* and *A. lasiocarpa* despite the declines predicted by species distribution models based on projected shifts in annual mean temperature (Bell et al., 2014a). This cooling may also favor snowpack retention, as well as buffer against warming-related shifts in understory vegetation composition (De Frenne et al.,

2013). However, the increase in diurnal temperature ranges resulting from cooling of overnight temperatures may produce a number of less predictable ecological effects. For example, broader warming trends may contribute to early spring snowmelt which may increase risks of frost damage to vegetation in beetle-killed stands experiencing colder overnight temperatures (Williams, Henry, & Sinclair, 2015).

Implications for Climate-Driven Ecosystem Transitions

Disturbances have the potential to accelerate shifts in forest species composition and ecosystem properties in response to climate change (Overpeck et al., 1990; Thom, Rammer, & Seidl, 2017). Abrupt and widespread mortality in dominant canopy species alters competitive interactions, opens up opportunities for new species to establish on forest floors, and may reduce rates of dispersal and regeneration, allowing species to be more rapidly replaced by more warm-adapted species (Johnstone et al., 2016). Our results indicate that disturbance also play an important role in regulating how organisms beneath the forest canopy experience warming trends. Because our study area is located in a region where climate suitability for subalpine forest species is projected to decline substantially by the end of the 21st century (Bell et al., 2014b), microclimate buffering from both topography and disturbance may have an important influence on when and where climatic tipping points are reached.

The warming observed within the West Fork Complex burn perimeter, in which most sampled sites experienced 100% canopy mortality, suggests that severe wildfires may be important processes accelerating climate-driven ecosystem transitions. Increased exposure to extreme high temperatures and soil drying may lead to reduced seedling establishment, predicting a decline in the previously dominant forest community (Stevens-Rumann et al., 2018; Turner, 2010). These shifts toward warmer and drier microclimates compound additional

limitations on forest community resilience resulting from reduced seed dispersal within large, high-severity burn patches (Harvey, Donato, & Turner, 2016) and alterations to soil water-holding capacity and biota (Certini, 2005; Savage, Mast, & Feddema, 2013).

It is less clear from our results how spruce beetle outbreak may interact with broader warming patterns to influence species persistence. Previous research has shown that regeneration is not typically inhibited in bark beetle-killed stands, although post-outbreak harvesting may shift regeneration dominance away from shade-tolerant species (Collins, Rhoades, Hubbard, & Battaglia, 2011). Our results suggest that unmanaged beetle-killed stands may be sufficiently shaded by standing dead trees to not experience an increase in daytime maximum temperatures. However, management actions such as salvage logging may result in post-disturbance conditions more closely mimicking those of a severely burned site with elevated daytime temperatures, thereby increasing the likelihood of regeneration failures due to increased soil surface warming and drying (Hood, Nelson, Rhoades, & Tinker, 2017). Additionally, stands may experience further temperature increases over time as standing dead trees fall. Fallen logs may create favorable microenvironments for seedling establishment, but it is not clear how these microclimates may interact with changes in below-canopy topoclimate to affect long-term recruitment and survival patterns. Processes of tree-fall and decomposition after beetle outbreaks will continue to impact stands for many decades, and how ecosystem shifts will be impacted by these long-term legacies is a remaining question.

Climate-driven ecosystem transitions are most likely to occur at the warm edges of species distributions, such as low-elevation, southwest-facing slopes lacking cold-air drainage or moisture-collecting features (Hoylman et al., 2018). Our results indicate that wildfires and bark beetle outbreak also play a role in determining the fine-scale spatial patterns of exposure to high

temperatures. However, interactions between disturbance-related changes to microclimate and overall warming trends are complex. Notably, bark beetle outbreaks may mitigate trends in increasing minimum temperatures. Because minimum temperatures have increased more rapidly than maximum temperatures over the last several decades in the central San Juans (Rangwala & Miller, 2010), spruce beetle outbreaks have the potential to enhance forest stand resilience against warming trends. Decreased overnight temperatures may help sites retain soil moisture throughout the growing season and prevent invasions by more warm-adapted species. However, it should be noted that needle loss from bark beetle outbreaks has been shown to accelerate snowmelt as a result of increased below-canopy solar radiation, resulting in depleted overall snowpack in spite of the fact that needle loss also reduces snowfall interception (Pugh & Small, 2013).

Conclusions

Our below-canopy temperature records indicate that forest microclimates are influenced by fine-scale topography as well as by canopy disturbance patterns in a mountain landscape severely impacted by wildfire and spruce beetle outbreaks. Severely burned sites experienced an overall temperature increase compared to unburned forest in similar topographic settings. However, decreasing canopy cover in unburned, beetle-killed sites was associated with decreases in overnight minimum temperatures and no significant change in daytime maximum temperatures. These results indicate that wildfires may play a role in accelerating climate-driven species transitions in mountain forests by compounding regional warming trends, particularly at the warm edges of distributions for high-elevation species. Reductions in minimum temperatures in severely beetle-killed forests may play some role in mitigating warming trends, at least as long as sites are dominated by standing dead trees with an undisturbed ground surface. These

differing effects of disturbance on fine-scale temperatures greatly complicate patterns of climate

change exposure on forests, particularly in landscapes with complex topography.

LITERATURE CITED

Abatzoglou, J. T., & Williams, A. P. (2016). Impact of anthropogenic climate change on wildfire across western US forests. *PNAS*, *113*(42), 11770–11775.

Ackerly, D. D., Loarie, S. R., Cornwell, W. K., Weiss, S. B., Hamilton, H., Branciforte, R., & Kraft, N. J. B. (2010). The geography of climate change: implications for conservation biogeography. *Diversity and Distributions*, *16*(3), 476–487.

Allen, C. D., Macalady, A. K., Chenchouni, H., Bachelet, D., McDowell, N., Vennetier, M., … others. (2010). A global overview of drought and heat-induced tree mortality reveals emerging climate change risks for forests. *Forest Ecology and Management*, *259*(4), 660–684.

Andrus, R. A., Harvey, B. J., Rodman, K. C., Hart, S. J., & Veblen, T. T. (2018). Moisture availability limits subalpine tree establishment. *Ecology*, *99*(3), 567–575.

Angus, J. (1994). The probability integral transform and related results. *SIAM Review*, *36*(4), 652–654.

Ashcroft, M. B. (2010). Identifying refugia from climate change. *Journal of Biogeography*, *37*(8), 1407–1413.

Ashcroft, M. B., & Gollan, J. R. (2012). Fine-resolution (25 m) topoclimatic grids of near-surface (5 cm) extreme temperatures and humidities across various habitats in a large (200 × 300 km) and diverse region. *International Journal of Climatology*, *32*(14), 2134–2148.

Austin, M. P., & Van Niel, K. P. (2011). Improving species distribution models for climate change studies: variable selection and scale. *Journal of Biogeography*, *38*(1), 1–8.

Bakka, H., Rue, H., Fuglstad, G. A., Riebler, A., Bolin, D., Illian, J., ... & Lindgren, F. (2018). Spatial modeling with R-INLA: A review. *Wiley Interdisciplinary Reviews: Computational Statistics, 10*(6), e1443.

Barry, R. G. (2008). *Mountain weather and climate* (3rd ed., Vol. 148). Retrieved from http://www.jstor.org/stable/633166.

Beers, T., Dress, P., & Wensel, L. (1966). Notes and observations: aspect transformation in site productivity research. *Journal of Forestry*, *64*(10), 691–692.

Bell, D. M., Bradford, J. B., & Lauenroth, W. K. (2014a). Early indicators of change: divergent climate envelopes between tree life stages imply range shifts in the western United States. *Global Ecology and Biogeography*, *23*(2), 168–180.

Bell, D. M., Bradford, J. B., & Lauenroth, W. K. (2014b). Mountain landscapes offer few opportunities for high-elevation tree species migration. *Global Change Biology*, *20*(5), 1441–1451.

Bergen, J. (1968). Cold air drainage on a forested mountain slope. *Bulletin of the American Meterological Society*, *49*(3), 301-.

Bristow, K., & Campbell, G. (1984). On the relationship between incoming solar-radiation and daily maximum and minimum temperature. *Agricultural and Forest Meteorology*, *31*(2), 159–166.

Bruening, J. B., Tran, T. J., Bunn, A. G., Weiss, S. B., & Salzer, M. W. (2017). Fine-scale modeling of bristlecone pine treeline position in the Great Basin, USA. *Environmental Research Letters*, *12*(1).

Carlson, A. R., Sibold, J. S., Assal, T. J., & Negron, J. F. (2017). Evidence of compounded disturbance effects on vegetation recovery following high-severity wildfire and spruce beetle outbreak. *PLoS ONE*, *12*(8).

Certini, G. (2005). Effects of fire on properties of forest soils: a review. *Oecologia*, *143*(1), 1–10.

Chen, J., Saunders, S. C., Crow, T. R., Naiman, R. J., Brosofske, K. D., Mroz, G. D., … Franklin, J. F. (1999). Microclimate in Forest Ecosystem and Landscape Ecology: Variations in local climate can be used to monitor and compare the effects of different management regimes. *BioScience*, *49*(4), 288–297.

Collins, B. J., Rhoades, C. C., Hubbard, R. M., & Battaglia, M. A. (2011). Tree regeneration and future stand development after bark beetle infestation and harvesting in Colorado lodgepole pine stands. *Forest Ecology and Management*, *261*(11), 2168–2175.

CSFS. (2018). *2017 Report on the Health of Colorado's Forests: Meeting the Challenge of Dead and At-Risk Trees* (p. 21). Fort Collins, CO: Colorado State Forest Service.

De Frenne, P., Rodríguez-Sánchez, F., Coomes, D. A., Baeten, L., Verstraeten, G., Vellend, M., … Verheyen, K. (2013). Microclimate moderates plant responses to macroclimate warming. *PNAS*, *110*(46), 18561–18565.

Dobrowski, S. Z. (2011). A climatic basis for microrefugia: the influence of terrain on climate. *Global Change Biology*, *17*(2), 1022–1035.

Dobrowski, S. Z., Abatzoglou, J. T., Greenberg, J. A., & Schladow, S. G. (2009). How much influence does landscape-scale physiography have on air temperature in a mountain environment? *Agricultural and Forest Meteorology*, *149*(10), 1751–1758.

Dobrowski, S. Z., Swanson, A. K., Abatzoglou, J. T., Holden, Z. A., Safford, H. D., Schwartz, M. K., & Gavin, D. G. (2015). Forest structure and species traits mediate projected recruitment declines in western US tree species. *Global Ecology and Biogeography*, *24*(8), 917–927.

ESRI. (2016). ArcGIS Desktop (Version 10.4). Redlands, CA: Enviornmental Research Systems Institute.

Frey, S. J. K., Hadley, A. S., Johnson, S. L., Schulze, M., Jones, J. A., & Betts, M. G. (2016). Spatial models reveal the microclimatic buffering capacity of old-growth forests. *Science Advances*, *2*(4).

Fuglstad, G.-A., Simpson, D., Lindgren, F., & Rue, H. (2018). Constructing Priors that Penalize the Complexity of Gaussian Random Fields. *Journal of the American Statistical Association*, *0*(0), 1–8.

Geiger, R. (1950). *The Climate Near the Ground*. Cambridge, MA: Harvard University Press.

Gelman, A., Hwang, J., & Vehtari, A. (2014). Understanding predictive information criteria for Bayesian models. *Statistics and Computing, 24*(6), 997-1016.

González, P., Garfin, G. M., Breshears, D. D., Brooks, K. M., Brown, H. E., Elias, E. H., … Udall, B. H. (2018). *Ch. 25: Southwest* (pp. 1101–1184). Washington, D.C.: U.S. Global Change Research Program.

Greiser, C., Meineri, E., Luoto, M., Ehrlen, J., & Hylander, K. (2018). Monthly microclimate models in a managed boreal forest landscape. *Agricultural and Forest Meteorology*, *250*, 147–158.

Harvey, B. J., Donato, D. C., & Turner, M. G. (2016). High and dry: post-fire tree seedling establishment in subalpine forests decreases with post-fire drought and large stand-replacing burn patches. *Global Ecology and Biogeography*, *25*(6), 655–669.

Holden, Z. A., Klene, A. E., Keefe, R. F., & Moisen, G. G. (2013). Design and evaluation of an inexpensive radiation shield for monitoring surface air temperatures. *Agricultural and Forest Meteorology*, *180*(Supplement C), 281–286.

Holden, Z. A., Swanson, A., Klene, A. E., Abatzoglou, J. T., Dobrowski, S. Z., Cushman, S. A., … Oyler, J. W. (2016). Development of high-resolution (250 m) historical daily gridded air temperature data using reanalysis and distributed sensor networks for the US Northern Rocky Mountains. *International Journal of Climatology*, *36*(10), 3620–3632.

Hood, P. R., Nelson, K. N., Rhoades, C. C., & Tinker, D. B. (2017). The effect of salvage logging on surface fuel loads and fuel moisture in beetle-infested lodgepole pine forests. *Forest Ecology and Management*, *390*, 80–88.

Hoylman, Z. H., Jencso, K. G., Hu, J., Martin, J. T., Holden, Z. A., Seielstad, C. A., & Rowell, E. M. (2018). Hillslope Topography Mediates Spatial Patterns of Ecosystem Sensitivity to Climate. *Journal of Geophysical Research: Biogeosciences*, *123*(2), 353–371.

Isaak, D. J., Wenger, S. J., & Young, M. K. (2017). Big biology meets microclimatology: defining thermal niches of ectotherms at landscape scales for conservation planning. *Ecological Applications*, *27*(3), 977–990.

Johnstone, J. F., Allen, C. D., Franklin, J. F., Frelich, L. E., Harvey, B. J., Higuera, P. E., … Turner, M. G. (2016). Changing disturbance regimes, ecological memory, and forest resilience. *Frontiers in Ecology and the Environment*, *14*(7), 369–378.

Landhaeusser, S. M., Deshaies, D., & Lieffers, V. J. (2010). Disturbance facilitates rapid range expansion of aspen into higher elevations of the Rocky Mountains under a warming climate. *Journal of Biogeography*, *37*(1), 68–76.

Lenoir, J., Graae, B. J., Aarrestad, P. A., Alsos, I. G., Armbruster, W. S., Austrheim, G., … Svenning, J.-C. (2013). Local temperatures inferred from plant communities suggest strong spatial buffering of climate warming across Northern Europe. *Global Change Biology*, *19*(5), 1470–1481.

Lindgren, F., & Rue, H. (2015). Bayesian spatial modelling with R-INLA. *Journal of Statistical Software, 63*(19), 1-25.

Lindgren, F., Rue, H., & Lindstrom, J. (2011). An explicit link between Gaussian fields and Gaussian Markov random fields: the stochastic partial differential equation approach. *Journal of the Royal Statistical Society Series B-Statistical Methodology*, *73*(4), 423–498.

Ma, S., Concilio, A., Oakley, B., North, M., & Chen, J. (2010). Spatial variability in microclimate in a mixed-conifer forest before and after thinning and burning treatments. *Forest Ecology and Management*, *259*(5), 904–915.

Meddens, A. J. H., Hicke, J. A., & Ferguson, C. A. (2012). Spatiotemporal patterns of observed bark beetle-caused tree mortality in British Columbia and the western United States. *Ecological Applications*, *22*(7), 1876–1891.

Meineri, E., & Hylander, K. (2017). Fine-grain, large-domain climate models based on climate station and comprehensive topographic information improve microrefugia detection. *Ecography*, *40*(8), 1003–1013.

MTBS. (2013). *Monitoring Trends in Burn Severity* [online data]. Retrieved from: mtbs.gov.

Overpeck, J. T., Rind, D., & Goldberg, R. (1990). Climate-induced changes in forest disturbance and vegetation. *Nature*, *343*(6253), 51–53.

Pugh, E. T., & Small, E. E. (2013). The impact of beetle-induced conifer death on stand-scale canopy snow interception. *Hydrology Research*, *44*(4), 644–657.

R Core Team (2019). R: A language and environment for statistical computing. Vienna, Austria: *R Foundation for Statistical Computing*. http://www.R-project.org/

Rangwala, I., & Miller, J. R. (2010). Twentieth century temperature trends in Colorado's San Juan Mountains. *Arctic, Antarctic, and Alpine Research*, *42*(1), 89–97.

Rother, M. T., & Veblen, T. T. (2016). Limited conifer regeneration following wildfires in dry ponderosa pine forests of the Colorado Front Range. *Ecosphere*, *7*(12).

Rue, Havard, & Held, L. (2005). *Gaussian Markov Random Fields: Theory and Applications* (1st ed.). New York: Chapman & Hall.

Rue, Håvard, Riebler, A., Sørbye, S. H., Illian, J. B., Simpson, D. P., & Lindgren, F. K. (2017). Bayesian Computing with INLA: A Review. *Annual Review of Statistics and Its Application*, *4*(1), 395–421.

Rue, H., Martino, S., & Chopin, N. (2009). Approximate Bayesian inference for latent Gaussian models by using integrated nested Laplace approximations. *Journal of the Royal Statistical Society: Series B (Statistical Methodology), 71*(2), 319-392.

Savage, M., Mast, J. N., & Feddema, J. J. (2013). Double whammy: high-severity fire and drought in ponderosa pine forests of the Southwest. *Canadian Journal of Forest Research*, *43*(6), 570–583.

Seidl, R., Thom, D., Kautz, M., Martin-Benito, D., Peltoniemi, M., Vacchiano, G., … Reyer, C. P. O. (2017). Forest disturbances under climate change. *Nature Climate Change*, *7*(6), 395–402.

Simpson, D., Rue, H., Riebler, A., Martins, T. G., & Sorbye, S. H. (2017). Penalising Model Component Complexity: A Principled, Practical Approach to Constructing Priors. *Statistical Science*, *32*(1), 1–28.

Stevens-Rumann, C. S., Kemp, K. B., Higuera, P. E., Harvey, B. J., Rother, M. T., Donato, D. C., … Veblen, T. T. (2018). Evidence for declining forest resilience to wildfires under climate change. *Ecology Letters*, *21*(2), 243–252.

Tennant, C. J., Harpold, A. A., Lohse, K. A., Godsey, S. E., Crosby, B. T., Larsen, L. G., … Glenn, N. F. (2017). Regional sensitivities of seasonal snowpack to elevation, aspect, and vegetation cover in western North America. *Water Resources Research*, *53*(8), 6908–6926.

Thom, D., Rammer, W., & Seidl, R. (2017). Disturbances catalyze the adaptation of forest ecosystems to changing climate conditions. *Global Change Biology*, *23*(1), 269–282.

Turner, M. G. (2010). Disturbance and landscape dynamics in a changing world. *Ecology*, *91*(10), 2833–2849.

Wilkin, K. M., Ackerly, D. D., & Stephens, S. L. (2016). Climate Change Refugia, Fire Ecology and Management. *Forests*, *7*(4).

Williams, C. M., Henry, H. A. L., & Sinclair, B. J. (2015). Cold truths: how winter drives responses of terrestrial organisms to climate change. *Biological Reviews*, *90*(1), 214–235.

CHAPTER 4: Canopy Structure, Seed Dispersal, and Fine-Scale Climate Interact to
Shape Seedling Response to Disturbance in a Rocky Mountain Subalpine Forest

Summary

Warming climates are creating disturbance regime shifts in western North American forests, particularly by causing large, severe wildfires and extensive bark beetle outbreaks. In this study we examined the response of seed dispersal and conifer seedling establishment to recent wildfire and spruce beetle (*Dendroctonus rufipennis*) outbreak in a subalpine spruce-fir forest in the San Juan Mountains, Colorado, and determined implications for ecosystem resilience. We assessed Engelmann spruce (*Picea engelmannii*) seed availability by establishing seed traps in areas burned by the West Fork Complex fire, and in surrounding unburned forest affected by the spruce beetle. We conducted conifer seedling counts at each seed trap site to assess recent (<10 years) establishment, and assessed effects of temperature on seedling abundance using Logtag® temperature sensors. These measurements were then used to determine 1) how seed availability varies within the burn area and across varying levels of spruce beetle severity, and 2) how seedling regeneration is affected by seed availability, temperatures, canopy cover, and understory cover. We found very low rates of both seed dispersal and conifer seedling establishment in the burned area, though there was abundant aspen regeneration at lower elevations. In unburned, beetle-killed forests, we found that the severity of spruce overstory mortality did not strongly affect seed availability but nevertheless appeared to have a strong negative effect on spruce seedling densities. Seedling densities for both spruce and subalpine fir (*Abies lasiocarpa*) were also influenced by below-canopy temperatures, aspect, and understory litter and shrub cover. These results indicate that the West Fork Complex fire has potentially resulted in a long-term loss of conifer forest. High-severity spruce beetle outbreaks have also limited regeneration,

although seedlings are still present in the majority of beetle-killed sites. Future patterns of re-establishment will also be strongly influenced by topography and future warming trends.

Introduction

Forest ecosystems of western North America have long experienced periodic disturbances from bark beetle outbreaks and wildfires. However, climate change creates doubt around whether ecosystems can be expected to recover as they have in the past (IPCC, 2014). Evidence from around the globe suggests that forest disturbance frequency, severity, and extent are increasing as a result of warming temperatures, and that these novel disturbance regimes may exceed species' recovery mechanisms (Allen et al., 2010; Seidl et al., 2017). Furthermore, warming temperatures and drought stress may create unsuitable conditions for re-establishment by tree species which originally established under much cooler climates decades or centuries ago (Johnstone et al., 2016).

For the past two decades, abnormally hot and dry conditions have caused unprecedented bark beetle outbreaks and wildfire activity in the southern Rocky Mountains (Bentz et al., 2010; Rocca, Brown, MacDonald, & Carrico, 2014). Bark beetles have caused tens of millions of hectares of conifer mortality across western North America, while annual area burned in the southern Rockies has more than tripled since the 1970's (Westerling, 2016). Recent studies documented declines in seedling recruitment following forest fires in the Rockies which have been attributed to warm, arid post-fire conditions (Harvey, Donato, & Turner, 2016; Rother & Veblen, 2016; Savage, Mast, & Feddema, 2013; Stevens-Rumann et al., 2018). Increasing fire size and severity may also contribute to reduced establishment, as non-serotinous species such as Engelmann spruce (*Picea engelmannii*) and subalpine fir (*Abies lasiocarpa*) are not able to disperse large distances into the interiors of burned patches with no available seed sources

(Harvey et al., 2016; Turner, Romme, & Gardner, 1999; Urza & Sibold, 2017). Impacts of bark beetle outbreaks on seedling recruitment have not been as widely documented, but there is evidence that higher-severity outbreaks may limit recruitment of shade-tolerant species (Pelz, Rhoades, Hubbard, & Smith, 2018).

There are several mechanisms by which increasing disturbance severity may reduce species' resilience to extreme events (Holling, 1973). In addition to reducing seed source availability within severe burn patches, severe wildfires may also alter soil chemistry, lead to severe erosion, and elevate ground-surface temperatures (Carlson, Sibold, Assal, & Negron, 2017; Certini, 2005; Carlson et al., *in prep*). Bark beetle outbreaks typically affect the canopy less than fire and do not disturb the soil surface, but may impact seedling regeneration by selectively killing large, seed-producing trees (Schmid & Frye, 1977). Canopy mortality additionally alters microclimate, light environments, and soil moisture on the ground surface, and may increase seedling exposure to warming temperatures (Dobrowski et al., 2015; Edburg et al., 2012). However, canopy disturbance can also promote regeneration with suitable temperature and moisture conditions and sufficient seed supply. Fires expose mineral soils and provide opportunities for seedling establishment (Johnstone & Chapin, 2006), while bark beetle outbreaks may release the growth of understory seedlings and create ideal seedling microhabitats under downed logs (Jonášová & Prach, 2004; Veblen, Hadley, & Reid, 1991).

Disturbances may complicate expected species shifts toward higher elevations and latitudes in response to climate change (Turner, 2010). Patches of overstory mortality with varying severity may result in differing patterns of seedling establishment, which may or may not correspond with warming patterns (Redmond & Kelsey, 2018). Because forests are slow-growing, and seedlings are more vulnerable to climate than adult trees, post-disturbance

98

establishment successes and failures will have long-term effects on the future trajectories of forests (Bell, Bradford, & Lauenroth, 2014; Perovich & Sibold, 2016). Understanding how forests are currently regenerating after severe overstory mortality events in the Rocky Mountains will improve understanding of future forest vulnerabilities to high temperatures and drought (Johnstone et al., 2016).

Disturbances may make species more vulnerable to climatic stress in subalpine forests of the southern Rockies (~2,700-3,600m in elevation; Dobrowski et al., 2015). Dominant spruce and fir species are shade-tolerant and do not benefit greatly from increased light availability following canopy removal (Knapp & Smith, 1982). Seedling germination and survival also depends on adequate soil moisture and snowpack (Andrus, Harvey, Rodman, Hart, & Veblen, 2018), which may be reduced by disturbance (Pugh & Small, 2013). However, seedlings may benefit from longer growing seasons (Hill, Ex, Aldridge, & Prolic, 2019). Furthermore, the topographic complexity of the southern Rockies may create fine-scale patches across the landscape where topographic conditions (i.e., north-facing slopes, high elevations, and cold-air drainages) allow sites to remain sufficiently cool and moist to continue supporting cold-adapted spruce and fir (Dobrowski, 2011). Canopy loss from bark beetle outbreaks may additionally result in cooling of overnight temperatures, mitigating the effects of warming on soil moisture and snowpack losses (Carlson et al., *in prep*).

The aim of this study was to determine how severe bark beetle outbreaks and wildfire in the San Juan Mountains of southwest Colorado have influenced seedling establishment rates. This region is warming rapidly, with an increase in mean annual temperature of ~1.6 °C since 2000 (PRISM climate data, http://prism.nacse.org). The area also experienced a severe drought from the fall of 2017 to the summer of 2018. Engelmann spruce (*Picea engelmannii*)-dominated

forests in this area have undergone one of the most severe outbreaks of spruce beetles (*Dendroctonus rufipennis*) of the ongoing North American outbreak, beginning ca. 2004 (CSFS, 2018), and in 2013 over 110,000 ha of spruce-fir forest were burned by the West Fork Complex wildfire. In order to improve understanding of the drivers of potential ecosystem transitions, we used hierarchical Bayesian models to assess the effects of each disturbance (spruce beetle outbreak and fire) on seed dispersal, understory composition, and post-disturbance seedling recruitment densities. We used a network of *in situ* temperature sensors to assess how seedling densities were affected by variations in below-canopy climate due to differences in canopy cover and topographic setting. Determining the nature of relationships between disturbance severity, fine-scale temperatures, and seedling recruitment will improve understanding of how subalpine forests are responding to the combined influences of warming and disturbance.

Methods

Study Area

Field sampling was located within a ~625 km^2 area around Wolf Creek Pass in the eastern San Juan Mountains (Figure 4-1). Terrain is steep and varied with elevations ranging from ~2,700 to 3,600 m. The forest is dominated by Engelmann spruce and subalpine fir (*Abies lasiocarpa*). White fir (*Abies concolor*), Douglas fir (*Pseudotsuga menziesii*), blue spruce (*Picea pungens*), and quaking aspen (*Populus tremuloides*) are also present. The high-elevation climate is characterized by mild summers, cold winters, and a short growing season. Most precipitation falls as winter snow (514 mm/year average) or rains brought by monsoonal storms in July-September (262 mm/year average). The area was burned by the West Fork Complex wildfire in 2013, a 44,515-ha event which burned at moderate to high severity (MTBS, 2013). Most of the unburned forest is in the early gray stage following the spruce beetle outbreak, in which most

killed trees have lost all needles but are still standing with fine twigs and branches remaining in the canopy.
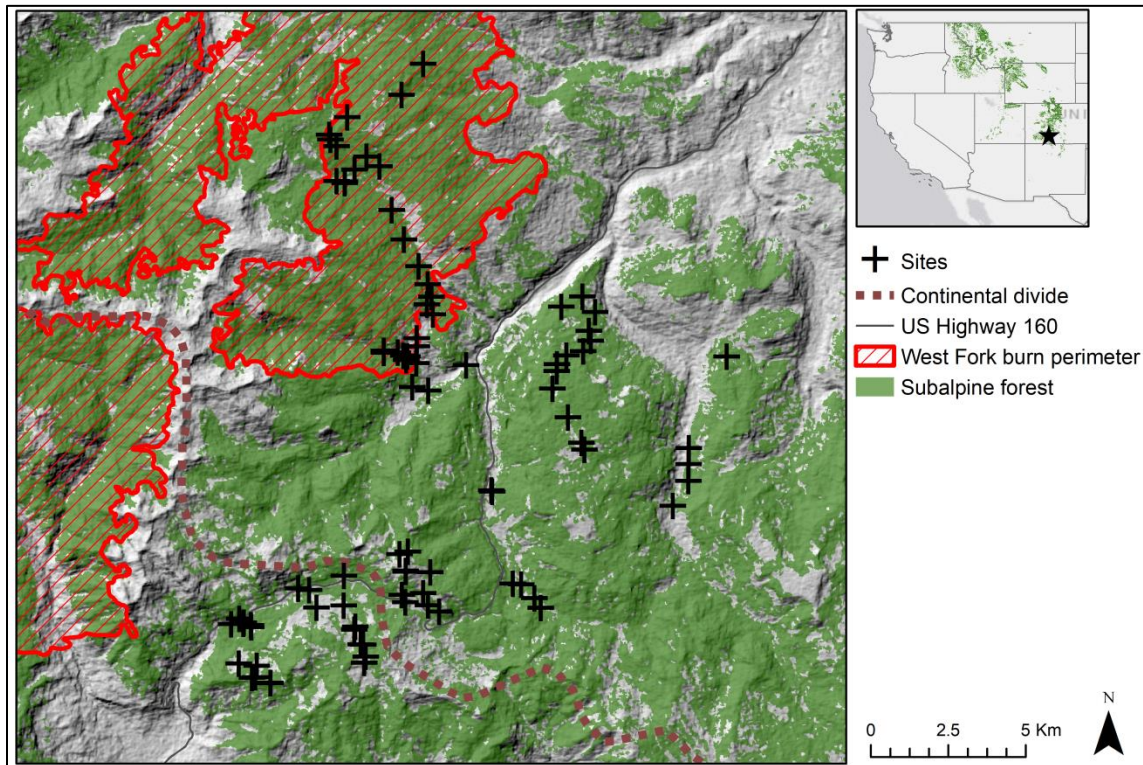
Figure 4-1. Map of study sites. Inset map shows the location of the study area within the western United States.

Field Data

    i.   Site Selection

We selected 58 sites in unburned forest and 27 sites in the West Fork Complex burn area to sample seedling abundance, seed dispersal, below-canopy temperatures, soil moisture, overstory mortality, understory composition, and seed counts. We selected sites in GIS to achieve a distribution of sites over gradients in elevation, aspect, topographic position, and spruce beetle outbreak severity. More sites were placed in unburned forest

in order to assess the effects of canopy cover gradients on temperature (Carlson et al., *in prep*) and seed abundance.

ii.   Seed Dispersal

We placed 30 cm × 30 cm square seed traps on the ground surface at each of our sites in order to sample wind-dispersed seed rain from *P. engelmannii* (PIEN) and other conifer species (FIR, mainly *A. lasiocarpa* with low abundances of *A. concolor* and *P. menziesii*). Insects and animals do not play a significant role in seed dispersal for any of these species (Alexander, 1987). Traps were square baskets constructed from fine mesh, covered with hardware cloth with 0.64-cm openings to prevent seed predation. The traps were then fixed to the ground with metal stakes. We initially placed the traps at each field site in early September, 2016, before the period of peak seed dispersal for PIEN (Alexander, 1987).

We collected seeds following snowmelt in June-early July of 2017 and again in late May-June of 2018. After separating PIEN seeds from litter and other material in the trap, we counted all viable conifer seeds. We used seeds from PIEN and FIR species to assess dispersal patterns in the burned area. In unburned sites, we only assessed the effect of PIEN seed counts on PIEN seedling abundance in order to assess the potential effect of spruce beetle outbreak on limiting seed dispersal. Because FIR species have not undergone major disturbance in our study area, we did not assess patterns in FIR seed abundance.

iii.   Temperature Data

We collected detailed temperature data for each of our sites using Logtag®
temperature sensors programmed to record every three hours. Sensors were placed inside
plastic radiation shields covered in reflective tape to prevent direct solar radiation, and
attached to tree trunks ~2 m above the ground. We initially placed sensors at each burned
and unburned site in the fall of 2016, at the same time that seed traps were placed. We
assessed seedling abundance in relation to temperatures recorded during the snow-free
season of 2017 (June-October). Temperature records were summarized as the mean of all
daily maximum and daily minimum temperatures over the growing-season period,
hereafter referred to as Tmax and Tmin.

We did not assess the effect of winter temperatures on seedling abundance for
three reasons: first, temperature records during the winter of 2016-2017 were unusable at
many sites due to influence of snow cover on the temperature sensors; second,
temperatures during the winter of 2017-2018 were affected by an exceptionally low
snowpack which may not be representative of the past decade in which our seedlings
established; and third, summer and winter temperatures were strongly correlated for
individual sites. While temperatures for a single growing season may not represent the
average conditions of the past several years of seedling recruitment, we assumed that
temperature records reflect topographic influences on climate that remain consistent over
time. Our goal was therefore not to determine absolute ideal temperatures for PIEN
seedlings, but to determine the extent to which seedling abundances are influenced by
these relative differences in temperature.

iv.   Canopy Cover and Topographic Characteristics

We assessed live canopy and overstory mortality at each unburned site within a 20 m × 20 m square plot area (**Error! Reference source not found.**). Plots were m easured from the tree where temperature sensors were fixed and extended 10 m in each of the four cardinal directions. We measured diameter at breast height (DBH) of all trees taller than breast height that were rooted within the plot and recorded species and live/dead status. DBH measurements were used to derive the total basal area of all live trees, of live PIEN, of live FIR, of live *P. tremuloides* (POTR), and of dead PIEN. To characterize site topography, we measured aspect and slope at all plot centers. We converted aspect to a relative northeast-to-southwest-facing scale using Taspect = sin(aspect + 45) + 1 (Beers, Dress, & Wensel, 1966).

v.   Understory

We measured understory composition using fifteen 1 m × 1 m subplots per plot (Figure 4-2). Subplots were placed at randomly selected intervals along the central north-south and east-west-running transects of the plot. We placed subplots using a PVC frame and visually estimated percent cover of each of eight understory classes: Moss, Grass, Forbs, Shrub, Litter, Bare, Coarse Woody Debris (CWD; defined as being >5 cm at the widest point), and Rock. Subplot percent cover estimates were then used to derive the mean and standard deviation of plot-level percent cover for each understory class.

vi.   Seedling Counts

We conducted seedling counts for each site during August-September of 2018. We measured the same 20 m × 20 m plot areas used to assess overstory and counted all tree species <1 m in height. Counts included both conifer and POTR seedlings. We

assessed seedling age for conifers by counting terminal bud scars associated with annual

growth, which has been shown to be a reasonably accurate method for aging PIEN

seedlings up to 14 years old (Urza & Sibold, 2013). In order to assess the effects of recent

disturbance on seedling impact we considered seedlings < 10 years old.
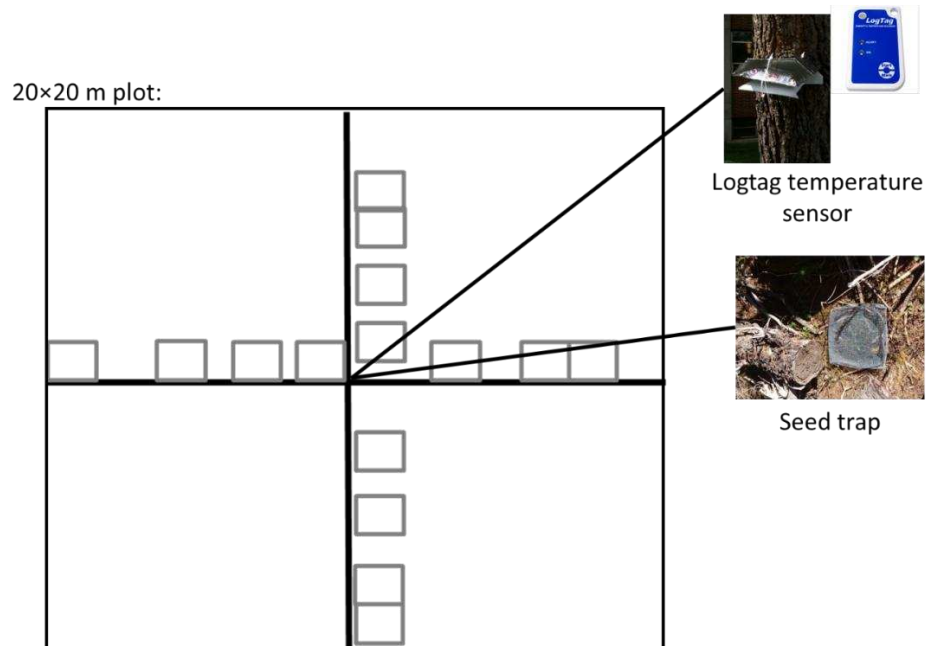
Figure 4-2. Diagram of field sampling design. Temperature sensors were mounted on tree trunks with seed traps placed at the base of the tree. Square area represents a 20×20 m plot centered around the sensor and seed trap along north-south and east-west axes, used to measure overstory basal area and seedling counts. Central lines represent transects used to place randomly spaced 1×1 m understory subplots (gray squares).

Analysis

Our analysis goals were to 1) determine the effect of disturbance on seed dispersal, and 2)

to determine the relative influence of seed dispersal, temperature, overstory, and understory on

post-disturbance PIEN and FIR seedling establishment. Due to low seedling counts in the burned

area, we only modeled abundances in unburned, beetle-killed sites. We assessed patterns of burn

severity on seed and seedling abundance in the burned area by mapping seedling counts over a

burn severity layer obtained from the Monitoring Trends in Burn Severity (MTBS) database

(https://mtbs.gov). For unburned sites, we used a Bayesian hierarchical modeling approach in order to account for uncertainty in understory cover and seed abundances. All models were fit by Markov Chain Monte Carlo simulations with 10,000 iterations, implemented with the JAGS (Just Another Gibbs Sampler) algorithm in the 'rjags' package in R (Plummer, 2017; Plummer, 2018; R Core Team, 2019).

i.   Seed Dispersal Model

We used a hierarchical Bayesian model to assess the relationship between live PIEN basal area and seed abundance in unburned sites. For sites with live PIEN, we calculated the basal area of all live PIEN trees at least 30 cm in diameter ($LivePIENOver30$). Although Alexander (1987) reported that a diameter of 38 cm is required for PIEN trees to become significant seed producers, there were only two sites with live trees of that diameter. Expected annual seed abundance at each site j was treated as a latent variable, $\lambda_{s,j}$, from which observed seed counts in 2017 and 2018 were drawn. Observed seed counts for each site and year i (s_{ij}) were modeled as a Poisson distribution with the mean, $\lambda_{s,j}$ predicted with the equations

$$\lambda_{s,j} \sim \text{gamma}\left(\frac{\mu_{s,j}^2}{\sigma_s^2}, \frac{\mu_{s,j}}{\sigma_s^2}\right)$$

$$\mu_{s,j} = \gamma_1 + \gamma_2\left(LivePIENOver30_j\right)$$

where γ_s's are unknown coefficients, $\mu_{s,j}$ is the mean of a gamma distribution predicting $\lambda_{s,j}$, and σ_s^2 is the unknown variance of the gamma distribution. μ_s and σ_s^2 were used to derive shape and rate parameters using moment-matching equations. γ's and σ_s^2 were assigned uninformative priors. The full posterior expression for the seed count model is

$$[\gamma_1, \gamma_2, \sigma_s^2 | \mathbf{s}] \sim \prod_{i=1}^{2} \prod_{j=1}^{58} \text{Poisson}(s_{i,j} | \lambda_{s,j})$$

$$\times \text{gamma}(\lambda_{s,j} | \gamma_1, \gamma_2, \sigma_s^2, LivePIENOver30)$$
$$\times \text{normal}(\gamma_1 | 0, 0.001)$$
$$\times \text{normal}(\gamma_2 | 0, 0.001)$$
$$\times \text{inverse gamma}(\sigma_s^2 | 0.001, 0.001)$$

ii.   Seedling Abundance Model

We used additional Bayesian models to determine how PIEN and FIR seedling counts varied with site temperature, aspect, overstory composition, and understory (all potential relationships are diagrammed in Figure 4-3; variable descriptions are given in Table 4-1). We fit models using both PIEN and FIR seedlings <10 years old as the response variable. For each site j, seedling count (y_j) was modeled as Poisson distributions with mean λ_j predicted by a linear combination of site variables (temperature, topography, and overstory; assumed to be measured without error), and hierarchical understory and seed count variables. The model is described by the equations

$$y_j \sim Poisson(\lambda_j)$$

$$\lambda_j = \exp(\beta_0 + \boldsymbol{\beta} X_j' + \boldsymbol{\beta}_U U_j' + \beta_s \lambda_{s,j})$$

where $\boldsymbol{X}$ is a matrix of predictor variables (those assumed to be measured without error), $\boldsymbol{U}$ is a matrix of latent understory cover values constrained by means and standard deviations of subplots, $\lambda_{s,j}$ is a latent variable representing annual mean seed count, and $\boldsymbol{\beta}, \boldsymbol{\beta}_U$ and β_s are coefficients. In these models, expected seed count (λ_s) was assigned an uninformative prior rather than being predicted by $LivePIENOver30$. This was because

a term for live PIEN overstory was already included in $\boldsymbol{X}$ as a direct effect on seedling

abundance. The full posterior expression for the seedling abundance model is

$$
\begin{aligned}
[\beta_0, \boldsymbol{\beta}_X, \boldsymbol{\beta}_U, \beta_s, \boldsymbol{\lambda}_s, \boldsymbol{U} | \boldsymbol{y}, \boldsymbol{s}] \sim & \prod_{i=1}^{2} \prod_{j=1}^{58} \text{Poisson}\left(y_j | \beta_0, \boldsymbol{\beta}_U, \boldsymbol{U}_j', \boldsymbol{\beta}_s, \lambda_{s,j}, \boldsymbol{\beta}_X, \boldsymbol{X}_j'\right) \\
& \times \text{Poisson}\left(s_{i,j} | \lambda_{s,j}\right) \text{gamma}\left(\lambda_{s,j} | 0.001, 0.001\right) \\
& \times \prod_{k=1}^{p_U} \text{beta}\left(\boldsymbol{U}_{j,k} | m_{j,k}, sd_{j,k}\right) \text{normal}(\beta_{U,k} | 0, 0.001) \\
& \times \prod_{l=1}^{p_X} \text{normal}(\beta_{X,l} | 0, 0.001) \\
& \times \text{normal}(\beta_s | 0, 0.001) \\
& \times \text{normal}(\beta_0 | 0., 0.001)
\end{aligned}
$$

where $m_{j,k}, sd_{j,k}$ are the observed mean and standard deviation of 15 understory subplots

at site j for understory category k, and are used for deriving shape and range parameters

for the beta distribution using moment-matching equations. β's were assigned

uninformative normal priors.
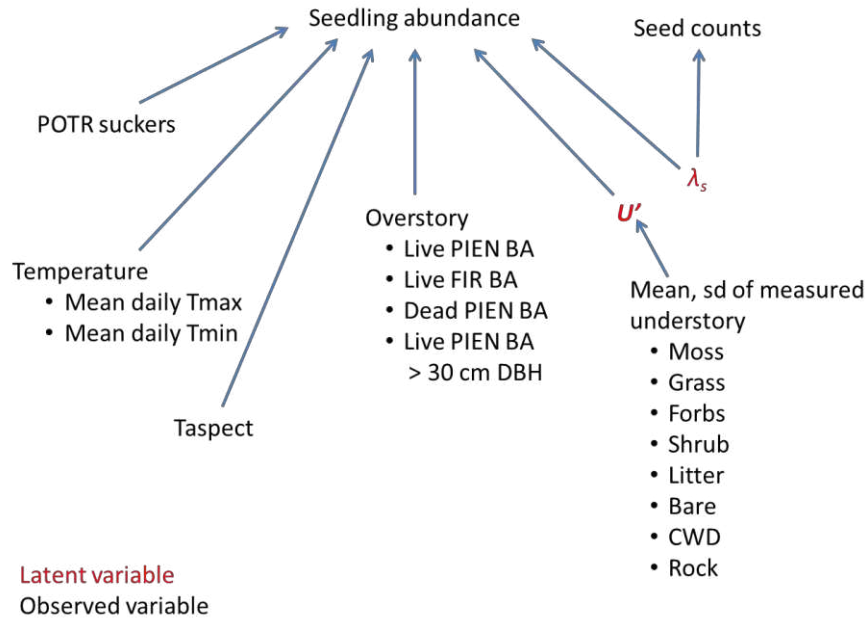
Figure 4-3. Diagram of hypothesized relationships between measured variables and seedling counts. Latent variables (red) are treated as unobserved, random variables in hierarchical Bayesian models.

Table 4-1. Candidate variables for Bayesian seedling abundance models.

Variable	Description
Site variables (X')	
Tmax	Mean growing-season daily maximum temperature
Tmax^2	Quadratic form of Tmax
Tmin	Mean growing-season daily minimum temperature
Tmin^2	Quadratic form of Tmin
Taspect	Transformed aspect measured at plot center (Beers et al., 1966)
Slope	Slope measured at plot center
LivePIEN	Basal area of live spruce trees > 5 cm in diameter
LiveFIR	Basal area of live fir trees (subalpine and white fir) > 5 cm in diameter
LivePIENOver30	Basal area of live spruce trees > 30 cm in diameter
POTR	Count of aspen seedlings < 1 m in height
Understory variables (U')	
Moss	Percent cover of each understory
Grass	category (drawn from beta

Forb	distributions defined by observed
Shrub	means and standard deviations from
Litter	15 subplots)
CWD	
Rock	
Bare	
Seed count (λ_s)	PIEN seed count (PIEN models only; mean of Poisson distribution for observed values)

iii.   Indicator Variable Selection

Due to the large number of predictor variables in the seedling abundance model (**Error! Reference source not found.**), we selected a parsimonious model using an indicator variable selection procedure (George & McCulloch, 1993). This involved adding a vector of binary indicator variable terms, **z**, to the model such that each variable n in the linear regression model is multiplied by $z_n * \beta_n$. The model was then fit using MCMC sampling, with each iteration assigning a value of 0 or 1 to z's to effectively include or exclude variables from the model. The posterior means of z's indicate overall variable importance (means closer to 0 mean variables are unimportant, means closer to 1 indicate greater importance). We assigned priors to z's and β's with the 'slab-and-spike' method described by Kuo & Mallick (1998), which uses independent distributions for both variables. The prior distribution for each z_m term was

$$z_m \sim \text{Bernoulli}(\rho)$$

where ρ was constrained by an informative beta prior resulting in a most likely value of 0.5. The prior distribution for each β_m was

$$\beta_m \sim \text{normal}(0, \tau)$$

where τ was assigned an uninformative inverse gamma prior. The full model expression with indicator variables included is

$$[\beta_0, \boldsymbol{\beta}_X, \boldsymbol{\beta}_U, \beta_s, \boldsymbol{\lambda}_s, \boldsymbol{U}, \boldsymbol{z}, \rho, \tau | \boldsymbol{y}, \boldsymbol{s}] \sim \prod_{i=1}^{2} \prod_{j=1}^{58} \text{Poisson}\left(y_j | \beta_0, \boldsymbol{\beta}_U, \boldsymbol{z}_U, \boldsymbol{U}_j', \beta_s, z_s, \lambda_{s,j}, \boldsymbol{\beta}_X, \boldsymbol{z}_X, \boldsymbol{X}_j'\right)$$

$$\times \text{Poisson}\left(s_{i,j} | \lambda_{s,j}\right) \text{gamma}\left(\lambda_{s,j} | 0.001, 0.001\right)$$

$$\times \prod_{k=1}^{p_U} \text{beta}\left(\boldsymbol{U}_{j,k} | m_{j,k}, sd_{j,k}\right)$$

$$\times \text{ normal}(\beta_{U,k} | 0, \tau) \text{Bernoulli}(z_{U,k} | \rho)$$

$$\times \prod_{l=1}^{p_X} \text{normal}\left(\beta_{X,l} | 0, \tau\right) \text{Bernoulli}(z_{X,l} | \rho)$$

$$\times \text{normal}(\beta_s | 0, \tau) \text{Bernoulli}(z_s | \rho)$$

$$\times \text{beta}(\rho | 5, 5)$$

$$\times \text{inverse gamma}(\tau | 0.001, 0.001)$$

$$\times \text{ normal}(\beta_0 | 0., 0.001)$$

We used the posterior means of z's to determine variable subsets to include in final models, using a threshold of 0.5. We then fit final models without indicators to find posterior distributions for β's.

Results

Seed Dispersal

We collected seeds from 26 of the 30 burned sites and 58 of the 60 unburned sites in at least one year. We were unable to obtain seed counts at the remaining sites due to lost traps or trap covers becoming separated. In the burned area, only two sites had non-zero PIEN seed counts in both years (average per-year counts of 1.5 and 0.5 seeds). Both sites were located less than 100 m from unburned edges (Figure 4-4). No FIR seeds were present in any seed collections in burned sites. Mean seed count in unburned sites was 5.0 seeds per year, with a maximum of 117 seeds collected in one year at a single site. There were 22 unburned sites with 0 seeds

counted in either collection year. The Bayesian regression model for unburned sites indicated that there is a positive relationship between expected mean seed count (λ_s) and site-level basal area of PIEN > 30 cm in diameter, with a 94.9% probability that the regression coefficient (γ_2) is greater than 0 (95% credible interval = -0.012 – 0.172; Figure 4-5).
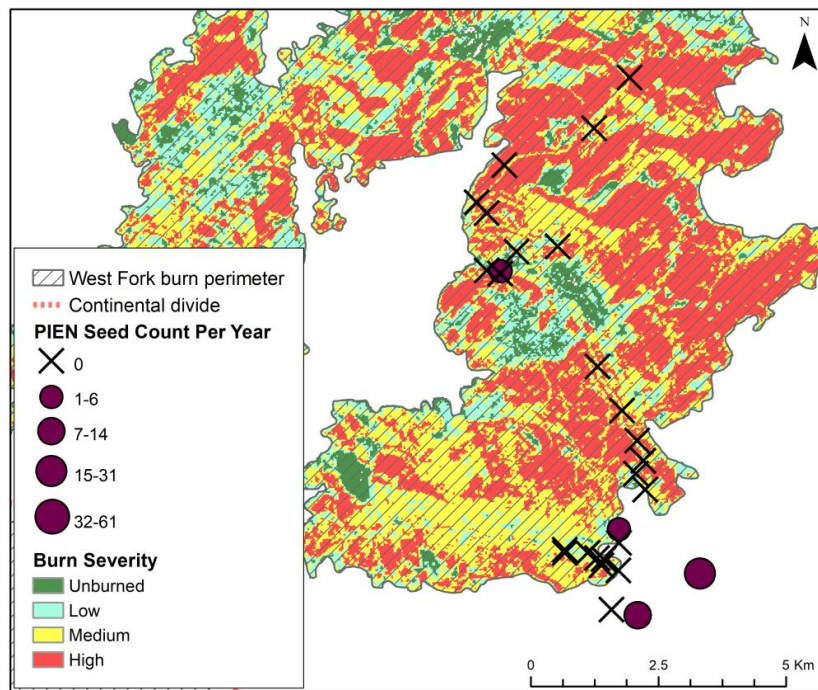
Figure 4-4. Map of seed counts in and adjacent to the West Fork Complex burned area, overlain with burn severity classes from MTBS. Counts are averaged between collection years in 2017 and 2018. Only sites where seed traps were recovered in at least one year are shown.
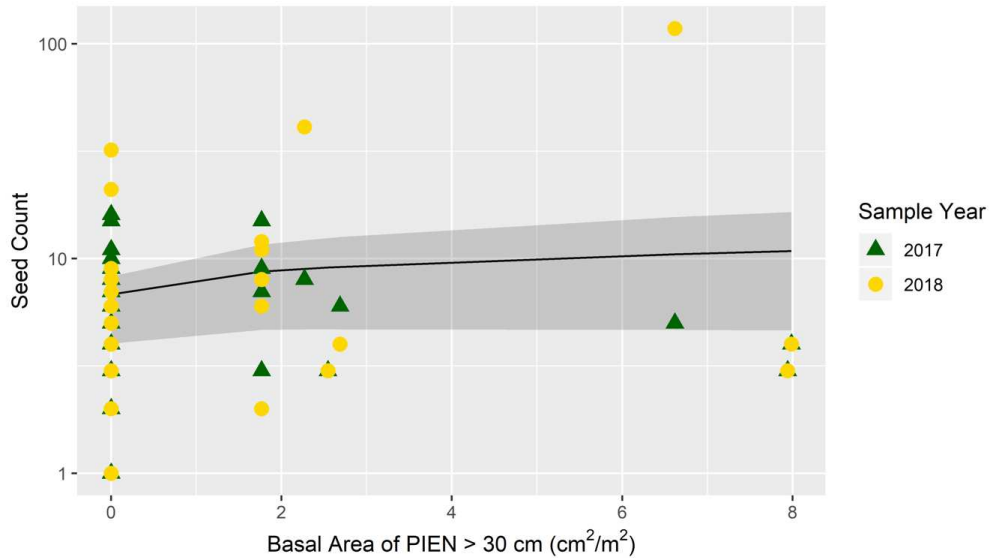
Figure 4-5. Modeled relationship between expected seed counts (s) and basal area of live PIEN > 30 cm in diameter in unburned forest. Black line=means of posterior distributions for s; gray shaded area=2.5th-97.5th percentile ranges. Points are observed values in both collection years.

Seedling Abundance

In the burned area, only three sites contained conifer seedlings established in the 5 years since the fire. Each of these sites was located < 100 m from unburned forest near the edge of the burn perimeter (Figure 4-6). These sites had also burned at low severity and contained seedlings older than 5 years which had survived the fire. None of the sites with seedlings had any viable seeds captured in seed traps, although one trap contained a single seed wing. In contrast to the low rates of conifer regeneration, many burned sites contained abundant POTR regeneration (mean density: 788.81 ± 1,460.5 suckers/ha). POTR suckers were only present at sites below 3,341 m in elevation (Figure 4-7).
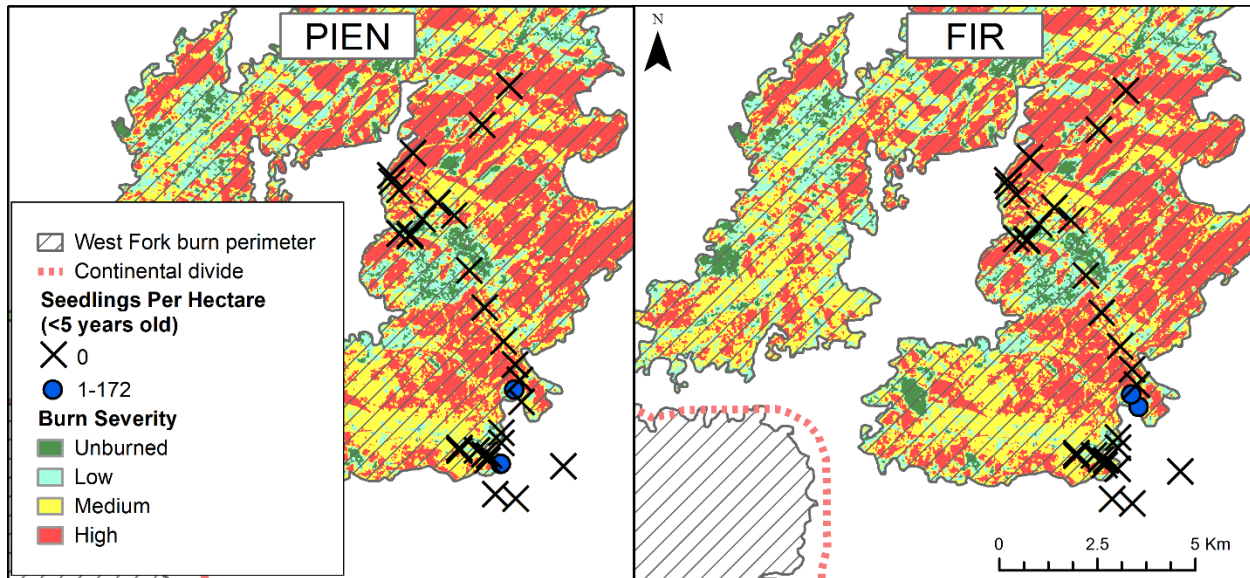
Figure 4-6. Map of seedlings in the West Fork Complex burn area that established since the year of the fire (2013), with burn severity classes from MTBS.
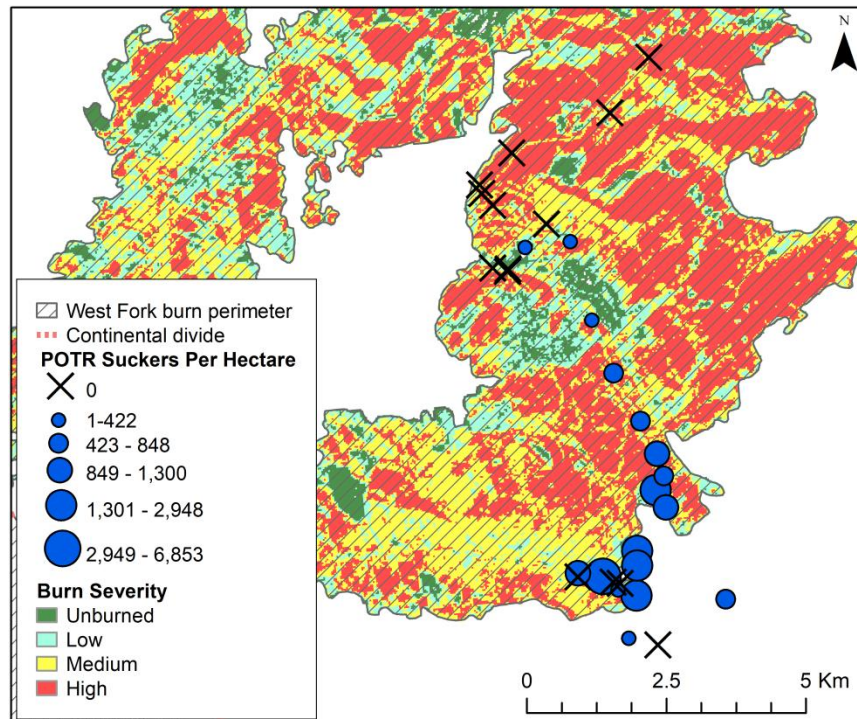
Figure 4-7. Map of POTR suckers in the West Fork Complex burn area, with burn severity classes from MTBS.

In unburned sites, the average density of sampled PIEN seedlings under 10 years old was 250.0 ± 420.7 seedlings/ha (mean ± one std. deviation) and the average density of PIEN seedlings 10 years or older was 252.2 ± 234.4 seedlings/ha. Ten sites contained no PIEN seedlings < 10 years old, although PIEN seedlings > 10 years old were present at all sites. The average density of FIR seedlings < 10 years old was 278.0 ± 427.6 seedlings/ha, and the density of FIR seedlings 10 years or older was 289.7 ± 344.8 seedlings/ha. Very few seedlings had established in the last three years (mean densities: 20.7 ± 57.6 seedlings/ha for PIEN, 19.0 ± 57.3 seedlings/ha for FIR). Temporal patterns in seedling establishment were similar for PIEN and FIR, with a majority of seedlings > 10 years old (Figure 4-8). Low abundances of seedlings established in 2016-2018 correspond with severe drought in 2018 as measured by the Palmer Drought Severity Index (PDSI; data from http://climateengine.org/). However, low PDSI values in 2012-2013 do not appear to affect seedling abundances.
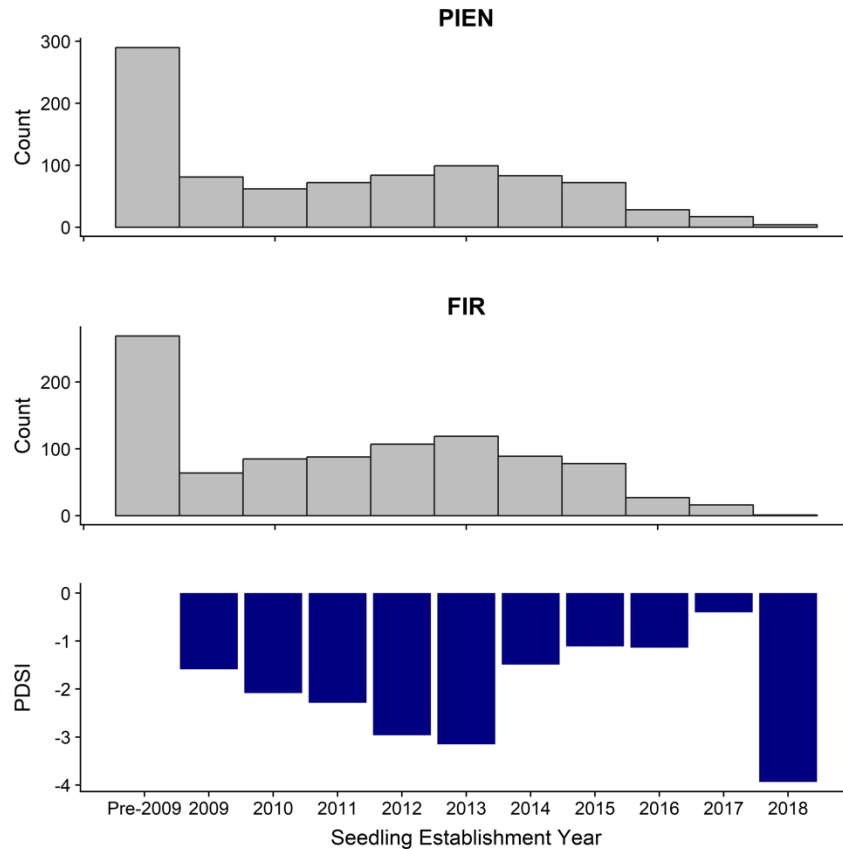
Figure 4-8. PIEN and FIR seedlings by year of establishment for seedlings up to 10 years old, compared to annual PDSI.

The indicator variable selection procedure for PIEN models resulted in a final model that included Tmax, Tmin, Taspect, DeadPIEN, LiveFIR, and all understory categories except Rock (Table 4-2). Seed count was not included. Although only the quadratic forms of Tmax and Tmin had mean z's > 0.5, we retained both the linear and quadratic forms of both variables. For FIR models, indicator variable selection resulted in a final model that included LiveFIR, POTR seedling count, and understory percent cover of Moss, Litter, CWD, and Bare. Temperature variables, Taspect, DeadPIEN, and understory percent cover of Grass, Forb, and Shrub were not included in FIR seedling models. Slope and LivePIEN were not included in either PIEN or FIR models.

Table 4-2. Posterior means of indicator variables (z's) for all explanatory variables in models predicting seedling abundances for both *P. engelmannii* (PIEN) and fir *spp*. (FIR). Values in bold are above the threshold of 0.5, and corresponding variables were included in final models. The full quadratic expressions of temperature variables were included. PIEN seed count was not considered in FIR models.

Variable	z – PIEN model	z – FIR model
Intercept	**1.00**	0.97
Site variables (X')		
Tmax	0.47	0.44
Tmax^2	**0.54**	0.44
Tmin	0.46	0.39
Tmin^2	**0.53**	0.44
Taspect	**0.86**	0.30
Slope	0.37	0.41
LivePIEN	0.29	0.34
DeadPIEN	**0.94**	0.28
LiveFIR	**0.82**	**0.99**
POTR	0.32	**0.69**
Understory variables (U')		
Moss	**0.52**	**0.90**
Grass	**0.64**	0.40
Forb	**0.56**	0.48
Shrub	**0.86**	0.41
Litter	**0.92**	**0.67**
CWD	**0.56**	**0.99**
Rock	0.38	0.45
Bare	**0.53**	**0.77**
PIEN seed count (s)	0.39	-

Variables in the final PIEN seedling abundance model with a >95% probability of being non-zero (and therefore strongly explaining seedling patterns) include Taspect, DeadPIEN, LiveFIR, Tmin (quadratic form), Shrub, and Litter (Table 4-3). PIEN seedling abundance shows a strongly positive response to Taspect (i.e., more north-facing aspects), a strongly negative response to increasing basal area of DeadPIEN, negative responses to increasing Shrub and Litter cover, and positive responses to increasing Bare and Grass cover (Figure 4-9). Seedling

abundance also decreases at the high ends of temperature ranges for both Tmax and Tmin, and

mean response to Tmin indicates an optimal temperature at the colder end of the sampled range

(~2 °C). Variables with a >95% probability of being non-zero in FIR models include LiveFIR,

POTR, CWD, and Bare (Table 4-3). FIR seedling abundance responds positively to increasing

LiveFIR overstory basal area and to increasing POTR seedling abundance, and responds

negatively to increasing CWD and Bare percent cover (Figure 4-10).

Table 4-3. Variables in PIEN and FIR seedling abundance models and probabilities that β's are greater or less than 0. (+) indicates that $\beta_{mean} > 0$; (-) indicates that $\beta_{mean} < 0$. Values above 0.95 are in bold, indicating a >95% probability that $\beta \neq 0$.

PIEN Model		FIR Model	
Variable	**Pr($\beta \neq 0$)**	**Variable**	**Pr($\beta \neq 0$)**
Taspect	**0.97 (+)**	LiveFIR	**>0.99 (+)**
DeadPIEN	**0.97 (-)**	POTR	**0.99 (+)**
LiveFIR	**>0.99 (+)**	Moss	0.92 (+)
Tmax	0.93 (-)	Litter	0.93 (+)
Tmax^2	0.91 (+)	CWD	**>0.99 (-)**
Tmin	**>0.99 (+)**	Bare	**0.97 (-)**
Tmin^2	**>0.99 (-)**		
Moss	0.65 (-)		
Shrub	**>0.99 (-)**		
Litter	**0.99 (-)**		
Bare	0.89 (+)		
CWD	0.54 (-)		
Grass	0.82 (+)		
Forb	0.65 (-)		
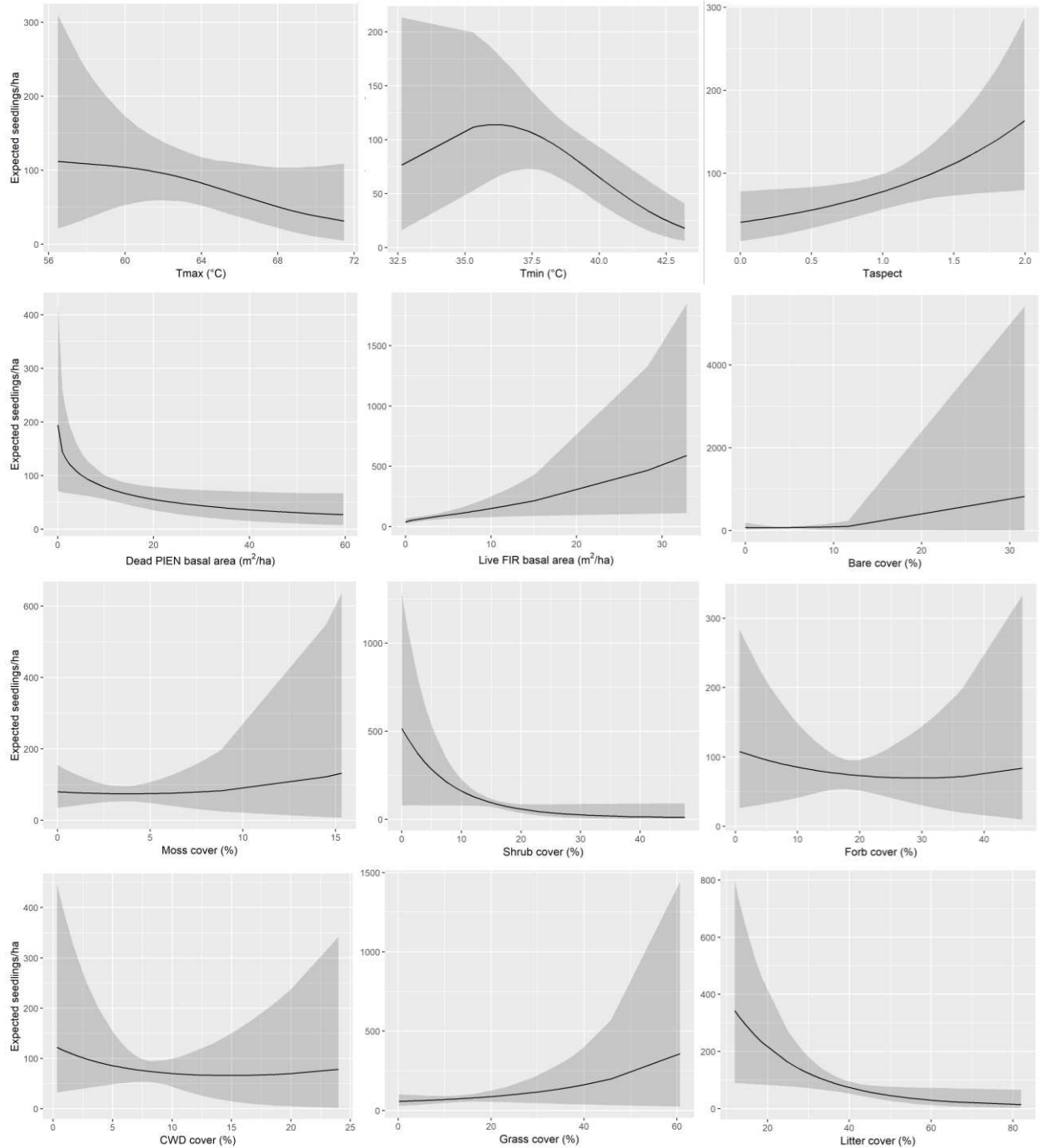
Figure 4-9. Marginal response plots for all variables included in final PIEN seedling abundance models. Plots show the expected response of seedling abundance to each variable when all other variables are held at their mean values. Black lines show posterior means of predicted responses, gray shaded area shows the 95% credible interval.
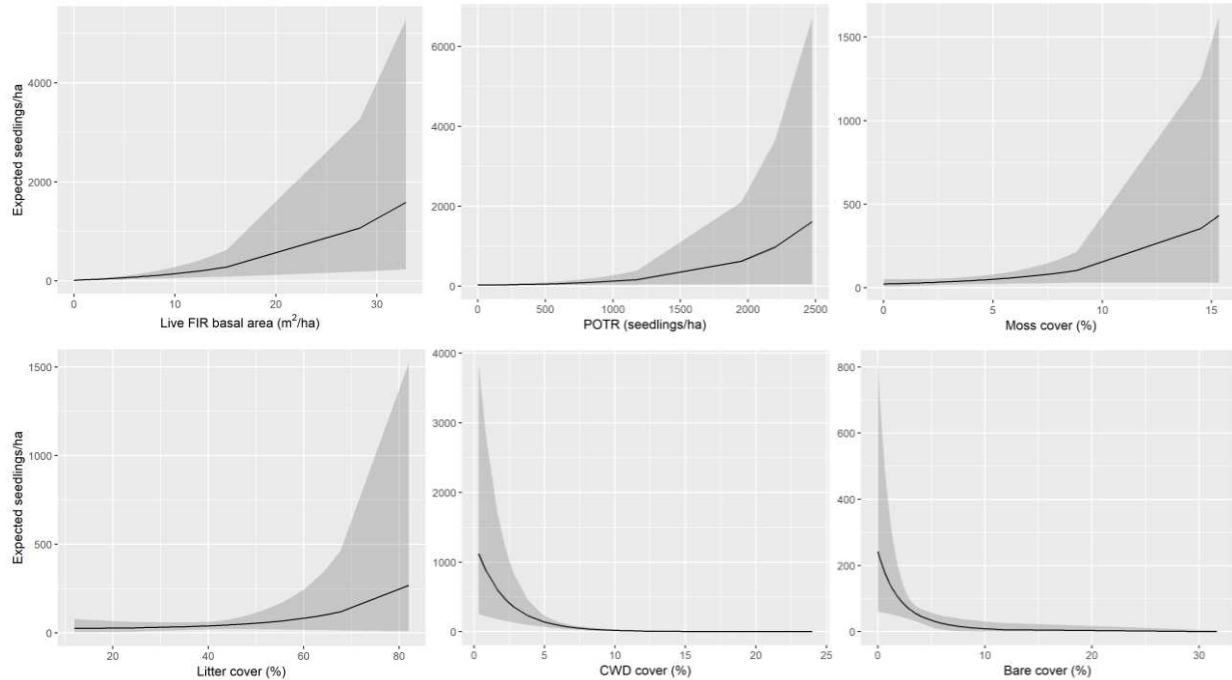
Figure 4-10. Marginal response plots for all variables included in final FIR seedling abundance models. Plots show the expected response of seedling abundance to each variable when all other variables are held at their mean values. Black lines show posterior means of predicted responses, gray shaded area shows the 95% credible interval.

Discussion

Patterns of Regeneration in the West Fork Burn Area

We did not observe any conifer regeneration in severely burned areas of the West Fork Complex burn area five years after the fire. Conifer re-colonization appeared to be constrained by lack of adequate seed dispersal, as seedling absence corresponded with an absence of available seed captured in seed traps and absence of live trees to serve as seed sources. Given that most of the forested area burned at high severity, we may expect to see these patterns of extremely low conifer regeneration throughout the interior of the burned area. We can infer from these results that much of the previously forested burned area will remain unforested for the foreseeable future. Current regeneration patterns suggest that lower elevations of the burn area

120

will remain aspen-dominated for the next several decades or longer while higher elevations with no aspen regeneration may remain unforested meadows.

Seed dispersal limitations are evident, as 90% of our seed traps in the burned area contained no conifer seeds. Seeds were only present in low numbers in traps located near the burn edge. This pattern was not unexpected given that Engelmann spruce and subalpine fir typically re-colonize burned areas by wind-dispersed seeds which do not typically travel farther than 100 m (Alexander, 1987). Although our seed trap design does not fully capture rare, long-distance seed dispersal events across the landscape (Nathan & Muller-Landau, 2000), the lack of seedlings at 90% of sites within the burned area suggests that these events are not leading to conifer re-establishment. Furthermore, regeneration has apparently not resulted from the pre-fire canopy seed bank. This can be an important seed source for post-fire regeneration in Engelmann spruce forests when seed production is abundant (Pounden, Greene, & Michaletz, 2014). In the West Fork Complex, it is very likely that pre-fire cone production was diminished by the severe spruce beetle outbreak which killed most large-diameter spruce trees in the previous decade (Carlson et al., 2017).

Declining conifer regeneration following wildfire has become a common pattern across the western United States in the last two decades, as a result of increasing post-fire drought stress and low seed availability due to increasing fire sizes (Stevens-Rumann & Morgan, 2019). These regeneration failures indicate that fires are catalyzing climate-driven ecosystem transitions. Our results provide an additional example of post-fire regeneration failure in a high-elevation forest type. We can attribute this apparent forest transition to lack of seed dispersal, although the absence of seeds in most of our study sites obscures the potential concurrent role of warming and drought in limiting seedling establishment (Harvey et al., 2016; Kemp, Higuera, Morgan, &

121

Abatzoglou, 2019; Urza & Sibold, 2017). Although droughts were not severe in the four years following the fire (Figure 4-8), mean annual temperatures at Wolf Creek Pass have warmed by an average of 0.44 °C since 1895 (PRISM climate data). Carlson et al. (*in prep*) found that mean temperatures in the burned area are elevated by ~0.5 °C compared to unburned areas. Re-establishing seedlings may therefore be experiencing temperatures significantly warmer than those experienced when the original forest established, which may be beyond a threshold for regeneration.

Patterns of Regeneration in Spruce Beetle-Killed Forest

Spruce beetle outbreak at Wolf Creek Pass has not resulted in regeneration failures and the apparent ecosystem transition that is observed in the West Fork Complex fire. Despite high canopy mortality of Engelmann spruce in most of our study sites, there is abundant advance regeneration in the sub-canopy by both PIEN and FIR seedlings > 10 years old. Low abundances of seedlings < 10 years old, which are assumed to have established after the beetle outbreak, are typical for severely beetle-killed spruce-fir forests (Astrup, Coates, & Hall, 2008; DeRose & Long, 2010). However, extremely low abundances of seedlings established in the last three years may indicate potential future trends that may arise from warming and severe droughts.

We observed a drop-off in seedling establishment from 2016-2018 which may be related to severe drought in 2018. While these drought conditions were not present in 2016-2017, the lagged effect might be attributed to mortality of newly established seedlings in fall 2017-summer 2018. We did not observe the same low seedling abundances in 2012-2013 despite a low PDSI in those years. Both droughts were characterized by hot summers, low monsoon-season precipitation, and early snowmelt, while the drought of 2017-2018 also included very warm fall temperatures and extremely low winter snow cover. In addition to growing-season soil moisture,

snowpack has been shown to strongly correlate with spruce and fir seedling establishment in both observational studies and growth experiments (Andrus et al., 2018; Kueppers et al., 2017). If warm fall-winter droughts such as the one in 2017-2018 are likely to occur more frequently in the San Juan Mountains in the near future, these events may limit future seedling establishment.

Our Bayesian analysis of site factors contributing to seedling abundance revealed that increasing temperatures may lead to greater declines in both PIEN and FIR establishment, especially on drier, southwest-facing slopes. Our temperature data only represents a single growing season and therefore is not necessarily representative of absolute temperature-abundance relationships, but temperature patterns are reflective of relative spatial difference in temperatures which depend on topographic setting (Carlson et al., *in prep*; Dobrowski, 2011). Our modeled temperature relationships therefore suggest that regional warming will cause PIEN and FIR seedling distributions to shift toward higher elevations, northeast-facing slopes, or valley bottoms with sufficient cold-air drainage to remain within their optimal temperature ranges. Due to differing responses to Tmax vs. Tmin, warming may be expected to affect PIEN distributions differently than FIR distributions.

Seedling abundance models also revealed that the severity of spruce beetle mortality (as measured by basal area of standing dead PIEN) has strong effects on PIEN seedling establishment in relation to temperature and other site factors. A possible explanation for this relationship is that spruce beetle outbreak results in seed limitations as large-diameter, cone-producing trees die off. There is limited evidence for this mechanism from our seed dispersal model, but our variable selection procedure indicated that seed counts did not explain PIEN seedling abundance. It is possible that our analysis is limited by only having seed collections over two years, which may not fully capture year-to-year variability in seed production.

Engelmann spruce produce bumper seed crops roughly every 2-5 years, and seed production is affected by multi-year weather conditions which impact various stages of seed development (Alexander, 1987; Buechling, Martin, Canham, Shepperd, & Battaglia, 2016). Longer-term seed monitoring may be needed to more accurately assess effects of spruce beetle outbreak on overall seed supply.

Our results show that spruce seedling abundance is affected by live canopy cover, with seedlings responding positively to increasing overstory FIR cover and negatively to increased spruce canopy loss. Although we did not see strong evidence that this is explained by seed dispersal, these relationships may be additionally influenced by changes in the below-canopy environment associated with live canopy. Dobrowski et al. (2015) observed that seedling densities correspond with undisturbed forest cover across the western U.S., and hypothesize that this may be due to canopy cover buffering microclimates against broader warming trends. Spruce beetle outbreak does not lead to greater below-canopy warming, but may lead to greater overnight cooling (Carlson et al., *in prep*) which may increase risk of frost damage at the onset of the growing season and potentially inhibit growth at cool edges of PIEN distribution (Carlson et al., *in prep;* Hill et al., 2019; Noble & Alexander, 1977). Canopy loss may also lead to greater rates of snow ablation and earlier snowmelt (Pugh & Small, 2013). An additional unexplored mechanism is the potential feedback between overstory die-offs and declines in below-ground ectomycorrhizal associations, which has been shown to reduce seedling growth and survival in lodgepole pine stands affected by mountain pine beetle (Karst et al., 2015).

Finally, our analysis explored the role of understory composition in determining seedling abundance. We found that there were likely to be fewer PIEN seedlings at sites with greater litter and shrub cover, consistent with current understanding that PIEN prefers to establish on exposed

mineral soil (Knapp & Smith, 1982; Noble & Alexander, 1977). Overstory mortality may be indirectly affecting PIEN regeneration by allowing for greater shrub growth as below-canopy light availability increases (Stone & Wolfe, 1996). Needle fall from the canopy may also initially increase understory litter cover following outbreak, creating a less favorable environment for PIEN seedling re-establishment. Furthermore, our results show that CWD did not favor seedling establishment for either PIEN or FIR and appeared to strongly inhibit FIR establishment. It should be noted that most CWD we observed was from recent tree-fall as a result of the beetle outbreak. This relationship may change over time as logs decompose and form moist micro-sites for seedling establishment.

Conclusions

This study assessed patterns of seedling regeneration in the West Fork Complex burn area and surrounding areas affected by a severe spruce beetle outbreak. Our results support two key conclusions: first, that conifer regeneration in the burned area is severely limited due to a lack of available seed sources; and second, that overstory mortality in spruce beetle-killed forests is confounding the response of seedling regeneration to temperature and other site characteristics. The extremely low seedling abundances in the West Fork burn area fit in with a pattern being observed across the western United States, in which increasing fire sizes and severities in tandem with increasing post-fire aridity are reducing rates of forest regeneration. In beetle-killed forest, the negative response of PIEN seedling establishment to increasing overstory mortality from spruce beetles has implications for long-term predictions of forest decline with climate change. While it is understood that temperature effects on seedling recruitment may vary at fine spatial scales in mountain forests, extensive canopy disturbances are also playing an important role in accelerating forest decline.

LITERATURE CITED

Alexander, R. (1987). *Ecology, Silviculture, and Management of the Engelmann Spruce-Subalpine Fir Type in the Central and Southern Rocky Mountains* (Agricultural Handbook No. 659). Washington, D.C.: U.S. Dept. of Agriculture Forest Service.

Allen, C. D., Macalady, A. K., Chenchouni, H., Bachelet, D., McDowell, N., Vennetier, M. et al. (2010). A global overview of drought and heat-induced tree mortality reveals emerging climate change risks for forests. *Forest Ecology and Management*, *259*(4), 660–684.

Andrus, R. A., Harvey, B. J., Rodman, K. C., Hart, S. J., & Veblen, T. T. (2018). Moisture availability limits subalpine tree establishment. *Ecology*, *99*(3), 567–575.

Astrup, R., Coates, K. D., & Hall, E. (2008). Recruitment limitation in forests: Lessons from an unprecedented mountain pine beetle epidemic. *Forest Ecology and Management*, *256*(10), 1743–1750.

Beers, T., Dress, P., & Wensel, L. (1966). Notes and observations: Aspect transformation in site productivity research. *Journal of Forestry*, *64*(10), 691–692.

Bell, D. M., Bradford, J. B., & Lauenroth, W. K. (2014). Mountain landscapes offer few opportunities for high-elevation tree species migration. *Global Change Biology*, *20*(5), 1441–1451.

Bentz, B. J., Régnière, J., Fettig, C. J., Hansen, E. M., Hayes, J. L., Hicke, J. A., et al. (2010). Climate Change and Bark Beetles of the Western United States and Canada: Direct and Indirect Effects. *BioScience*, *60*(8), 602–613.

Buechling, A., Martin, P. H., Canham, C. D., Shepperd, W. D., & Battaglia, M. A. (2016). Climate drivers of seed production in *Picea engelmannii* and response to warming temperatures in the southern Rocky Mountains. *Journal of Ecology*, *104*(4), 1051–1062.

Carlson, A.R., Sibold, J.S., & Negron, J.F. *in prep*. Topoclimate patterns are affected by wildfire and spruce beetle disturbance in a Rocky mountain forest.

Carlson, A. R., Sibold, J. S., Assal, T. J., & Negron, J. F. (2017). Evidence of compounded disturbance effects on vegetation recovery following high-severity wildfire and spruce beetle outbreak. *PLoS ONE*, *12*(8).

Certini, G. (2005). Effects of fire on properties of forest soils: A review. *Oecologia*, *143*(1), 1–10.

CSFS. (2018). *2018 Report on the Health of Colorado's Forests*. Fort Collins, CO: Colorado State Forest Service.

DeRose, R. J., & Long, J. N. (2010). Regeneration response and seedling bank dynamics on a *Dendroctonus rufipennis*-killed *Picea engelmannii* landscape. *Journal of Vegetation Science*, *21*(2), 377–387.

Dobrowski, S. Z. (2011). A climatic basis for microrefugia: The influence of terrain on climate. *Global Change Biology*, *17*(2), 1022–1035.

Dobrowski, S. Z., Swanson, A. K., Abatzoglou, J. T., Holden, Z. A., Safford, H. D., Schwartz, M. K., & Gavin, D. G. (2015). Forest structure and species traits mediate projected recruitment declines in western US tree species. *Global Ecology and Biogeography*, *24*(8), 917–927.

Edburg, S. L., Hicke, J. A., Brooks, P. D., Pendall, E. G., Ewers, B. E., Norton, U. et al. (2012). Cascading impacts of bark beetle-caused tree mortality on coupled biogeophysical and biogeochemical processes. *Frontiers in Ecology and the Environment*, *10*(8), 416–424.

George, E. I., & McCulloch, R. E. (1993). Variable selection via Gibbs sampling. *Journal of the American Statistical Association, 88*(423), 881-889.

Harvey, B. J., Donato, D. C., & Turner, M. G. (2016). High and dry: Post-fire tree seedling establishment in subalpine forests decreases with post-fire drought and large stand-replacing burn patches. *Global Ecology and Biogeography*, *25*(6), 655–669.

Hill, E., Ex, S., Aldridge, C., & Prolic, C. (2019). Overstory density, short growing seasons, and moisture limit Engelmann spruce establishment over time in high-elevation managed stands. *Canadian Journal of Forest Research*, *49*(1), 64–75.

Holling, C. S. (1973). Resilience and stability of ecological systems. *Annual Review of Ecology and Systematics*, *4*(1), 1–23.

IPCC. (2014). Climate Change 2014: Synthesis Report. Contribution of Working Groups I, II, and III to the Fifth Assessment Report of the Intergovernmental Panel on Climate Change. (p. 151). Geneva, Switzerland.

Johnstone, J. F., Allen, C. D., Franklin, J. F., Frelich, L. E., Harvey, B. J., Higuera, P. E. et al. (2016). Changing disturbance regimes, ecological memory, and forest resilience. *Frontiers in Ecology and the Environment*, *14*(7), 369–378.

Johnstone, J. F., & Chapin, F. S. (2006). Effects of soil burn severity on post-fire tree recruitment in boreal forest. *Ecosystems*, *9*(1), 14–31.

Jonášová, M., & Prach, K. (2004). Central-European mountain spruce (*Picea abies* (L.) Karst.) forests: Regeneration of tree species after a bark beetle outbreak. *Ecological Engineering*, *23*(1), 15–27.

Karst, J., Erbilgin, N., Pec, G. J., Cigan, P. W., Najar, A., Simard, S. W., & Cahill, J. F., Jr. (2015). Ectomycorrhizal fungi mediate indirect effects of a bark beetle outbreak on secondary chemistry and establishment of pine seedlings. *New Phytologist*, *208*(3), 904–914.

Kemp, K. B., Higuera, P. E., Morgan, P., & Abatzoglou, J. T. (2019). Climate will increasingly determine post-fire tree regeneration success in low-elevation forests, Northern Rockies, USA. *Ecosphere*, *10*(1), e02568.

Knapp, A. K., & Smith, W. K. (1982). Factors influencing understory seedling establishment of Engelmann spruce (*Picea engelmannii*) and subalpine fir (*Abies lasiocarpa*) in southeast Wyoming. *Canadian Journal of Botany*, *60*(12), 2753–2761.

Kueppers, L. M., Conlisk, E., Castanha, C., Moyes, A. B., Germino, M. J., de Valpine, P. et al. (2017). Warming and provenance limit tree recruitment across and beyond the elevation range of subalpine forest. *Global Change Biology*, *23*(6), 2383–2395.

Kuo, L., & Mallick, B. (1998). Variable selection for regression models. *Sankhyā: The Indian Journal of Statistics, Series B*, 65-81.

MTBS. (2013). *Monitoring Trends in Burn Severity* [online data]. Retrieved from: mtbs.gov.

Nathan, R., & Muller-Landau, H. C. (2000). Spatial patterns of seed dispersal, their determinants and consequences for recruitment. *Trends in Ecology & Evolution*, *15*(7), 278–285.

Noble, D. L., & Alexander, R. R. (1977). Environmental Factors Affecting Natural Regeneration Engelmann Spruce in the Central Rocky Mountains. *Forest Science*, *23*(4), 420–429.

Pelz, K. A., Rhoades, C. C., Hubbard, R. M., & Smith, F. W. (2018). Severity of Overstory Mortality Influences Conifer Recruitment and Growth in Mountain Pine Beetle-Affected Forests. *Forests*, *9*(9).

Perovich, C., & Sibold, J. S. (2016). Forest composition change after a mountain pine beetle outbreak, Rocky Mountain National Park, CO, USA. *Forest Ecology and Management*, *366*, 184–192.

Plummer, M. (2017). JAGS: Just Another Gibbs Sampler [software version 4.3.0]. https://sourceforge.net/projects/mcmc-jags/files/JAGS/4.x/Windows/

Plummer, M. (2018). rjags: Bayesian Graphical Models Using MCMC [R package version 4-8]. https://CRAN.R-project.org/package=rjags.

Pounden, E., Greene, D. F., & Michaletz, S. T. (2014). Non-serotinous woody plants behave as aerial seed bank species when a late-summer wildfire coincides with a mast year. *Ecology and Evolution, 4*(19), 3830–3840.

Pugh, E. T., & Small, E. E. (2013). The impact of beetle-induced conifer death on stand-scale canopy snow interception. *Hydrology Research*, *44*(4), 644–657.

R Core Team (2019). R: A language and environment for statistical computing. Vienna, Austria: *R Foundation for Statistical Computing*. http://www.R-project.org/

Redmond, M. D., & Kelsey, K. C. (2018). Topography and overstory mortality interact to control tree regeneration in spruce-fir forests of the southern Rocky Mountains. *Forest Ecology and Management*, *427*, 106–113.

Rocca, M. E., Brown, P. M., MacDonald, L. H., & Carrico, C. M. (2014). Climate change impacts on fire regimes and key ecosystem services in Rocky Mountain forests. *Forest Ecology and Management*, *327*, 290–305.

Rother, M. T., & Veblen, T. T. (2016). Limited conifer regeneration following wildfires in dry ponderosa pine forests of the Colorado Front Range. *Ecosphere*, *7*(12).

Savage, M., Mast, J. N., & Feddema, J. J. (2013). Double whammy: High-severity fire and drought in ponderosa pine forests of the Southwest. *Canadian Journal of Forest Research*, *43*(6), 570–583.

Schmid, J., & Frye, R. (1977). *Spruce beetle in the Rockies* (No. Gen. Tech. Rep. RM-49). Fort Collins, CO: US Forest Service, Rocky Mountain Forest and Range Experiment Station.

Seidl, R., Thom, D., Kautz, M., Martin-Benito, D., Peltoniemi, M., Vacchiano, G. et al. (2017). Forest disturbances under climate change. *Nature Climate Change*, *7*(6), 395–402.

Stevens-Rumann, C. S., Kemp, K. B., Higuera, P. E., Harvey, B. J., Rother, M. T., Donato, D. C. et al. (2018). Evidence for declining forest resilience to wildfires under climate change. *Ecology Letters*, *21*(2), 243–252.

Stevens-Rumann, C. S., & Morgan, P. (2019). Tree regeneration following wildfires in the western US: a review. *Fire Ecology*, *15*(1), 15.

Stone, W. E., & Wolfe, M. L. (1996). Response of understory vegetation to variable tree mortality following a mountain pine beetle epidemic in lodgepole pine stands in northern Utah. *Vegetatio*, *122*(1), 1–12.

Turner, M. G. (2010). Disturbance and landscape dynamics in a changing world. *Ecology*, *91*(10), 2833–2849.

Turner, M. G., Romme, W. H., & Gardner, R. H. (1999). Prefire heterogeneity, fire severity, and early postfire plant reestablishment in subalpine forests of Yellowstone National Park, Wyoming. *International Journal of Wildland Fire*, *9*(1), 21–36.

Urza, A. K., & Sibold, J. S. (2013). Nondestructive Aging of Postfire Seedlings for Four Conifer Species in Northwestern Montana. *Western Journal of Applied Forestry*, *28*(1), 22–29.

Urza, A. K., & Sibold, J. S. (2017). Climate and seed availability initiate alternate post-fire trajectories in a lower subalpine forest. *Journal of Vegetation Science*, *28*(1), 43–56.

Veblen, T. T., Hadley, K. S., & Reid, M. S. (1991). Disturbance and Stand Development of a Colorado Subalpine Forest. *Journal of Biogeography*, *18*(6), 707–716.

Westerling, A. L. (2016). Increasing western US forest wildfire activity: Sensitivity to changes in the timing of spring. *Philosophical Transactions of the Royal Society B: Biological Sciences*, *371*(1696), 20150178.

CHAPTER 5: Synthesis

The goal of my dissertation was to better understand how forest recovery patterns are being affected by disturbance severities and interactions which appear to exceed any recorded precedent in the Southern Rockies. Because these disturbances are linked to a rapid warming trend throughout the region, regeneration patterns may be indicative of the potential for disturbance-mediated ecosystem transitions driven by shifting climate suitability. In my research I considered three potential mechanisms by which disturbances may facilitate change: (1) recovery patterns being influenced by compounded disturbance interactions, (2) loss of canopy cover influencing the exposure of regenerating seedlings to warming trends, and (3) regeneration responses to temperature being mediated by disturbance effects on seed availability or other changes to the micro-environment. Understanding these factors allows for a more complete understanding of the role of disturbance in shaping forest ecosystem responses to climate change.

The geographic region selected for my dissertation work played an important role in my study design and interpretation of results. I chose to study the effects of the West Fork Complex fire and surrounding spruce beetle-killed forest because this area represented a region with particularly severe disturbance effects. The San Juan mountain range is at the southern edge of the North American distribution for the subalpine spruce-fir forest type (i.e., the "warm" edge), indicating that widespread mortality could begin a process of extirpation as these forest types shift to higher, cooler latitudes. My results found that this may be the case in areas affected by the West Fork Complex fire, but is not clearly so in unburned forests affected by the spruce beetle outbreak. However, there are some indications that high-severity spruce beetle outbreak may be making forests more vulnerable to forest decline with future warming and wildfires.

131

In Chapter 2, I found that there was a negative correlation between remotely sensed pre-fire spruce beetle outbreak severity and vegetation cover two years after the West Fork Complex fire. Quantifying outbreak severity has posed a challenge for researchers working in forests where beetle evidence has been destroyed by naturally occurring wildfire. However, I was able to obtain a reliable estimate using a simple Landsat-derived vegetation change index (dNDMI), which correlated well with field measurements of dead spruce basal area when compared with the dNDMI from imagery taken at the time of field sampling ($R^2 = 0.67$). Using this index, I was able to model the relationship between beetle-caused canopy mortality and post-fire NDVI. The analysis also accounted for several other topographic and fire weather variables, derived from publicly available digital elevation models, weather station data, and fire perimeters.

This landscape-scale approach was highly advantageous in terms of using archived Landsat imagery to study a long-term disturbance and recovery process. Focusing on multi-year patterns highlights an important consideration for understanding disturbance interactions between beetle outbreak and fire – namely, that pre-fire disturbance can have compounded disturbance impacts beyond those affecting immediate post-fire overstory mortality, which has been the most common metric of fire severity used in previous studies. A reasonable hypothesis is that bark beetle outbreaks cause needles and branches to fall to the ground, increasing surface fuel loads and causing more intense burning of soil matter. However, this study approach was limited in its ability to identify causal mechanisms. Future research may build upon this understanding of landscape-scale pattern by investigating the processes explaining how bark beetle outbreaks may lead to increased soil burn severity, and how this process may affect longer-term ecosystem development.

In Chapter 3, I used a detailed network of below-canopy temperature sensors to determine that fine-scale temperature patterns in forests are mediated by canopy modification from disturbance. I found that burned areas experienced an overall warming of ~0.5 °C compared to unburned forest, and that spruce beetle-killed forests experienced a cooling of overnight minimum temperatures with decreasing canopy cover (by up to ~1.0 °C) and little change in daytime maximum temperatures. In my topographically complex study area, the magnitude of these temperature effects was comparable to those from variations in elevation, aspect, cold-air drainage, and exposure. While it is well-understood that forest canopies buffer microclimates against both extreme hot and cold temperatures and may play a role in reducing tree species' exposure to broader warming patterns, my study was the first, to my knowledge, to explicitly model how this buffering effect can be impacted by disturbance.

My results reveal that disturbance can play a role in pushing ecosystems beyond thresholds of climate suitability, but that this role varies with different disturbance types and severities. Severe wildfire appears to exacerbate warming and may potentially limit regeneration in regions where warm and dry conditions are beginning to exceed physiological limits for seedling re-establishment. Partial canopy disturbance from bark beetle outbreaks, on the other hand, had a more complex effect. Loss of canopy led to greater overnight cooling through radiative heat loss, but standing dead trees and understory vegetation apparently provide enough ground surface shading to prevent daytime temperatures from largely increasing. Recognizing how these topoclimate patterns are influenced by different disturbance types and severities will help to improve understanding of how abrupt disturbances may interact with shifting climatic suitability for forest species, help to identify ecologically important refugia, and help to avoid

oversimplistic assumptions about how warming temperatures will cause species distributions to shift.

In Chapter 4, I built upon the understanding of disturbance effects on below-canopy temperature gained in Chapter 3 to model how other factors may be influencing regeneration success in combination with temperature. I found that (1) both seed dispersal and seedling regeneration for conifers are currently very limited in the West Fork burn area, and (2) there is a negative correlation between Engelmann spruce seedling regeneration and overstory spruce mortality in spruce beetle-killed forest stands. From these results I can conclude that the size and severity of the West Fork fire has greatly limited seed availability in the interior of the burn and that this is likely to limit forest recovery for the foreseeable future. From the results of Chapter 3 I may infer that exacerbated warming could be limiting seedling establishment, but the overall lack of seedlings in my study sites precludes statistical analysis to determine support for this hypothesis. In beetle-killed stands, I did not find evidence that the decline in seedling abundance with increasing overstory mortality was explained by seed limitation. While my 2-year study design could not fully account for potential temporal variability in seed production, other factors may explain this effect. These include effects on soil moisture resulting from increased solar radiation reaching the ground surface, changes to understory resulting from canopy opening, or potential loss of symbiotic mycorrhizae with overstory decline.

Results from within the West Fork burn area fit into other recent studies noting limited seedling regeneration following wildfire throughout the western US. These instances have raised speculations that wildfires are triggering widespread ecosystem transitions in a warming climate. Regeneration failures have most often been attributed to post-fire drought and/or seed dispersal limitations resulting from large, high-severity burns. The results of my study provide another

example of seedlings failing to re-establish following fire due to a lack of seed dispersal, and is one of relatively few examples in a high-elevation subalpine forest type. Although subalpine forests experience colder temperatures and higher precipitation compared to lower-elevation conifer forests, and therefore experience fire less frequently, warming may drive more widespread fires and subsequent ecosystem transitions in the near future. Conversely, regeneration in beetle-killed forests did not appear to be so severely limited. Advance regeneration and continued seedling establishment indicates that these forests will be resilient to the current beetle outbreak, although it is unclear how this recovery trajectory may be modified by warming and future disturbances. Reduced seedling establishment with increasing spruce beetle outbreak severity may be an indicator of reduced resilience to future stress, which may persist for several decades before smaller surviving trees reach maturity.

Overall, the results of my dissertation provide new insights into disturbance recovery trajectories in the southern Rocky Mountains. I investigated factors in my research which may have been overlooked in previous research into forest disturbance and recovery processes, including how the effects of interacting disturbances may manifest in long-term recovery patterns, how climate change exposure may be misunderstood due to disturbance impacts to the below-canopy environment, and how regeneration response to changing temperatures may be mediated by a number of ecological changes brought on by disturbance. Better understanding of these complexities will help researchers to understand how climate change may impact societally important forest resources, and to better adapt and prepare for future change.